



Open your mind. LUT.

Lappeenranta **University of Technology**

Faculty of Technology

Mechanical Engineering

Eric Martial Mvola Belinga

Applications and Benefits of Adaptive Pulsed GMAW

Supervisors: Professor Jukka Martikainen

Dr. (Tech) Paul Kah

ABSTRACT

Lappeenranta University of Technology

Faculty of Technology

Mechanical Engineering

Author: Eric Martial Mvola Belinga

Title: Applications and Benefits of Adaptive Pulsed GMAW

Year: 2012

Master's Thesis

124 Pages, 62 figures, 19 Tables, 7 Appendices.

Supervisors: Professor Jukka Martikainen

Dr. (Tech.) Paul Kah

Keywords: Adaptive pulsed, GMAW, high power energy, heat input

In ship and offshore terminal construction, welded cross sections are thick and the number of welds very high. Consequently, there are two aspects of great importance; cost and heat input. Reduction in the welding operation time decreases the costs of the work force and avoids excessive heat, preventing distortion and other weld defects. The need to increase productivity while using a single wire in the GMAW process has led to the use of a high current and voltage to improve the melting rate. Unfortunately, this also increases the heat input. Innovative GMAW processes, mostly implemented for sheet plate sections, have shown significant reduction in heat input (Q), low distortion and increase in welding speed.

The aim of this study is to investigate adaptive pulsed GMAW processes and assess relevant applications in the high power range, considering possible benefits when welding thicker sections and high yield strength steel. The study experimentally tests the usability of adaptive welding processes and evaluates their effects on weld properties, penetration and shapes of the weld bead.

The study first briefly reviews adaptive GMAW to evaluate different approaches and their applications and to identify benefits in adaptive pulsed. Experiments are then performed using Synergic Pulsed GMAW, WiseFusionTM and Synergic GMAW processes to weld a T-joint in a horizontal position (PB). The air gap between the parts ranges from 0 to 2.5 mm. The base materials are structural steel grade S355MC and filler material G3Si1. The experiment investigates heat input, mechanical properties and microstructure of the welded joint.

Analysis of the literature reveals that different approaches have been suggested using advanced digital power sources with accurate waveform, current, voltage, and feedback control. In addition, studies have clearly indicated the efficiency of lower energy welding processes. Interest in the high power range is growing and a number of different approaches have been suggested. The welding experiments in this study reveal a significant reduction of heat input and a weld microstructure with the presence of acicular ferrite (AF) beneficial for resistance to crack propagation. The WiseFusion bead had higher dilution, due to the weld bead shape, and low defects.

Adaptive pulse GMAW processes can be a favoured choice when welding structures with many welded joints. The total heat reduction mitigates residual stresses and the bead shape allows a higher amperage limit. The stability of the arc during the process is virtually spatter free and allows an increase in welding speed.

ACKNOWLEDGEMENT

I would like to express my gratitude to my supervisor, Professor Jukka Martikainen, who gave me the opportunity to work in the LUT Welding Laboratory and improve my skills in a stimulating working environment. In addition, I would like to thank Dr. Paul Kah for his expert guidance throughout this study. It has been an honour for me to work under his supervision and to benefit from his scientific knowhow and experience.

I would like to thank next the personnel of the Lappeenranta University of Technology Welding Laboratory with whom the experiments were conducted, especially Esa Hiltunen, Antti Heikkinen and Antti Kähkönen.

Although it has been some time since my early age, I want to thank my father, Belinga Engelbert, and my mother, Mvondo Ngonu Delphine. They guided my first steps and dedicated themselves to making sure that I had a well-rounded education. I learnt from them the first notions of mechanical engineering and the importance of hard work. Additionally, I want to thank my four sisters and six brothers, especially Mewoli Nathalie Bernadette and Mbeng Martin Michel Patrick, for their commitment and support in my life. Last but not least, I thank Jaana Janhunen for her loving and kind attention.

Lappeenranta, 2012

Mvola Belinga Eric Martial

LIST OF SYMBOLS AND ABBREVIATIONS

Symbol	Unit	Meaning
A		Amperage
AC-GMAW		Alternative Current GMAW
AF		Acicular Ferrite
ASME		American Society of Mechanical Engineers
ASTM		American Society for Testing and Materials
atm		atmospheric pressure
Ar		Argon
BM		Base Metal
CO ₂		Carbon Dioxide
cm		Centimetre
CMT		Cold Metal Transfer
CRA		Corrosion Resistance Alloy
CSC		Controlled Short Circuit
CTOD		Crack Tip Opening Displacement
CTWD		Contact Tip to Work Distance
CV		Constant Voltage
DA		Digital Analogic
DC		Direct Current
DCEN		Direct Current Electrode Negative
DCEP		Direct Current Electrode Positive
DP-GMAW		Dual Pulsed GMAW
Fem		Plasma Suction Force
Fg		Gravitational Force
FL		Fusion Line
F _m		Electromagnetic Force
Fr		Backlash Force
Fs		Surface Tension Force
FZ		Fusion Zone
GBF		Grain Boundary Ferrite
GMAW		Gas Metal Arc Welding
HAZ		Heat Affected Zone
H ₂		Hydrogen
He		Helium
HNO ₃		Nitric Acid
I	A(Amperage)	Intensity

IIW		International Institute of Welding
Is	A(Amperage)	Welding Current
K		Kelvin
kW		Kilowatt
MAG		Metal Active Gas
MIG		Metal Inert Gas
Min		Minute
ms		Micro second
N ₂		Nitrogen
O ₂		Oxygen
ODPP		One Drop Per Pulse
P	Watt	Power
PA		Flat (Weld flat joint at 45 degrees)
PB		Fillet Weld in Horizontal Position
P-GMAW		Pulsed GMAW
RMD		Regulated Metal Deposition
SCR		Steel Catenary Riser
S355MC		Thermo-mechanically rolled steel, yield strength 355 MPa
SAW		Submerged Arc Welding
SMA		Shielded Metal Arc
STT		Surface Tension Transfer
TIG		Tungsten Inert Gas
T.I.M.E		Transferred Ionized Molten Energy
TMCP		Thermo-mechanical Controlled Process
U	V(voltage)	Voltage
V		Voltage
VP-GMAW		Variable Polarity GMAW
VT		Visual Test
WF		Widmanstätten Ferrite
WM		Weld Metal
WPS		Welding Procedure Specification
Wfs	m/min	Wire feed speed
Ws	cm/min	Welding speed
WZ		Weld Zone

BACKGROUND

The basic concept of GMAW or MIG/MAG was introduced in the 1920's but the process did not become commercially available until 1948. At first, it was considered to be, fundamentally, a high-current density, small diameter, bare metal electrode process using an inert gas for arc shielding. The primary application of this process was for welding aluminium. As a result, the term MIG (Metal Inert Gas) was used and this is still a common reference for the process. Subsequent process developments included operation at low-current densities and pulsed direct current, application to a broader range of materials, and the use of reactive gases (particularly CO₂) and other gas mixtures. This latter development has led to formal acceptance of the term gas metal arc welding (GMAW) for the process because both inert and reactive gases are now used. [1]

There are two operating modes of GMAW; semiautomatic and automatic modes. With GMAW, all commercially important metals such as carbon steel, high-strength low alloy steel, stainless steel, aluminium, copper, titanium and nickel alloys can be welded in all positions by choosing the appropriate shielding gas, electrode, joint design and welding variables.

Interest in welding processes providing high melting rates has increased considerably in recent times. A high melting rate means higher productivity and, consequently, lower costs of production, which is most certainly of interest to any industry. A higher melting rate involves not only a larger quantity of filler material melted, but also higher energy input to the weld, which may have unfavourable effects on mechanical properties. In high-productivity welding, it is necessary to be cautious and take into account the chemical composition and mechanical properties of the materials treated.

In the literature and in practice, numerous methods exist for increasing productivity in arc welding. First, consumable electrodes such as solid wire and

cored wire were used as a way to improve welding productivity and deposition rates. In the 1970s, when robotic welding was first adopted, productivity was improved by an increase in the arc time factor. The welding process was often the same as used earlier for manual welding. In the 1990s, improved methods were introduced and developed, especially mechanised welding. The first improvement was single wire, and later double wire was used. The latest advancement is the use of a laser-hybrid process, as a combination of the laser and GMAW processes. [2]

TABLE OF CONTENTS

ABSTRACT	ii
ACKNOWLEDGEMENT.....	iv
LIST OF SYMBOLS AND ABBREVIATIONS	v
BACKGROUND	vii
LIST OF FIGURES	xiii
LIST OF TABLES	xvi
1 INTRODUCTION.....	1
1.1 The objective of the work.....	2
1.2 The limits of the work.....	2
2 CONVENTIONAL GMAW.....	4
2.1 The process principle	4
2.2 Arc characteristics.....	5
2.3 Heat input to the weld	8
2.4 Heat flow during welding.....	9
2.5 Forces acting during metal transfer	10
2.6 Effect of shielding gas on the drop transfer	13
2.7 Classification of different types of arc.....	14
2.7.1 Pulsed arc	15
2.7.2 Spray arc	16
2.7.3 Short arc.....	16
2.8 Metal transfer mechanism	17
2.9 Welding parameters	21
2.9.1 Current	21
2.9.2 Voltage.....	25

2.9.3 Inductance	25
2.9.4 Welding Speed	26
2.9.5 Electrode Extension.....	27
2.9.6 Shielding Gas	29
2.9.7 Gas flow rate	31
2.9.8 Electrode Diameter.....	32
3 HIGH ARC ENERGY	34
3.1 High current short circuiting arc.....	34
3.2 High current spray arc.....	36
3.3 High arc energy effect on the joint properties	38
4 ADAPTIVE PULSED GMAW WELDING PROCESSES.....	44
4.1 Modified short arc GMAW methods	45
4.2 Modified pulsed GMAW methods	47
4.2.1 Synergic control	48
4.2.2 Self-regulating control.....	49
4.2.3 Dual-pulse	49
4.2.4 AC pulse	50
4.3 Mechanically assisted metal transfer GMAW	52
4.4 Combination of waveform and reversal electrode motion control.....	53
4.5 Combination GMAW metal transfer mode.....	55
4.6 Determination of heat input with complex waveform	56
5 COMPARISON BETWEEN CONVENTIONAL AND ADAPTIVE GMAW .	58
6 ADAPTIVE GMAW PROCESS: WISEROOT™, WISEFUSION™ AND WISEPENETRATION™	61
6.1 WiseRoot™	61
6.2 WiseThin™	63

6.3	WisePenetration™	63
6.4	WiseFusion™ function	65
7	EXPERIMENTS	67
7.1	Usability of the process	67
7.2	Materials	68
7.2.1	Base metals	68
7.2.2	Filler metal	70
7.2.3	Shielding gas	71
7.3	Experimental set-up	71
7.4	Experimental Procedure	72
7.4.1	Sample preparation	72
7.4.2	Visual inspection of the specimens	73
7.4.3	Metallographic specimens preparation	74
7.4.4	Vickers hardness test	74
7.4.5	Bead penetration measurement	75
7.4.6	Dilution analysis	76
8	RESULTS AND DISCUSSION	77
8.1	Heat input	77
8.2	Visual inspection of the weld	78
8.3	Macro-sections analysis	80
8.4	Dilution analysis	86
8.5	Microstructure analysis	88
8.6	Vickers hardness test	96
9	CONCLUSIONS	99
10	FURTHER RESEARCH	102
11	SUMMARY	103

REFERENCES	105
APPENDICES	118

LIST OF FIGURES

Figure 1. GMAW process equipment: (1) Reel or drum, (2) Drive rollers (3) Flexible conduit, (4) Hose package, (5) Welding gun, (6) Power source [2,9]....	5
Figure 2. Schematic diagram, static characteristic curve of the arc [13]	7
Figure 3. Temperature distribution in MIG welding of aluminum at 250 A without regard to the influence of metal vapour [14]	7
Figure 4. Arc potential (U) distribution between the electrode and the workpiece [2]	8
Figure 5. Schematic of temperature-time traces for three points located along a line perpendicular to a weld during passage of a moving welding heat source for 1018 steel [16].....	10
Figure 6. Forces acting during droplet transfer [20]	12
Figure 7. Forces acting on the drop at a steel electrode tip (argon plasma velocity: 100 m/s) [21].....	13
Figure 8. Distribution of temperature and current density in the arc and the forces involved with different shielding gases [23].....	14
Figure 9. Arc types and their working ranges, solid wire d=1.2 mm shielding gas: argon-rich mixtures [24]	15
Figure 10. Pulsed arc waveform and droplet detachment sequences [25]	16
Figure 11. Transfer by spray arc [27].....	16
Figure 12. Voltage and current short circuit metal transfer mode [25].....	17
Figure 13. Penetration vs welding current for 80 cm/min with different voltages[32]	22
Figure 14. Penetration characteristics of DCEP and DCEN arcs [10].....	22
Figure 15. Relationship between weld bead geometry and EN ratio [34]	24
Figure 16. Penetration vs arc voltage graph for 80 cm/min welding speed [32].....	25
Figure 17. Relationship between reactor inductance (L) value and welding current waveform [35].....	26
Figure 18. Penetration vs welding speed graph for 22V arc voltage [32].....	27
Figure 19. Contact Tip-to-Work Distance (CTWD) [6]	28

Figure 20. Melting rate as a function of welding current and wire extension length with 1.6 mm solid wire in a TIME welding gas mixture [36]	29
Figure 21. Electric (a) and thermal conductivity (b) of shielding gases at pressure of 1 atm [38, 39].....	30
Figure 22. Evolution of the penetration with different shielding gas mixtures, with short-circuits (S.C) and spray (S) transfer [41].....	31
Figure 23. Effect of gas flow rate on average weld bead penetration [42]	32
Figure 24. Comparison of melting rates in welding with a covered electrode, a solid wire and a cored wire, respectively [43].....	33
Figure 25. Percentage surface fraction of non-metallic inclusions in the weld metals [48]	40
Figure 26. Fractions of different forms of ferrite in recrystallised structures of weld metals. [48]	41
Figure 27. Fracture energy in Charpy V-notch tests at -20 °C for weld metals produced in shields of the investigated gases at different intensity of current [48]	42
Figure 28. Configuration of digitally-controlled arc welding machine [59].....	45
Figure 29. Setting of arc frequency by inductance, capability of control of short-circuit and arcing time [35].....	47
Figure 30. Pulse waveform of synergic control [72]	49
Figure 31. Pulse waveform of self-regulating control [72]	49
Figure 32. Dual-pulsed current waveform [77].....	50
Figure 33. Current waveform for AC pulsed GMA welding [80].....	51
Figure 34. Waveform current (Is) and voltage (Us) with electrode alternative feeding motion (Wfs) [90].....	54
Figure 35. Process course, each two positive (EP) and negative (EN) Advanced CMT cycles [88]	55
Figure 36. Graph comparing calculated heat input to actual heat input for P-GMAW [100]	57
Figure 37. Current waveform of WiseRoot compared with a conventional current waveform [106].....	61
Figure 38. Welding current changes with the stick-out length [107].....	65

Figure 39. Pulse sequence where the filler droplet short-circuits before detaching [107]	66
Figure 40. Welding equipment and setting.....	72
Figure 41. Welding design and electrode orientation in horizontal position	73
Figure 42. Weld profile description	75
Figure 43. Profile repartition of hardness test	75
Figure 44. Bead penetration measurement	76
Figure 45. Filler metal dilution [114].....	76
Figure 46. Increasing gap values bead appearance of the Synergic Pulsed GMAW process welded specimen.....	78
Figure 47. Increasing gap values bead appearance of the Synergic GMAW process welded specimen.	79
Figure 48. Increasing gap values sample using WiseFusion™, 35% short circuit... 79	
Figure 49. Increasing gap values sample using WiseFusion™, 50% short circuit... 80	
Figure 50. Increasing gap values sample using WiseFusion™, 20% short circuit... 80	
Figure 51. Cross section dilution analysis at 0 air gap (a) Synergic pulsed GMAW (b) Default curve 35% short circuit	81
Figure 52. Cross section dilution analysis at 1 mm gap (a) Synergic Pulsed GMAW (b) WiseFusion 35% short circuit, (c) 50% , (d) 20% and (e) Synergic GMAW83	
Figure 53. Cross section dilution analysis at 2 mm gap (a) Synergic Pulsed GMAW (b) WiseFusion 35% short circuit, (c) 50%, (d) 20% and (e) Synergic GMAW 85	
Figure 54. Microstructure of specimen P1.1 Base metal S 355 MC.....	90
Figure 55. Microstructure of specimen P1.1 (a) HAZ-Base and (b) Weld	91
Figure 56. Microstructure of specimen P2.1 (a) HAZ-Base and (b) Weld	92
Figure 57. Microstructure of specimen P3.1 (a) HAZ-Base and (b) Weld	93
Figure 58. Microstructure of specimen P4.1 (a) HAZ-Base and (b) Weld	94
Figure 59. Microstructure of specimen P5.1 (a) HAZ-Base and (b) Weld	95
Figure 60. Hardness test results comparison between specimen P1.0 and P2.0.....	96
Figure 61. Hardness test results comparison P1.1, P2.1, P3.1, P4.1 and P5.1	97
Figure 62. Hardness test results comparison P1.2, P2.2, P3.2, P4.2 and P5.2	98

LIST OF TABLES

Table 1. Transfer heat efficiency in GMAW process [11].....	9
Table 2. IIW Classification of metal transfer [28].....	19
Table 3. Classification of controlled transfer mode [30]	20
Table 4. Classification for extended operating mode techniques [30].....	20
Table 5. High current short circuit application and benefits	36
Table 6 High current spray - application and benefits	37
Table 7. Welding parameters example high energy GMAW [48].....	39
Table 8. Comparison between conventional and adaptive GMAW process [102]...	59
Table 9. Chemical properties of S355 MC [109].....	69
Table 10. Tensile properties transverse of S355 MC [109].....	69
Table 11. Chemical properties of the consumable electrode [111]	70
Table 12. Welding experiment parameters.....	77
Table 13. Specimen designation	81
Table 14. Weld dimension at 0 mm gap.....	82
Table 15. Weld dimension at 1 mm gap.....	84
Table 16. Weld dimension at 2 mm gap.....	86
Table 17. Dilution comparison of P1.0 and P2.0.....	87
Table 18. Dilution comparison at 1 mm air gap	87
Table 19. Dilution comparison at 2 mm air gap	88

1 INTRODUCTION

The development of new materials creates new challenges for the welding processes used and thereby generates special requirements, such as, welding thin sheet plate, zinc coated plate, stainless steel and high strength steel and dissimilar. The new requirements have in the past decade been subject to particular attention, which has led to major innovations in the field of welding in general and GMAW in particular. GMAW has benefited from new technological advances like any other field of industry. Developments in electronics have enabled the creation of new components with a higher feedback response rate [3, 4]. Digitalisation and the inverter are significant advances for arc welding because they result in better control of the arc and transmission of metal as consequence of a more precise and strict monitoring of the voltage and current waveform. In addition, information sensed at the electrode tip and the CTWD are fully integrated in the algorithm [5]. It is possible today to control by algorithm; the current, voltage, displacement of the electrode and the flow of shielding gas. New methods of welding have demonstrated their successful application in welding thin sheet plate, dissimilar joint and metal sensitive to heat input. It should be noted that these new processes are used more in the conventional voltage range, characterised by a current lower than 200 A and demonstrate significant reduction in heat input, sparks and smoke.

A major trend today, the development of adaptive GMAW to higher current and voltage, offers advantages such as high deposition rate and welding speed and reduces the excessive heat that generates distortion. Utilization of adaptive GMAW is currently limited to materials sensitive to heat and to thin sheet metal. Adaptive GMAW provides an improvement in productivity but its use is limited when welding metals of high thicknesses. Using the arc welding process on larger thicknesses requires sufficient energy to eliminate the risk of defects such as insufficient penetration, and lack of fusion between passes and edges of the workpiece. However, when using excessive high energy the intermetallic is affected and results in poor quality of physical properties. Conventional GMAW

process at high levels has been subjected to a high level of sparks, resulting in extra cost for cleaning, noise and smoke, and an unstable process that affects the chemical and physical characteristics of the welded joint.

This study is carried out to identify conditions permitting adoption of new arc welding methods within the range of high-power energy, which will enhance the usability of adaptive GMAW, and to assess the limits and benefits. Furthermore, the results gathered will form the basis for experiments to test the usability of an adaptive pulsed GMAW and establish optimal applications. Experiments will define necessary settings for the best results and compare the effectiveness of droplet detachments control approach to previous ones.

1.1 The objective of the work

The objective of this research is to investigate the applications and benefits of adaptive pulsed GMAW. The adaptive GMAW process is reviewed and applications in the high energy range are identified. In addition, Synergic GMAW, Synergic Pulsed GMAW and WiserFusionTM are assessed for structural plate steel S355MC. In these experiments, the consumable electrode is G3Si1 and the binary shielding gas mixture 82 % Ar + 18 % CO₂. A single pass on a T-joint (fillet weld), at horizontal position (PB), is performed on an increasing gap from 0 to 2.5 mm. Results on the appearance of the bead and the mechanical and microstructure of the weld joint are analysed and compared. The power source FastMIG 450 from Kemppi is used to perform the experiments.

1.2 The limits of the work

The work is limited to adaptive GMAW processes based on current and voltage waveform control, adaptive by wire feeding control, adaptive by combined current and wire feeding control, adaptive by pulsed control, and adaptive by short arc frequency. The study focuses on pulsed GMAW processes using a single consumable electrode. Therefore, processes operating with multiple filler

wire, such as TAMDEM, or hybrid processes, like those combining laser or TIG with GMAW, are not mentioned in this thesis.

2 CONVENTIONAL GMAW

This section considers the conventional GMAW process, which refers to basic control of metal transfer. An understanding of the conventional GMAW process enables, later in this study, comparison with the adaptive GMAW processes. Firstly, the principle of the process is presented and illustrated with basic components of the welding equipment. Next, the notion of the arc characteristic is presented to show in which circumstances the arc generates the necessary temperature to melt the electrode and to demonstrate the different forces involved in producing metal deposition. Finally, the metal transfer mechanism and its classification are presented.

2.1 The process principle

The gas metal arc welding process (GMAW) is an electric arc welding process that is distinguished from others by a continuously fed consumable electrode. The welding process to complete the junction of two materials needs a minimum equipment set-up as shown in Figure 1. While initial settings are required to be defined by the operator, the equipment provides for automatic self-regulation of the electrical characteristics of the arc. The welding operation is performed either manually by the welder for semiautomatic controls, where the operations are the gun positioning and travel speed and direction, or with full automatic control.

The main role of the power source is to provide the current and voltage required to maintain the arc and the transfer mechanism of the molten metal from the electrode to the weld pool. A shielding gas provider device supplies protection and regulates the flow and mixing quantities indicated for the process. A wire unit designed to supply the electrode, and whose role is to feed the electrode through the torch at a precise speed, is an integral part of the equipment. The arc length and the current (wire feed speed) are automatically maintained by the equipment and appropriate settings. The torch is used to properly position the electrode and control the flow of gas to the work area. An anode or cathode,

depending on the state of the electrode required, is set to the workpiece, in order to establish an arc between the electrode and the workpiece. [6-8]

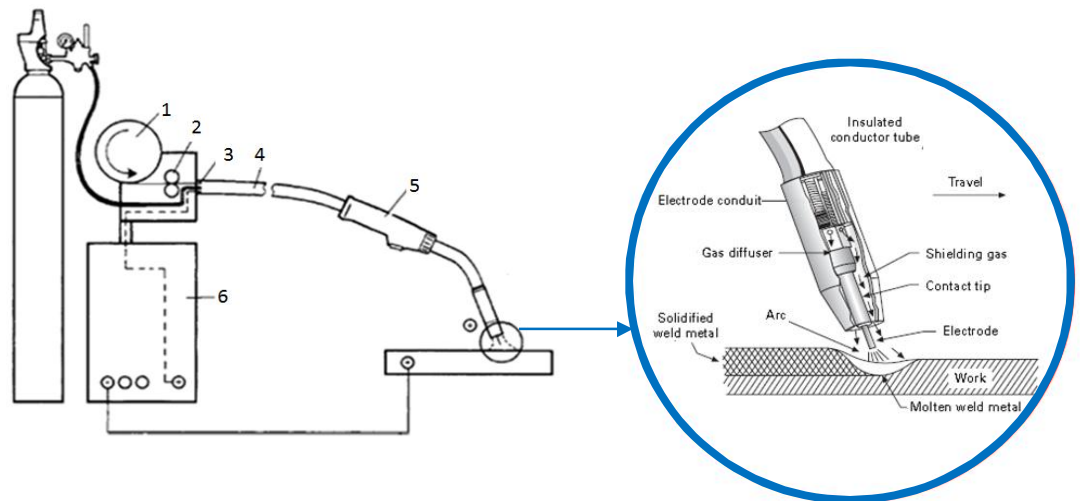


Figure 1. GMAW process equipment: (1) Reel or drum, (2) Drive rollers (3) Flexible conduit, (4) Hose package, (5) Welding gun, (6) Power source [2, 9]

Knowledge of variable parameters and their control is essential to achieve welds with satisfactory quality standards. The variables depend on each other; therefore, changing one consequently affects others. Skill and experience are needed to select optimum settings for each application. The optimum values are affected by the type of base metal, electrode composition, welding position, and quality requirements. Thus, there is no single set of parameters that gives optimum results in every case. [6]

2.2 Arc characteristics

An arc is a column of ionised gas (plasma) created by the passage of an electric current between two electrodes. The electrodes have to be quite close together (less than 6 mm) and the gas in the space between them has to readily ionise for a stable arc to be created. Unstable arcs extinguish easily.

Although the arc can be considered as an electrical resistance or impedance, it only approximates Ohm's law at higher current. At low current, the arc voltage increases as the current is reduced. Welding arcs have a power of the order of 0.6 to 36 kW. This energy creates a column of hot plasma (ionised gas) which is quite stiff because of electromagnetic forces. It is these electromagnetic forces that cause transfer of material from the electrode to the workpiece, mould and shape the weld pool, and even in some cases hold the molten weld pool in place. The temperature of the arc plasma reaches approximately 6000°C in the GMAW process [10]. The arc is characterised in terms of its properties: stability, degree of ionisation, and stiffness. The main factors influencing arc properties are shape of the anode and cathode, emissivity of the cathode, composition of the ionised gas/vapour mixture, and electrode material. [11]

It is usual for the arc to be moved along the joint at a steady travel speed. The arc must generate enough energy to fuse the base and filler material. If it is moved too quickly, fusion does not occur. Even if fusion occurs, the weld bead may cool rapidly and crack. If it is moved too slowly the weld pool is large and may be uncontrollable, or other metallurgical problems may occur. In structural steel, excessively high arc energy may produce welds with low ductility and toughness. In quenched and tempered steel, weld strength may be low because of the extension of the higher heat affected zone (HAZ) and longer cooling rate time, which affect the microstructure formation and grain size. [12]

The relationship between voltage and current with a constant length of the arc is known as the static characteristic. The characteristic curve in GMAW is a function of arc length, gas composition and protective material electrode. In the diagram shown in Figure 2 the characteristic curve is divided into two parts, the Ayrton and Ohm. Only the Ohm part is used for welding because the Ayrton area is unstable. The curves I_1 and I_2 represent different arc lengths. [13]

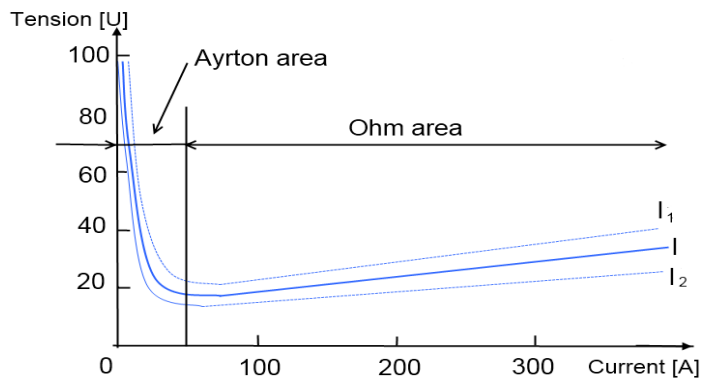


Figure 2. Schematic diagram, static characteristic curve of the arc [13]

The temperature profile of the electric arc areas in the GMAW process has different layers of temperatures and is dependent on the composition of the shielding gas used. The maximum temperature in the centre of the arc can reach 20.000K, as shown in Figure 3. [14]

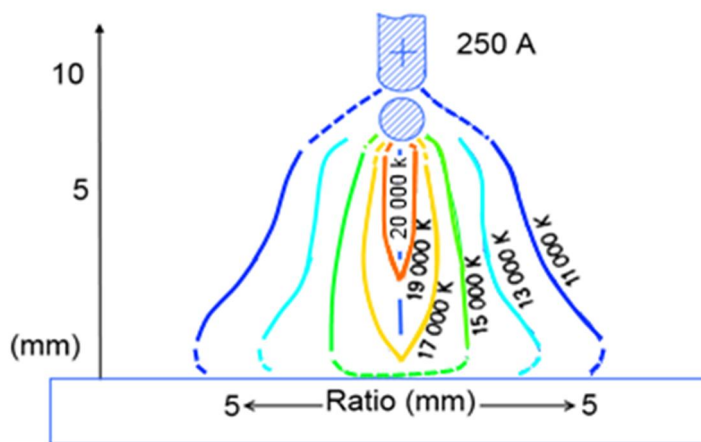


Figure 3. Temperature distribution in MIG welding of aluminum at 250 A without regard to the influence of metal vapour [14]

The arc can be divided into the anode region, cathode region and the arc column. Normally the wire electrode is the anode, the positive polarity, and the workpiece the cathode, the negative polarity (Fig. 4). In the arc, heat losses by heat conduction appear close to the surface of the wire electrode and the workpiece. These anode and cathode regions of the arc therefore have considerable voltage

drops (see Fig. 4). In spite of their small size, more than half of the total voltage drop is found in this area. Thermal balance is achieved because the heat that is conducted into the electrode and the joint is replaced by electric energy. [2]

Heat generated in the anode region melts the wire and heats the melted drop. In the same way, heat generated in the cathode area will heat and melt the joint faces.

As the anode voltage can be considered as a constant voltage drop, the heating effect is proportional to the current. The melting rate is thereby also proportional to the current and, at least in theory, independent of the voltage setting. [2]

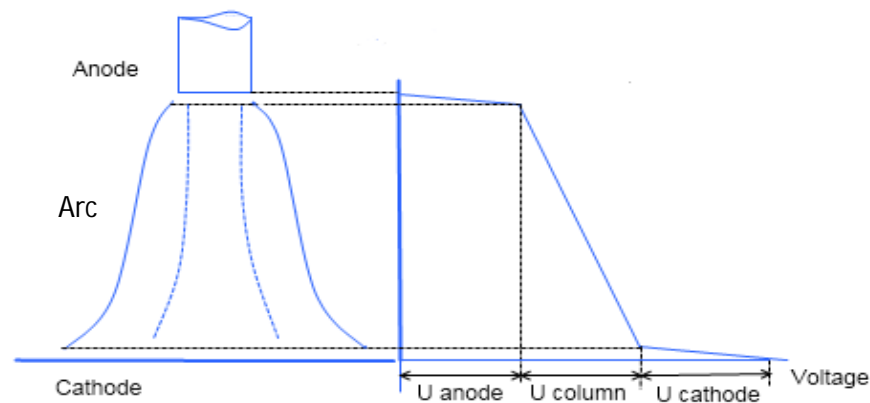


Figure 4. Arc potential (U) distribution between the electrode and the workpiece [2]

2.3 Heat input to the weld

When energy or heat is transferred from a source to the workpiece to produce a weld, the transfer is not perfect. There are many opportunities for energy to be lost between the welding source and the workpiece in fusion welding processes. There are also opportunities for loss within the workpiece. There can be radiant losses in the form of infrared, visible and/or ultraviolet light, convection losses to the air or shielding gases, and conduction losses to filler wires or the mass of the workpiece surrounding the region of energy deposition. There can also be losses of heat with loss of mass in the form of metal vapour or molten metal, called spatter. The effects of possible loss of energy between the source and the workpiece, or within

the workpiece, depend on the characteristics of the specific welding process, the workpiece, and the mode of energy deposition. The heat efficiency commonly found for GMAW processes is 0.8; however, the value can be specific for each metal transfer mode, as illustrated in Table 1. [11]

Table 1. Transfer heat efficiency in GMAW process [11]

Metal transfer mode	Transfer heat efficiency
Globular or short-arc transfer mode	0.60-0.75
Spray transfer mode	0.65-0.85

The sum of all losses determines the energy or heat transfer efficiency of the process. This transfer efficiency is expressed as a fraction ranging from 0.0 to 1.0 that lowers the net energy or heat input according to a modified form of Eq. (1), to give: [11]

$$Q = \frac{60 \times U \times I}{1000 \times V} \times \eta \quad (1) [11]$$

Where

Q : Heat input (kJ/mm)

U : Welding voltage (volts)

I : Welding current (amps)

V : Travel speed (mm/min)

η : Efficiency factor for GMAW is 0.8

2.4 Heat flow during welding

The temperature flow depends significantly on the location of the heating source. The variation of temperature with time, often referred to as the thermal cycle, affects the microstructure, residual stresses, and the extent of distortions in the weldment. Control of these temperature fields and cooling rates is essential to

ensure sound welds with the desired fusion-zone geometry, chemical composition, and microstructure, as well as with low residual stress and distortion [15]. The temperature-time curves in Figure 5 are situated respectively to the temperature level, as the distance from the weld centerline increases. The maximum temperature decreases with increasing distance from the source, more or less abruptly, depending on the temperature gradient that characterizes the particular process, and the procedure temperature returns asymptotically to the ambient temperature. [11]

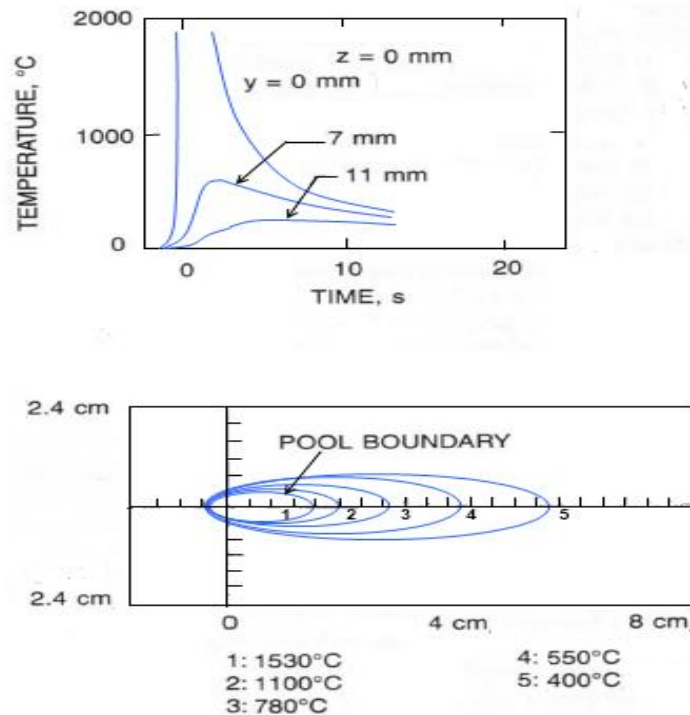


Figure 5. Schematic of temperature-time traces for three points located along a line perpendicular to a weld during passage of a moving welding heat source for 1018 steel [16]

2.5 Forces acting during metal transfer

A drop of the metal melt, formed at the electrode tip, is simultaneously exposed to several forces, as shown in Figure 6 and 7, the presence and ratio of which are responsible for the drop weight and frequency of drop transfer into the weld pool.

The main forces determining the processes of drop formation and transfer in arc welding are the gravitational force (F_g), surface tension force (F_s), electromagnetic force (F_m), and force of reactive pressure of the vapours. It should be noted that the magnitude and direction of these forces might vary with changes in the conditions and modes of welding. Depending on the welding process used, all of these forces or just some of them may influence the transfer of filler wire metal. In order to understand better the role of each of these forces, the action of these forces can be considered separately. [17]

Surface tension forces (F_s) are the major forces that keep the drop at the electrode tip. The dimensions of the electrode drops always increase with the increase in these forces. Most of the published reports state that the surface tension forces contain the electrode metal drop at the electrode tip during the entire process of its growth and detachment. However, data from some researchers [18] indicate that in arc welding processes, the surface tension forces change the direction of their action at the drop-detachment stage, thus promoting the breaking up of a liquid-metal bridge, and may even impart [19] additional velocity to the drop transferring into the weld pool. [17]

In arc welding processes, the electromagnetic force (F_m) has a considerable influence on the electrode-metal transfer. The occurrence of this force is due to the interaction of the conductor (through which the electric current passes) and the magnetic field induced by this current. Electrode-metal transfer is greatly dependent on the magnitude of the reactive forces. These forces arise as a result of evaporation of a part of the metal from the drop surface and the flow rate of gases as a result of chemical interaction of the metal melt with the slag or the gas. [17]

In addition to the above forces, the electrode-metal transfer may also be influenced by aerodynamic forces, for example the plasma suction force (F_{em}). This aerodynamic force only occurs in those cases in which powerful plasma (gas) flows arise.

Thus, the magnitude and action of the forces affecting the transfer of electrode metal depend on the chosen fusion welding process, the welding modes, the properties of the base and electrode materials, the composition of the slag and the gaseous medium. Therefore, the precise role of each individual force in the process of electrode-metal transfer is different and will be specific to each concrete case. [17]

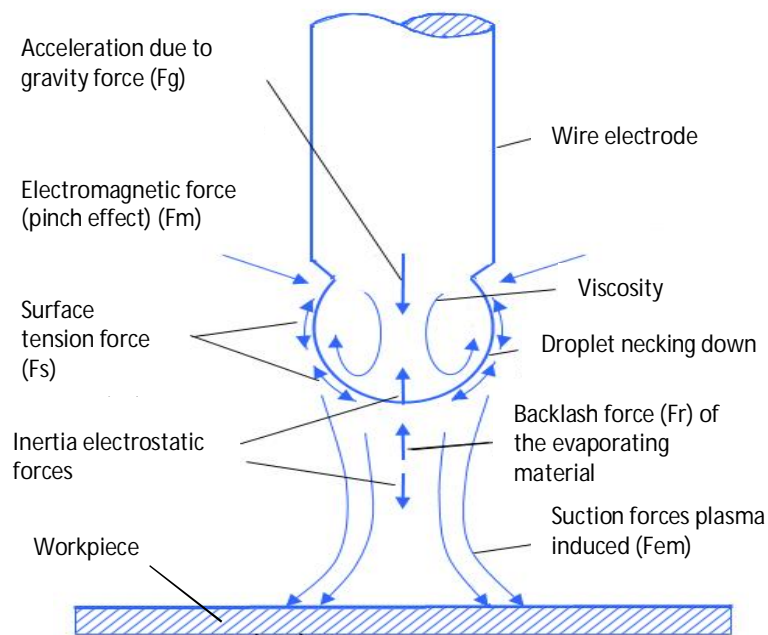


Figure 6. Forces acting during droplet transfer [20]

The effect of velocity differences in the shielding gas is not significant and decreases as the current increases. This is because the influence of the electrode-magnetic force (F_m) becomes dominant as the current increases (Figure 7) [21].

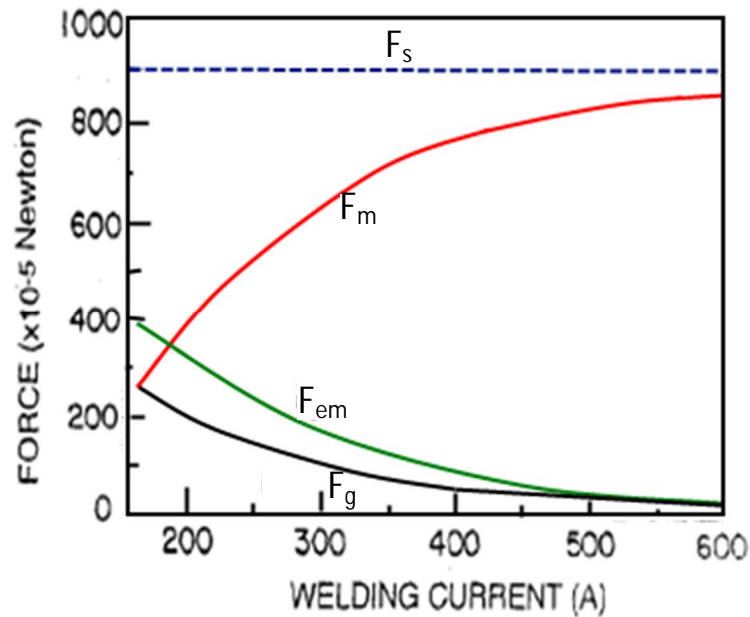


Figure 7. Forces acting on the drop at a steel electrode tip (argon plasma velocity: 100 m/s) [21]

2.6 Effect of shielding gas on the drop transfer

The type of material transfer mode strongly depends on the type of shielding gas used during the GMAW process. The shielding gas affects the intensity of the forces acting upon the droplet. In consumable electrode welding, different gases can have quite different effects on the mode of molten metal transfer. Helium, for example, does not usually produce an axial spray, regardless of current level or polarity; transfer remains globular. Spray transfer is also difficult to achieve with active gases such as nitrogen or carbon-dioxide. The harsh globular transfer and spatter associated with carbon dioxide as a shielding gas can be offset by adding argon to stabilize the arc and improve transfer. [11]

Small additions of oxygen or carbon dioxide are commonly added to argon to stabilize the arc, lower or raise the globular-to-spray transition current, respectively, and improve wetting and bead shape, especially for welding steel. [11]

In argon, the current-carrying arc core is wider and envelops the wire electrode end, as in Figure 8. This generates electromagnetic forces which bring about the detachment of the liquid electrode material. This so-called “pinch effect” causes a metal transfer in small drops. The pointed shape of the arc attachment in carbon dioxide produces a reverse-direction force component, that is, the molten metal is pushed up until gravity has overcome that force component and material transfer in the form of very coarse drops appears. [22]

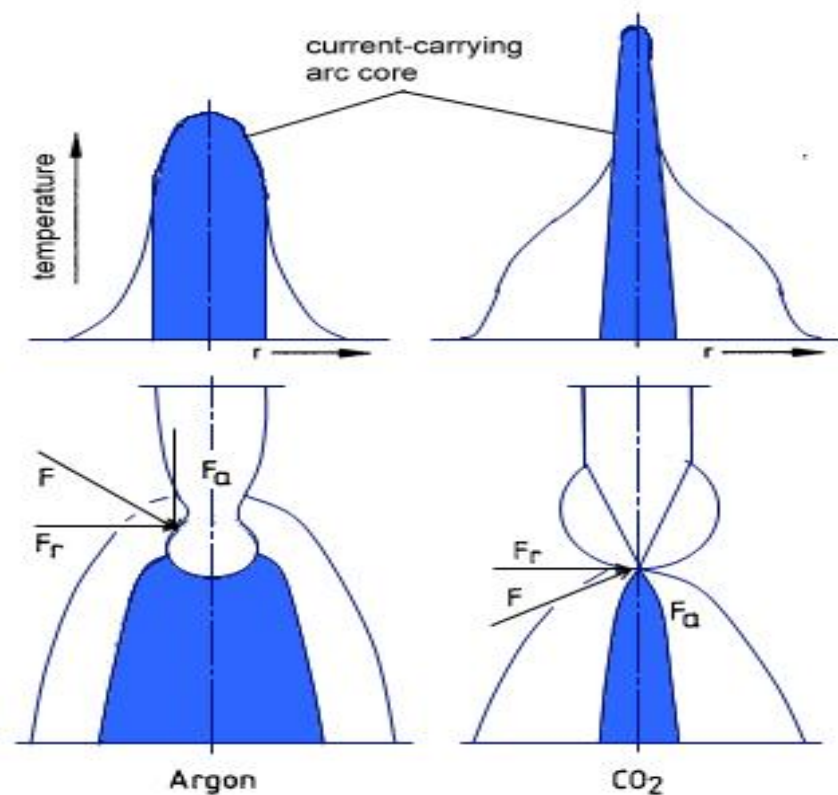


Figure 8. Distribution of temperature and current density in the arc and the forces involved with different shielding gases [23]

2.7 Classification of different types of arc

In the GMAW process, different types of arc can be generated, depending on the current, voltage and shielding gas input. Figure 9 shows the different types of arc generated based on the power loaded. In general, three main groups of arc can be distinguished; pulsed arc, spray arc and short circuiting arc. The peak current of

pulsed arc is located at the same area as conventional spray arc. This sub-section presents basic information about these categories, which will later be useful in understanding of the metal transfer mechanism.

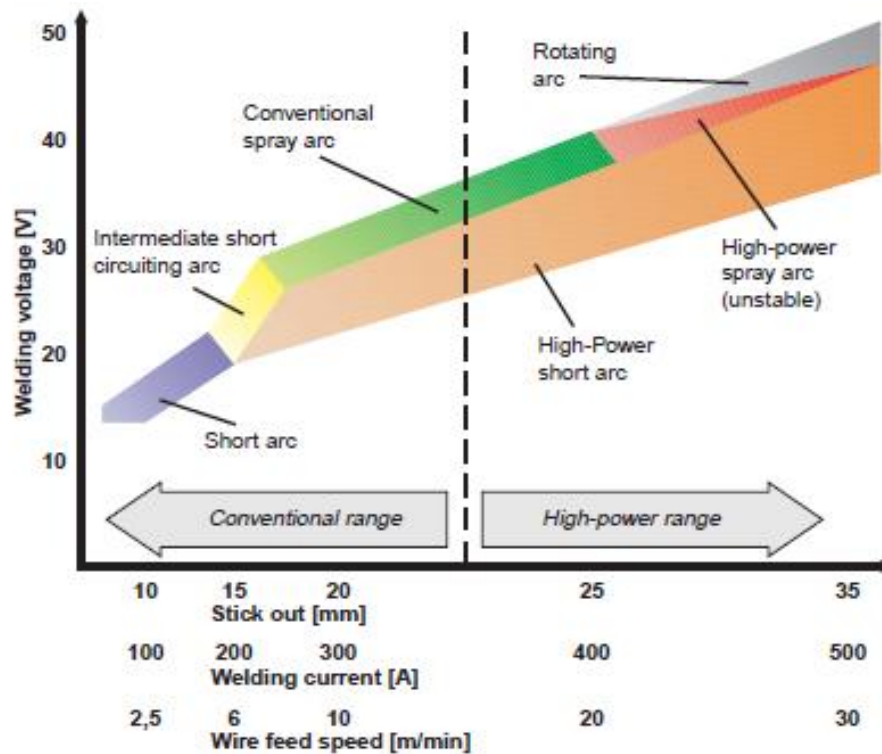


Figure 9. Arc types and their working ranges, solid wire $d=1.2$ mm shielding gas: argon-rich mixtures [24]

2.7.1 Pulsed arc

A pulsed arc occurs at high current and the resulting magnetic forces are directed downwards, which helps the droplet to be released from the surface tension at the electrode. The droplet transfer is characterised by a stream of small droplets. The current waveform consists of a background current that sustains the arc burning period and a peak current for the transfer of the metal (see Figure 10). Although the current amplitude in each pulse is high, the average current - and thus the heat input to the joint - can be kept low.

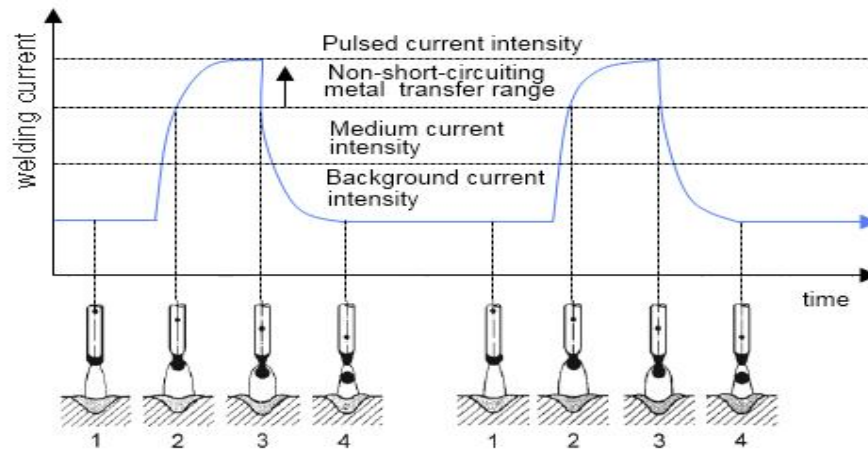


Figure 10. Pulsed arc waveform and droplet detachment sequences [25]

2.7.2 Spray arc

Spray transfer is the transfer mode with a high-speed wire feed and high voltage. The transfer of the metal occurs without formation of short circuits, with much smaller droplets than the diameter of the wire. Figure 11 shows schematically the transfer with very fine droplets. The diagrams of voltage and current are very stable in this process. Because of the high energy in the process, the arc is applicable for spray welding of thick plates and flat (PA) and horizontal (PB) positions [26].

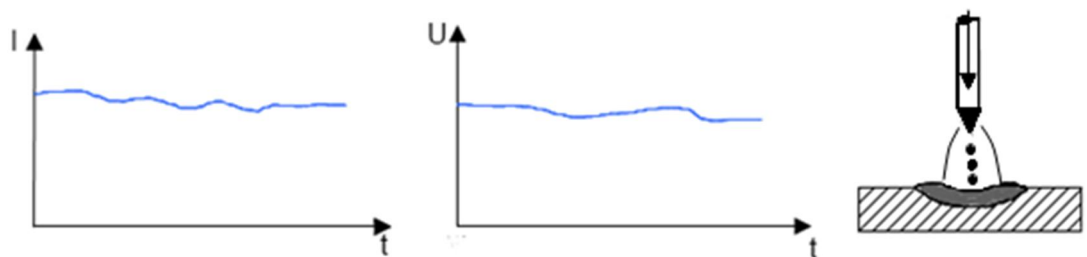


Figure 11. Transfer by spray arc [27]

2.7.3 Short arc

The short arc is characterised by a period of burn arc and a short circuit when the bridge occurs between the electrode and weld pool during molten metal transfer.

Figure 12 shows current and voltage waveform and droplet detachment sequences seen with a high speed camera [1, 2, 6]. The magnetic forces are smaller and are directed upwards. With the short circuiting arc transfer, the droplet hanging at the tip of the electrode tends to increase in size and the process runs the risk of being unstable. A way to overcome this problem is to keep the arc length so short that the droplets dip into the pool before they have grown too much. Surface tension will then start the transfer of the melted material and the tail of the droplet will be constricted by the magnetic forces, the so-called "pinch effect". No metal is transferred in the form of free droplets across the arc gap. The stability of short circuiting transfer is very sensitive to variations in the shielding gas, the chemical composition of the electrode and the properties of the power source and wire feed system. [16]

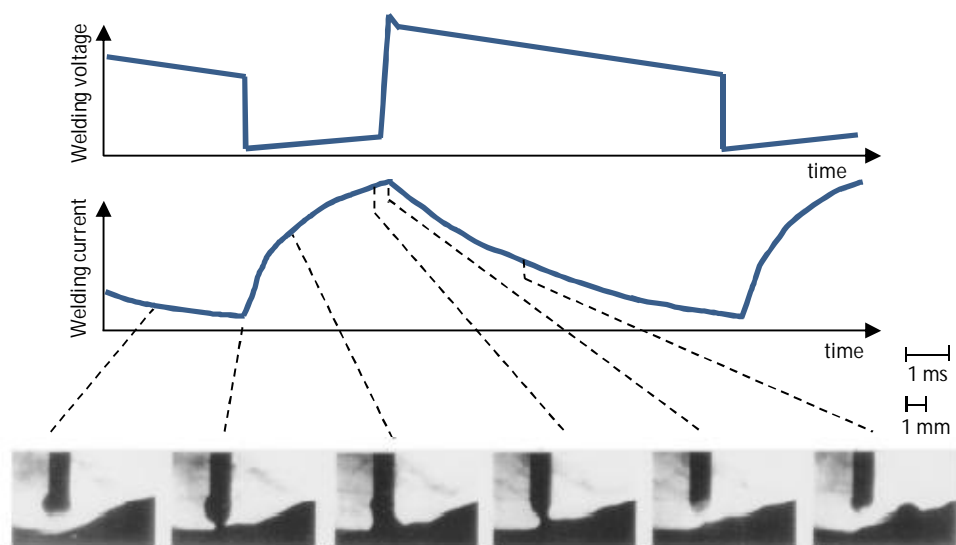


Figure 12. Voltage and current short circuit metal transfer mode [25]

2.8 Metal transfer mechanism

The first formal classification of metal transfer modes, given in Table 2, was proposed during the XII Commission of the International Institute of Welding (IIW) in 1976 by Anon [28]. Metal transfer modes were divided into three main groups; free flight, bridging and slag protected transfer. Free flight occurs when

molten metal detaches from the electrode and moves toward the pool through the arc plasma. The classification was based on the drop size; under the current effect, the size of drop transfer decreases when the current increases. According to J. F. Lancaster (1984) [7], drops formed at moderate current GMAW are roughly spherical and close to the wire diameter (globular transfer). At relatively high current, the tips of the electrode are reduced to a conical form, and relatively small size drops are projected to the pool (projected spray transfer). The increase in current, within the permissible range, results in smaller drop flow at a higher frequency (streaming transfer). At higher current the flow molten metal rotates and thus was classified on this basis (rotating transfer).

Other unstable transfer mechanisms were also classified based on repulsion of large drops at lower currents (repelled transfer) and explosive small drops at very high current (explosive transfer). In addition, the thermal conductivity of the material considerably affects the metal transfer; for instance, copper and aluminium alloys have higher conductivity than steel, which results in a higher deposition rate. At 200 A steel has 10 drop detachments per second and copper transfer is twice that of steel. Aluminium produces 170 drops per second. [7]

Short circuiting transfer is associated with low current and voltage according to the classification by J. F. Lancaster (1984) [7] and was characterised by the bridge transfer from the electrode tip to the weld pool. In addition, a slag transfer mode was added although this belongs to submerged arc welding (SAW) rather than GMAW process.

Table 2. IIW Classification of metal transfer [28]

Transfer Modes		Welding Process	
Free flight transfer	Globular	Drop	Low current GMA
		Repelled	CO ₂ shielded GMA
	Spray	Projected	Intermediate current GMA
		Stream	Medium current GMA
		Rotating	High current GMA
	Explosive		SMA (coated electrode)
Bridging transfer	Short-circuiting		Short arc GMA
	Bridging without interruption		Welding with filler wire addition
Slag protected transfer	Flux wall guided		SAW
	Other modes		SMA, cored wire, electroslag

Improvements in the power source over the last two decades have led to accurate control of the arc and droplet detachment. The power sources have been designed to follow a specific current and voltage waveform, as well as the motion of the wire feeder to guarantee the timing of metal transfer.

The transition zone has been one of the difficulties when setting non-bridge transfer. An investigation by J. Ma (1982) [29] provided relevant information about the transfer mechanism in the transition zone between globular and spray transfer.

By considering the early stage of changes in power source development, J. Norrish in 2003 [8] proposed a review of the definition of the metal transfer mode in GMAW. A distinction is made between three categories: (1) natural metal transfer, which refers to conventional transfer modes; (2) controlled transfer techniques, which are a group of current and waveform control methods, as well as wire feeding motion control; and (3) extended operating mode techniques, which are control techniques related to wire extension, variable polarity and any other heavy duty GMAW process new developments.

Tables 3 and 4 present the classification for controlled transfer and extended operating mode techniques, respectively, according to the classification proposed by [8] and reviewed by [30].

Table 3. Classification of controlled transfer mode [30]

Metal Transfer Modes		Welding Process
Controlled spray	Pulsed transfer	GMAW using variable frequency pulse and drop spray transfer
Controlled Short Circuiting	Current controlled dip transfer	GMAW using current controlled power source
	Controlled wire feed short circuit mode	GMAW with wire feed oscillation

Table 4. Classification for extended operating mode techniques [30]

Metal transfer modes		Application
Short circuiting GMAW	Extended stick out GMAW	High deposition short circuit transfer GMAW
	Low frequency pulsed	Pulsed mean current for gap filling
Pulsed transfer GMAW	Multi-wire	Multi-wire GMAW
	Low frequency pulsed	Modulated pulsed transfer welding of Aluminium
	Variable polarity	Welding of thin sections and single sided root runs
Spray transfer GMAW	Rotating spray	High current extended stick out
	Electrode negative	Flux cored wire or special gas mixture
Spray transfer SAW	Electrode negative	
	Extended stick out	
	AC/ variable polarity	

The technology has been improving in recent years and the power source has benefited from intelligent control, giving more flexibility to innovations in the GMAW process. Recently, Danut Iordachescu et al [31] noticed that sketch has become an important means to illustrate the metal transfer mode and this was introduced in a review of the metal transfer mode.

2.9 Welding parameters

Welding parameters affect the way the molten electrode is transferred to the workpiece, the arc stability, spatter generation, weld bead geometry and overall weld quality. The main parameters of the process are current, voltage, travel speed, electrode extension and electrode diameter, although others, such as electrode orientation, electrode composition and shielding gas, also have a direct influence on the metal transfer mechanisms. These parameters are not independent. The current and voltage, for example, are correlated; voltage depends not only on the arc length but also on the electrode extension and the shielding gas [1, 2, 6, 10, 32, 33].

2.9.1 Current

Current and voltage considerably affect the mechanism of transfer; at low current and voltage molten metal is not projected to the weld pool, the transfer occurs by short circuiting mode. When the current and voltage are relatively high, molten drop sizes are close or slightly bigger than the electrode diameter and the transfer is in globular mode. At higher current and voltage, drop sizes are smaller than the electrode and transfer occurs in spray modes.

The graphs in Figure 13 reveal that for a speed of 80 cm/min, the increase in penetration for 22 V is 2.35 mm, for 24 V it is 0.5 mm, and for 26 V the increase is 0.55mm when the current value increases from 95 A to 115 A (increase of 20 A). [32]

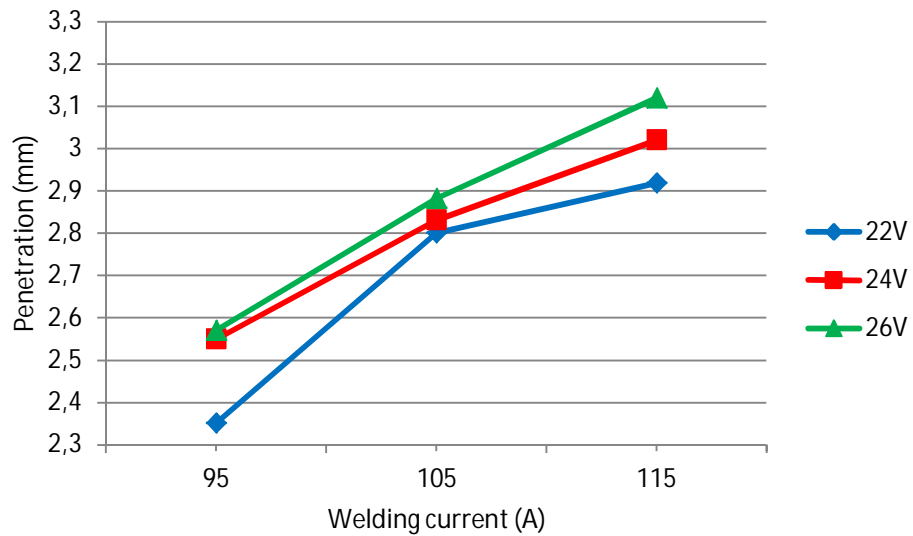


Figure 13. Penetration vs welding current for 80 cm/min with different voltages [32]

Direct current electrode positive (DCEP) is the most commonly used current in GMAW because it gives a stable electric arc, low spatter, good weld bead geometry and the greatest penetration depth. [1]

AC pulsed GMAW is welding which repeats Direct Current Electrode Positive (DCEP) and Direct Current Electrode Negative (DCEN) in a cycle based on the EN ratio. This welding has the advantages of both DCEP and DCEN (Figure 14). The occurrence of burn-through is low because the heat input is lower than that of DC pulsed GMAW. In addition, spatter hardly occurs because of ODPP (One Drop per Pulse) metal transfer. [33]

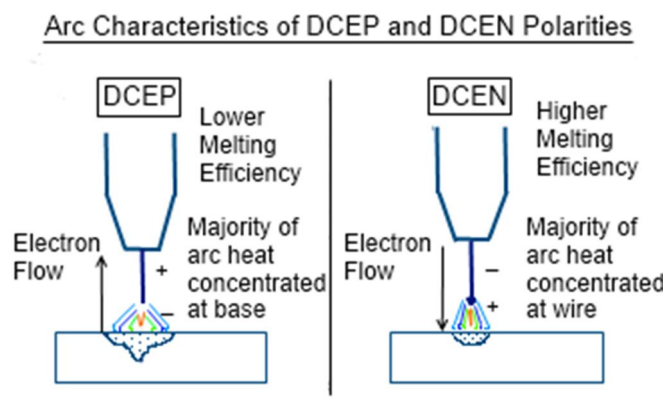
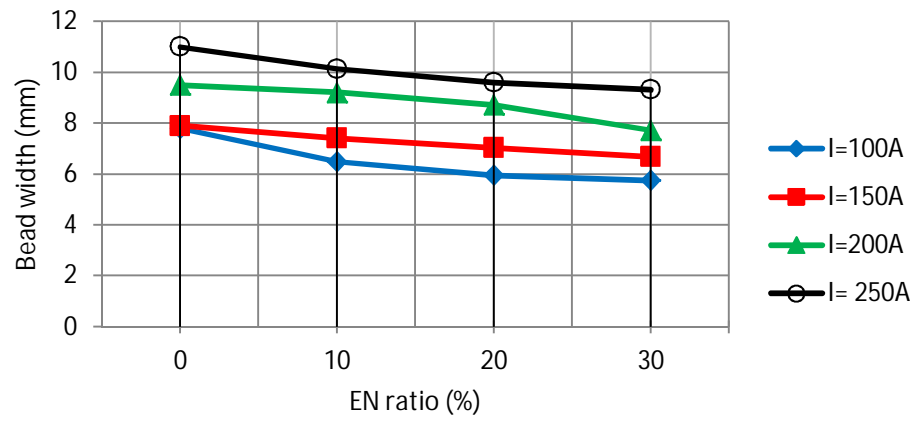
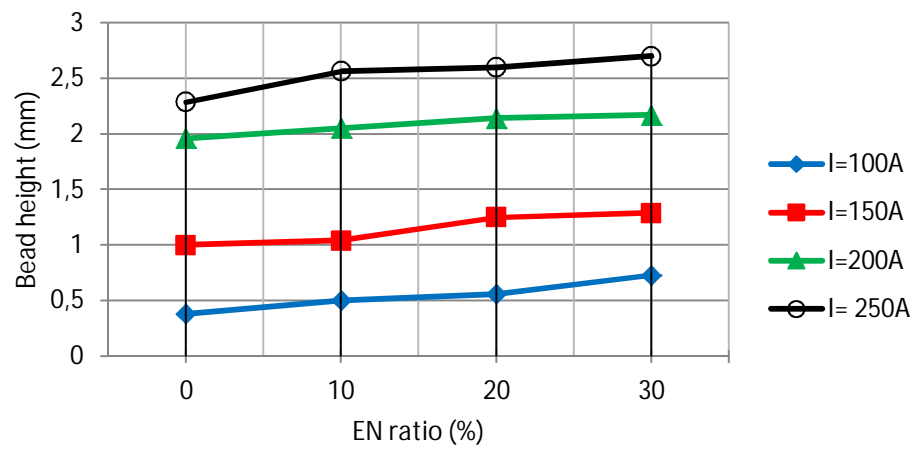


Figure 14. Penetration characteristics of DCEP and DCEN arcs [10]

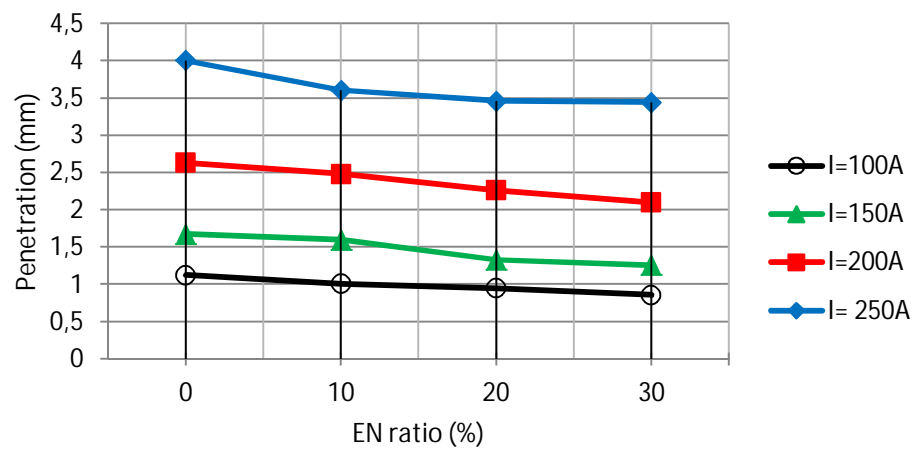
Analyses of the impact of the welding process parameters of AC pulsed GMAW on bead shape have been carried out in a welding experiment by W. J. So et. al. [33]. To measure the macro-section of the weld bead, 8 mm thick steel, grade SM490 was tested (bead-on-plate-welding test). ER 70S-6 (1.2 mm in diameter) and 95% Ar + 5% CO₂ (20 m/min) were used as the wire and shielding gas. The Contact-Tip-to-Work Distance (CTWD) was set to 15 mm. Figure 15 (a), (b) and (c) show the change in bead width, bead height and penetration with the change in welding current and EN ratio at a welding speed of 0.5 m/min. For the same welding current, bead width and penetration decreased while bead height increased as the EN ratio increased; this because DCEN time increased with the increase in EN ratio, and heat input to the base metal decreased because of direct wire heating after creation of the arc root in non-melted wire. [34]



(a) Bead width



(b) Bead height



(c) Penetration

Figure 15. Relationship between weld bead geometry and EN ratio [34]

2.9.2 Voltage

Arc voltage is directly related to current, as indicated above, and increased arc length increases voltage. Arc voltage also depends on the shielding gas and electrode extension. An increase in arc voltage widens and flattens the weld bead. Low voltages increase the weld reinforcement and excessively high voltages can cause arc instability, spatter and porosity, and even undercut. [2, 6]

The graphs in Figure 16 show that for a speed of 80 cm/min, the increase in depth of penetration for 95 A, 105 A and 115 A is 0.19, 0.15 and 0.18 mm, respectively, for an increase of 4 V. [32]

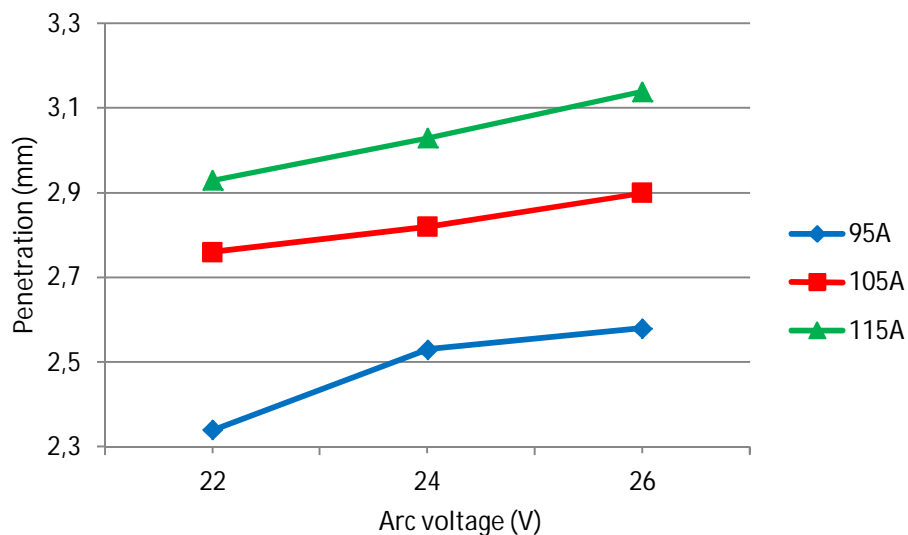


Figure 16. Penetration vs arc voltage graph for 80 cm/min welding speed [32]

2.9.3 Inductance

It is often possible to adjust the inductance of the power source to fit the wire size to give the right welding properties. Short circuiting arc welding is the process type most sensitive to inductance change; Figure 17 shows the relationship between the inductance and the current waveform. A low value gives a distinct and concentrated arc but spatter will increase. A higher value gives a somewhat

wider bead and a softer sounding. Too high inductance gives bad stability with a tendency for stubbing. Inductance may be replaced by greater drooping characteristics curves of the power source. In inverter power sources, the dynamic properties of the power source are normally managed by digital or electronic control circuits. [2, 6]

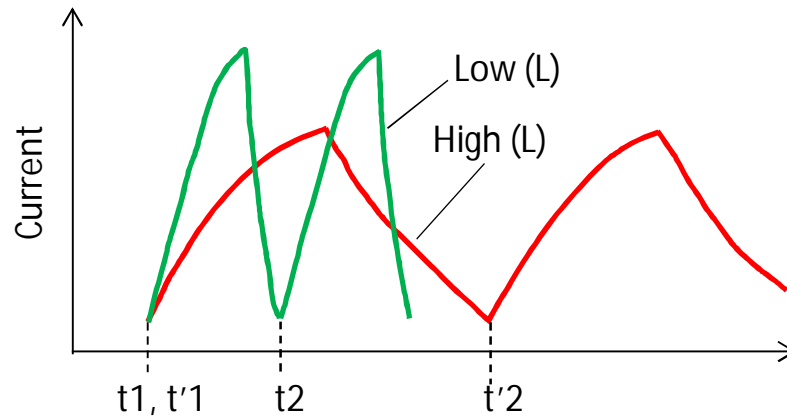


Figure 17. Relationship between reactor inductance (L) value and welding current waveform [35]

2.9.4 Welding Speed

Increase in welding speed leads to growth in productivity. Increase in the welding speed results in a decrease in the linear heat input to the workpiece and the filler metal deposition rate per unit of length. The initial increase in welding speed can cause some increase in penetration depth, because the arc acts more directly in the parent material, but further increase in speed decreases penetration and can cause undercut, due to insufficient material to fill the cavity produced by the arc. [2, 6]

The graphs in Figure 18 suggest that as the welding speed increases, the depth of penetration increases. However, it decreases as the speed is increased beyond 60 cm/min. This indicates that for any welding condition, there is an optimum value of welding speed beyond which if the speed is increased, the depth of penetration decreases. [32]

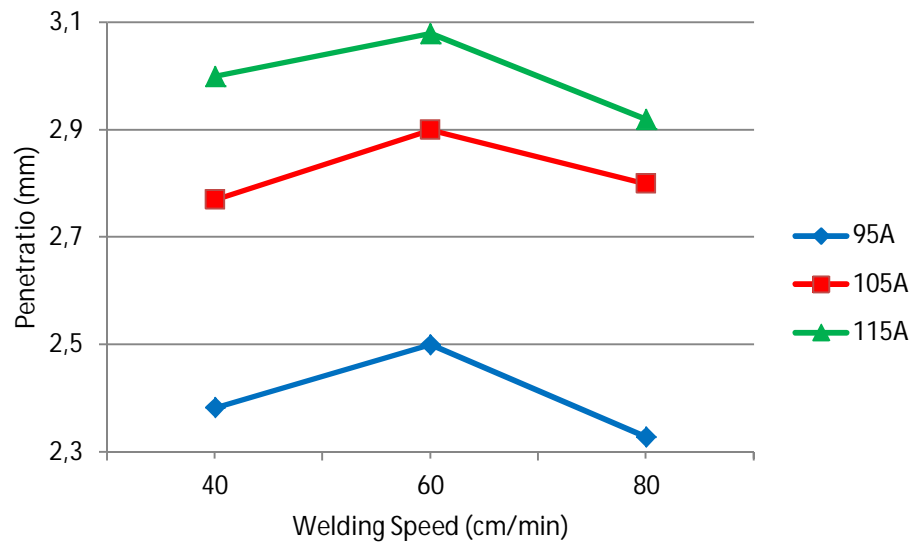


Figure 18. Penetration vs welding speed graph for 22V arc voltage [32]

2.9.5 Electrode Extension

The electrode extension is the electrode length that is out of the contact tube (Fig. 19). An increase in electrode extension produced by an increase in the torch distance to the work-piece for a specific set of parameters increases the electrode melting rate because of the Joule effect. Electrode extension ranges from 5 to 15 mm for dip transfer, being higher (up to 25 mm) for the other transfer modes. [2, 6]

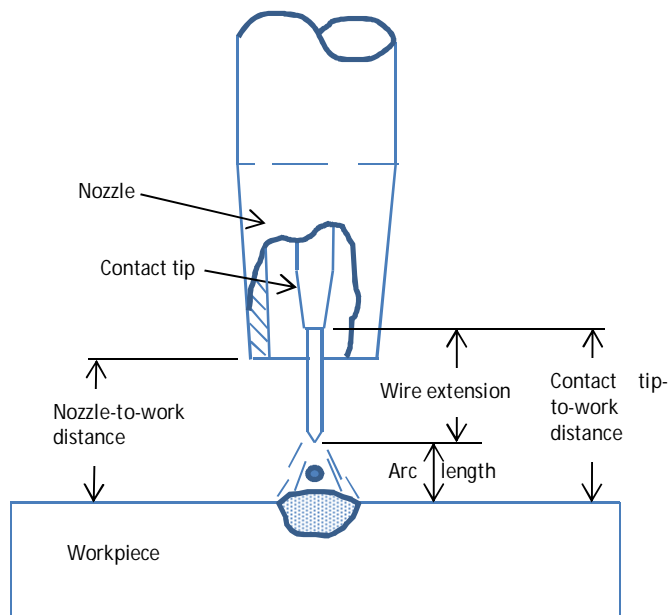


Figure 19. Contact Tip-to-Work Distance (CTWD) [6]

In a study of the melting rate in TIME-shielding arc welding with a solid wire, measurements were performed by varying wire extension lengths. The results of measurement for three different wire extension lengths are shown in Figure 20. As expected, the melting rate increases with the increase in the wire extension length, because of the increase in heating of the wire extension due to its ohmic resistance. [36]

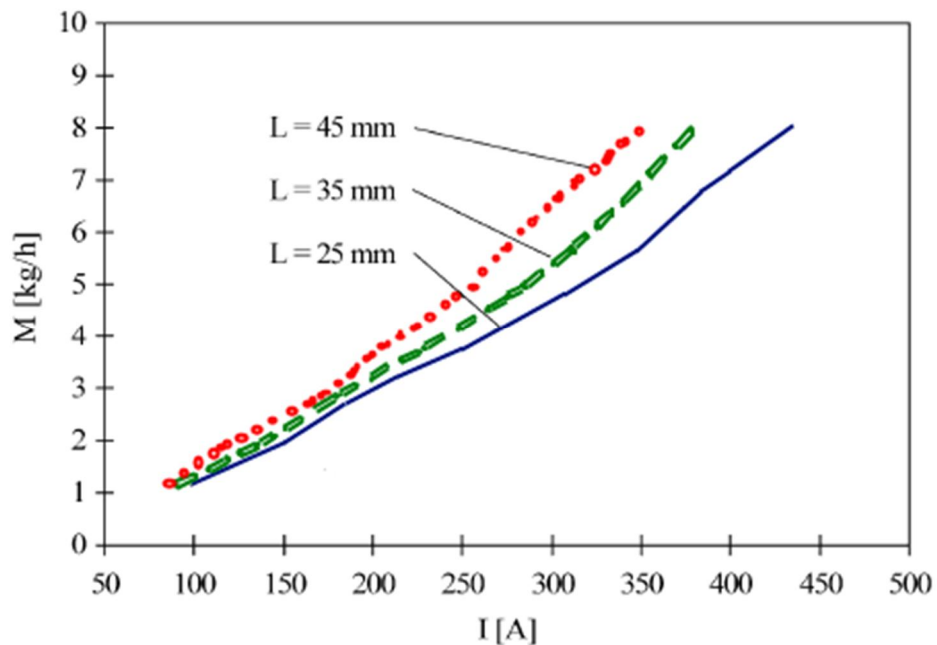


Figure 20. Melting rate as a function of welding current and wire extension length with 1.6 mm solid wire in a TIME welding gas mixture [36]

2.9.6 Shielding Gas

Shielding gases have an effect on arc stability, metal transfer mode, weld bead shape and melting rate, as well as protecting the weld from the atmosphere. Figure 21(a) shows that an increase in temperature also increases electrical conductivity. In Figure 21(b), showing thermal conductivity of the most frequently used gases as a function of temperature, it is clearly indicated that molecular gases (hydrogen, oxygen and carbon dioxide) have the highest thermal conductivity at lower temperatures (around 3000 K) and inert gases, helium and argon, at higher temperatures (around 9000 K). Thermal conductivity of gas affects the temperature of the arc and that of the weld pool. Gases used in GMAW can be pure gases, binary, ternary, and exceptionally, quaternary mixtures. Common pure gases are argon, helium, carbon dioxide and oxygen. The first two are inert gases and are used principally in welding of light alloys, nickel, copper and reactive materials. Helium has a higher ionization potential than argon, providing larger weld pools, but is more expensive. Carbon dioxide is an active gas and is used in

welding of carbon steels. It produces high levels of spatter but provides high penetration depth. [37-39]

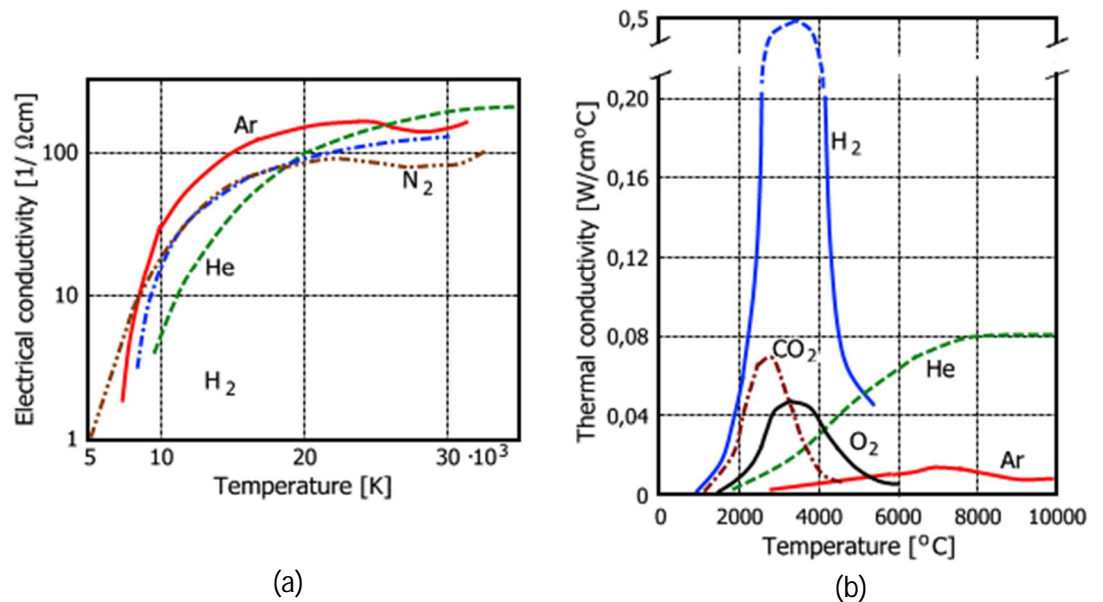


Figure 21. Electric (a) and thermal conductivity (b) of shielding gases at pressure of 1 atm [38, 39]

Binary mixtures, commonly argon/carbon dioxide (up to 20% CO_2), are used in the welding of carbon and low alloy steels, argon/oxygen (up to 5% O_2), for stainless steels, and argon/helium (up to 75% He) for nonferrous materials. The addition of oxygen or carbon dioxide to argon stabilizes the welding arc and changes the bead shape [40]. The main objective of adding helium to argon is to increase heat input, and consequently welding speed, and to reduce the incidence of weld porosity.

Figure 22 shows the effect of the shielding gas mixture on the penetration of a PB weldment. It can be seen that the penetration increases with the increase in CO_2 content in the mixture in both binary and ternary shielding mixtures. This behaviour can be explained by the arc force, which relates the depth of penetration with the arc length and current intensity. [41]

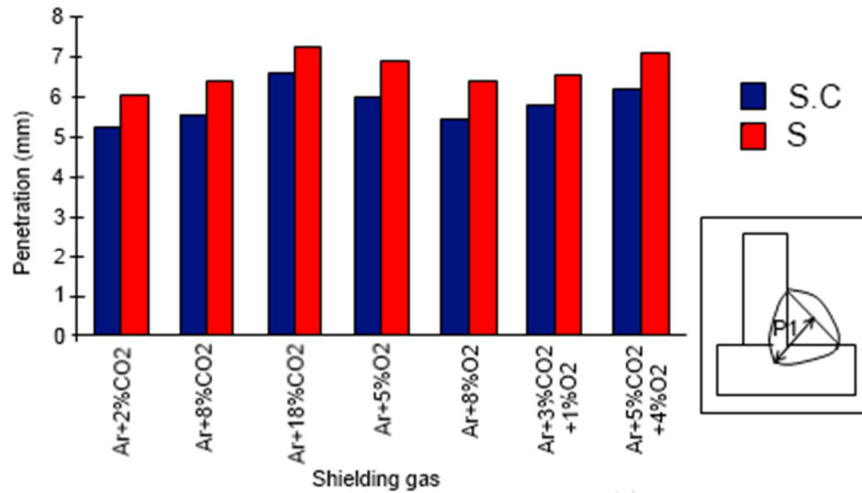


Figure 22. Evolution of the penetration with different shielding gas mixtures, with short-circuits (S.C) and spray (S) transfer [41]

The most common ternary mixtures are argon/oxygen/carbon dioxide, which is used in welding of carbon steels, and argon/helium/carbon dioxide and argon/carbon dioxide/hydrogen, for welding stainless steels. Ternary mixtures are intended to improve weld bead profile, increase tolerance to material contamination and promote higher travel speeds. [2, 6]

2.9.7 Gas flow rate

The flow rate of the shielding gas has an important influence on the quality of the weld metal and the surface of the weld. Too low a flow gives inadequate protection since air contaminates the gas. On the other hand, if the flow is too high, there will be turbulence when the gas exits from the nozzle, and oxygen and nitrogen are drawn into the arc. In both cases, the result will be welds contaminated with oxides and nitrides, and porosity. [2, 6]

Figure 23 shows the effect of gas flow rate and wire diameter on average weld bead penetration. The average weld bead penetration was adjusted by taking the average of all measured values with the same gas flow rate for a particular wire diameter, but without considering the effects of welding speed, arc current and welding voltage. It can be seen here that a higher weld bead penetration is

obtained with a larger wire diameter, but the effect of gas flow rate on weld bead penetration seems to have little significance. [42]

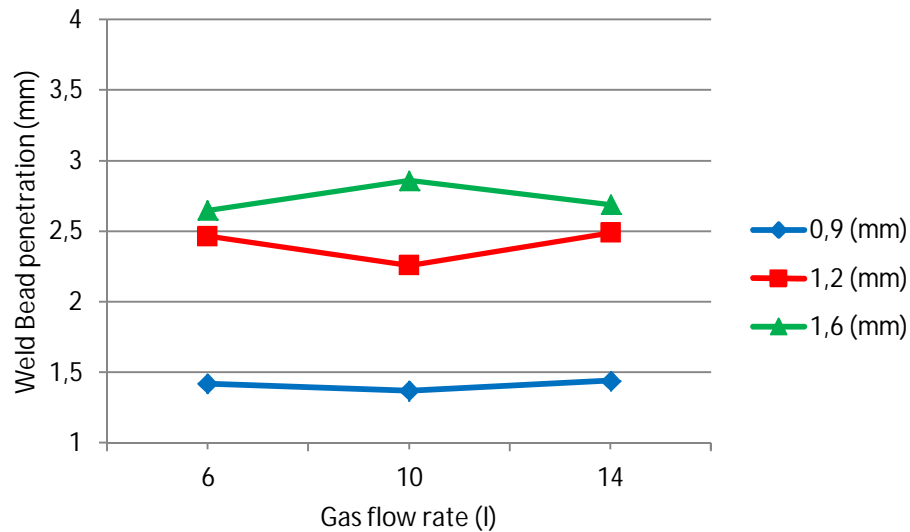


Figure 23. Effect of gas flow rate on average weld bead penetration [42]

The gas flow must be adapted to the arc. At low current, 10 litres per minute can be sufficient, while at higher welding data, up to 20 litres can be required. Welding with aluminium needs more gas than steel because of its higher reactivity to air, which is likely to lead to porosity, and the higher heat required to compensate the thermal expansion. [2, 6]

2.9.8 Electrode Diameter

The chemical composition of the electrodes is similar to that of the materials being welded. The most usual electrode diameters are 0,8, 1,0, 1,2 and 1,6 mm. Electrodes of lower diameter are used for thin materials. Electrodes of 1,2 and 1,6 mm diameters are utilized in welding thicker materials and need higher currents, which produce larger weld pools. Electrodes of 1,6 mm diameter are not recommended for positional applications, because operational difficulties as the diameter of the electrode increases lead to a lack of accuracy. Figure 24 presents a comparison of melting rates in welding with a covered electrode, a solid wire and

a cored wire. The melting rate increases as the diameter of the wire decreases and the current grows. [2, 6, 43]

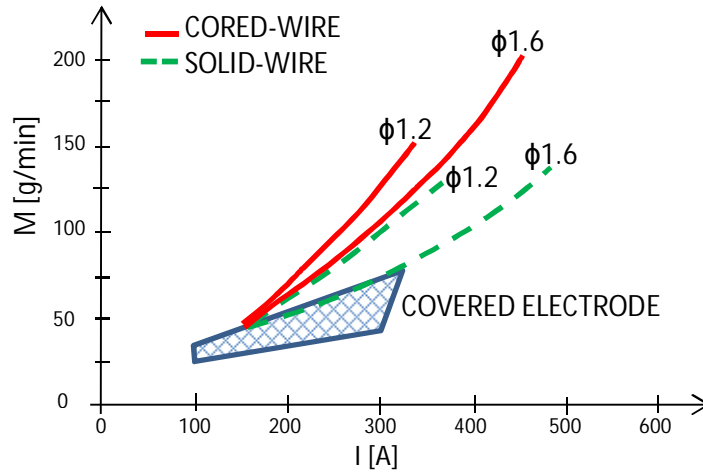


Figure 24. Comparison of melting rates in welding with a covered electrode, a solid wire and a cored wire, respectively [43]

3 HIGH ARC ENERGY

Investigations carried out by many manufacturers of welding equipment and materials into opportunities for improving the efficiency of the GMAW welding process have resulted in the introduction of some new variants of this method. In particular, these explore specific characteristics of the arc that come into being when the high energy of the system is combined with high rates of wire feed, longer CTWD and the chemical composition of the shielding gas. The deposition rate reached in processes of this kind is 10-14 kg/hr, but when high-energy sources are employed, it may even rise to some 27 kg/hr. The area of applications covered by high arc energy welding methods includes the manufacture of constructions welded in thick plates and in thick-walled tubing. The ever-growing popularity of these variants of high arc welding is associated with the high efficiency of the arc compared with the standard GMAW process, and with the good properties of welds which are deposited at high values of arc parameters. According to some research [44-46], the differences between individual variants of the process manifest themselves almost entirely in the chemical composition of the recommended shielding gases, leaving other characteristics of the process almost unchanged. However, other works [36, 47, 48] indicate that the gas mixture has a negligible effect on the efficiency and the weld properties.

3.1 High current short circuiting arc

The high-power short arc, called a RapidArc or ForcedArc, is characterized by the use of a reduced welding voltage. At its earlier approach the process was performed with moderately lower voltage combined with a high wire feed speed and welding current which resulted in a high penetration (forced) short arc with a high frequency, approximately 150-400 Hz [2].

The droplet attachment at the end of the electrode grows until it touches the molten pool via a shorting bridge. In consequence, the arc extinguishes, and thus, the high welding current causes a high pinch force, which constricts the shorting

bridge to an increasingly greater extent. Finally, the surface tension of the molten pool takes off the droplet [49]. The arc re-ignites and the process is repeated [45]. Thus, the liquid end of the electrode periodically causes short circuits. The radial force of the magnetic field may deflect the droplet a little out of its symmetry axis [50]. In contrast to conventional short-arc welding, the short-circuit duration is shorter because of the more extreme pinch effect, and the droplet frequency is higher [24].

The arc has a sharper sound than a conventional short arc. The relatively low welding voltage enables a faster welding speed without undercut. At the same time, the risk for large weld reinforcement (due to the low voltage) is limited by selection of an appropriate combination of the welding parameters, such as welding speed, shielding gas mixture and gas flow rate. An argon-based (92 % Ar + 8 % CO₂) shielding gas is used with a higher gas flow than normal (20 l/min) [2].

The process is used for welding smaller weld sizes with high travel speeds. Table 5 presents some important applications and the benefits of the high-energy short circuit GMAW process. Thin sheet and medium thick steels (up to 12 mm) are suitable for welding with a high current short circuiting arc since the heat input is low but with maintained fusion capacity (lower thermal losses to the material due to the high travel speed). Mechanised welding is necessary to make full use of the process. In addition, due to the long electrode extension, approximately 20-35 mm, an automated system is required for good repeatability to ensure a high weld quality. The welding position also has an important role; high quality weldments are achieved in the horizontal position (PA). Solid wires with diameters between 0.8 and 1.2 mm are used and deposition rates between 8 and 18 kg/h can be achieved. An interesting aspect of this method is that normal welding equipment can be used. [2]

Table 5 High current short circuit application and benefits

Process	Cross section	Position	Electrode	CTWD	Deposition rate
High energy short circuit	Up to 12 mm	PA	Solid wire Diameter 0.8-1.2 mm	20-35 mm	8-18 kg/h

There has been some discussion about the classification of this process. The high power short arc was classified by J. Norrish [8] in the category of extended stick out GMAW in the group of short-circuiting transfer. According to N. V. Pepe [51], this process works as a pulse spray transfer process. The process has improved significantly with digitalised power source and control of current and voltage waveforms.

3.2 High current spray arc

The material transfer of a conventional spray arc depends on the amperage and on the shielding gas. In the lower current range, principally in the case of shielding gases containing carbon dioxide (CO₂), the droplet is separated directly at the electrode, whereas, the formation of a longer molten part of the wire electrode can be observed with increased welding current, especially when using argon/oxygen mixtures. [24]

The upper current range of the conventional spray arc, in contrast, is characterized by an axial flow transfer. This type of transfer requires the arc to embed a sufficiently long part of the end of the electrode in order to supply enough heat [49]. Shielding gases of low thermal conductivity - such as argon or gas mixtures containing a high percentage of argon - meet this criterion. They cause a wide current-carrying arc column with a relatively narrow heat-carrying marginal zone and low temperatures [23].

In contrast to this, carbon dioxide leads more heat into the marginal zones of the arc and forms a very narrow, hot arc core of high current density. The arc only touches the droplet at one point, where it embeds the end of the electrode with argon. [24]

The aim of use of a high current spray arc is to increase productivity by increasing the deposition rate. Table 6 presents some important applications and the benefits of the high-energy short circuit GMAW process. Solid wire with diameters between 1.0 and 1.2 mm are used and deposition rates slightly above 20 kg/h can be achieved when welding in the best position, the flat position. Large weld sizes and thicker plates up to 20 mm are feasible. The spray arcs used are the same as in the TIME concept, but a difference lies in the shielding gas. For all rapid processing arc types, a more cost efficient shielding gas with the main composition 92 % Ar and 8% CO₂ is used. The gas flow is higher than normal, often 20-30 l/min. A large electrode stick-out is used and a wire-straightening device in the wire feeding system increases the accuracy of the weld positioning. The welding equipment should have a current capacity of at least 600 A and stepless voltage control. High-speed wire feeding up to 50 m/min is used and the stability of the wire feeding is the key to a stable process. [6, 24]

Table 6 High current spray - application and benefits

Process	Thickness	Position	Gas flow rate	Electrode	Welding speed	Deposition rate
High current spray	Up to 20 mm	PA	20-30 l/min	Solid wire 1.0-1.2 mm	Up to 50 m/min	Up to 20 kg/h

The rotating arc shows a broad penetration profile and a smooth surface transition in the weld toe region. However, the penetration depths decrease compared to the moderated spray. The stability of rotating arcs has been

discussed. [52] If the frequency of the rotation is unstable, a risk of unwanted spatter and porosity due to turbulence around the weld pool can occur. Furthermore, there is a less suitable mixed arc region in between the stable rotating arc region and the moderated spray region. Therefore, it is important to select stable welding parameters, not too close to the arc region boundary. For this reason, to promote stable rotation or inhibit rotation, special shielding gases have been developed - this is the basis for other high-speed welding concepts with the spray arcs. Improvements in power sources have generated another way to control the arc stability, through a suitable selection of power source characteristics. [53]

3.3 High arc energy effect on the joint properties

The higher risk of defects in welding with a high-energy GMAW process is a consequence of the effect that heat input has on microstructures in the weld and fusion zone, and the large heat affected zone. Poor chemical properties of the weldment dramatically affect the mechanical properties of the joint. Investigations by M. Suban [36] and B. Czornog [47] related to the high energy GMAW process have contradicted claims that single wire heavy duty welding processes absolutely need special shielding gas mixtures for the arc to be stable and have shown that there were no significant difference of shape and mechanical properties of the weld related to shielding gases mixture.

Investigations into high arc efficiency GMAW welding carried out at The Welding Institute of Poland covered the areas of padding or overlying welds, weld metals, and joints welded in Ar-CO₂ and ternary Ar-He-CO₂ (variable helium content) gas mixtures. The results of these investigations show that with a current intensity of up to 450 A, the process is stable in the shield of any of the gas mixtures used. Equally, the shapes of padding welds and the mechanical properties of weld metals and joints do not show any significant differences associated with the composition of the shielding gas in spite of the variation in chemical analysis. [53]

Another investigation focused on the properties of welds and joints when using the high-energy GMAW process [48]. The work concentrated on assessing the effect of the chemical composition of the arc shield on the characteristic properties of the weld metals and the properties of the welded joints. The welding was carried out with a semi-automatic, Magomig-550 welder manufactured by the OZAS Company of Opole, equipped with a standard thyristor source of current and a wire feeder operating at a rate of 25 m/min. Electrode wires 1.2 mm in diameter were used. Table 7 shows specimen number, shielding gas mixture and current applied to investigate the effects of higher energy on the weld properties: [48]

Table 7. Welding parameters example high energy GMAW [48]

Specimens	Shielding gas	Current [A]
1	60 % Ar + 30 % He +10 % CO ₂ (60/30/10);	300
2		350
3		400
4	75 % Ar + 15 % He + 10 % CO ₂ (75/15/10)	300
5		350
6		400
7	90 % Ar + 10 % CO ₂ (90/10)	300
8		350
9		400
10	60 % Ar + 30 % He + 10 % CO ₂ (60/30/10);	300
11		350
12		400
13	86 % Ar + 12 % CO ₂ + 2 % O ₂ (Argomiks U12)	300
14		350
15		400
16	90 % Ar + 10 % CO ₂ (90/10)	400
17	60 % Ar + 30 % He + 10 % CO ₂ (60/30/10);	400

The properties of the weld metals deposited were determined by the high arc energy GMAW method. Test pieces grade 18G2A were welded using a G3Sil

wire in conjunction with 90/10, 75/15/10 and 60/30/10 gas mixtures, and a current intensity of 300, 350 and 400 A. For comparison, an investigation was also carried out into the weld metals deposited with a G2Mo (copper coated Mo bearing mild steel solid wire electrode) type of wire in the commercial Argomiks U12 mixture. [48]

The metallographic examinations included a quantitative assessment of non-metallic inclusions, and of the primary and secondary weld structures. The investigation into the presence of non-metallic inclusions was made with an automatic Pericolor 5000 picture analyser on etched and un-etched micro sections, while the examination of the structures was carried out with a Neophot 2 optical microscope and a Hitachi 4200 scanning microscope. Figures 25 illustrate the percentage of surface fraction of non-metallic inclusions in the weld metals; there is a slight tendency of an increase in non-inclusions dependent on the amperage growth. A dramatic drop is observed at series number 6 and a moderate drop at series number 3, which are related to the presence of Helium. Series numbers from 10 to 12 are welded with G2Mo electrode. [48]

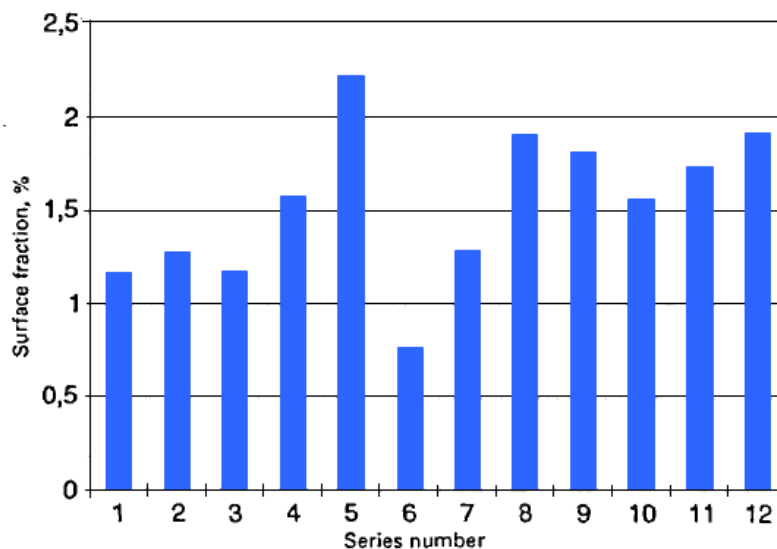


Figure 25. Percentage surface fraction of non-metallic inclusions in the weld metals [48]

Quantitative and qualitative analyses of the secondary structures of non-recrystallised weld metals were carried out. Volume fractions of various forms of ferrite, in particular free, laminar and fine-acicular ferrite, were determined in individual layers. Mean values based on ten measurements are given in Figure 26. A fine acicular ferrite microstructure is advantageous over other microstructures because its chaotic ordering increases toughness. The bar graph shows that the presence of fine acicular ferrite is greater at 400 A, independent of the gas mixture. [48]

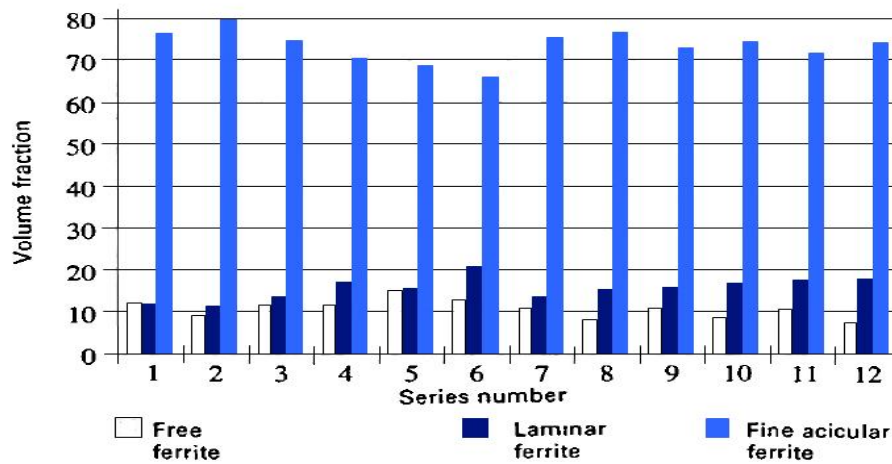


Figure 26. Fractions of different forms of ferrite in recrystallised structures of weld metals [48]

Figure 27 shows that the lowering of the impact strength of the weld metals with a rise in the welding energy was general and occurred with all the weldments with the one exception of those produced by the G2Mo consumable electrode. The latter exception is associated with the chemical composition of this particular wire (an addition of molybdenum refines the structure). The 90/10 mixture produced the highest impact strength of the weld metals deposited with the G3Si1 wire. [48]

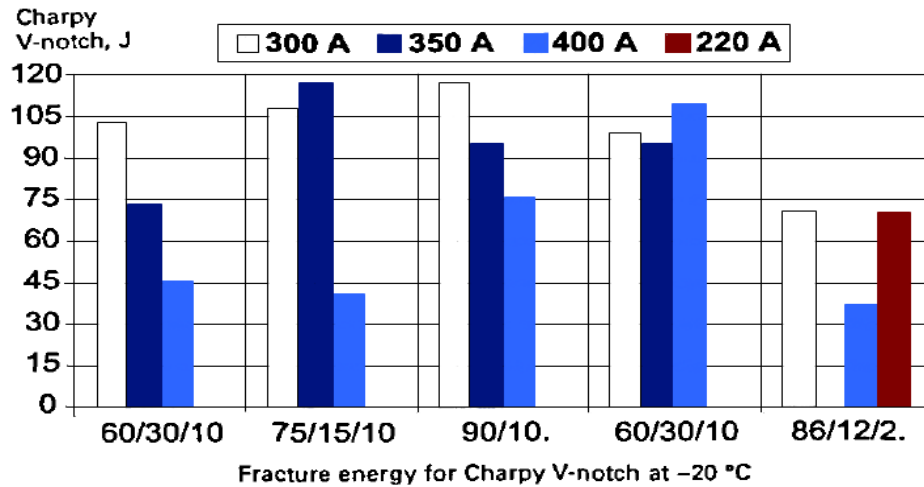


Figure 27. Fracture energy in Charpy V-notch tests at -20 °C for weld metals produced in shields of the investigated gases at different intensity of current [48]

The information reviewed in this section clearly indicates that within the range of the investigated welding parameters, the addition of helium does not have any noticeable effect on the welding process and its outcome. It is therefore possible to use the simple and cheap Ar-CO₂ mixture in GMAW process using high arc energy levels. The fears occasionally expressed by some specialists that the ductile properties of the welds deposited by the high arc energy GMAW method will be low [12] have not been confirmed. Both the fatigue strength and CTOD tests produced satisfactory results. This is due to a relatively low fraction of non-metallic inclusions in the welds and to the satisfactory structures of fine-acicular ferrite, and, generally, of fine ferritic and pearlitic phases predominating in the zone subjected to thermal effects generated during the deposition of subsequent weld runs. [48]

Although careful selection of welding parameters, material composition and electrode orientation, extension of the electrode and higher welding speed contribute to an increase in productivity, another alternative would be to modify the arc behaviour such that the arc pressure at the transition line decreases, but the hot region remains approximately the same. More knowledge of the welding arc is necessary to implement this approach effectively and a process promoting arc

control for adaptive pulsed GMAW could have the benefit of an improvement in the weld quality. [54]

4 ADAPTIVE PULSED GMAW WELDING PROCESSES

In the GMAW process, the welding wire becomes the electrode. The welding wire, i.e. the electrode, melts owing to the arc heat and forms droplets, which transfer to the base material. Accordingly, arc length and position of the arc generation change intermittently.

The stability of the transfer phenomenon is directly linked to the weld quality and workability. This is why, all over the world, manufacturers of welding machines, welding consumables and gases, and universities and research institutes have predominantly been focusing on the performance of the power source, the composition of shielding gases and the chemical composition of wires to develop welding systems that would contribute to improvements in productivity and quality.

Traditionally, use of a constant voltage (CV) power source with inductance control proved to be excessively sensitive to arc length variations, with high wire feed speed and current respond. Therefore, feed-forward controls - also known as digital or reactive controls - have been introduced, where the current can be modified independently from the wire speed. Advances in process control have been made, especially using feed-forward algorithms, as demonstrated by their excellent adaptability to steps responses when compared to traditional feedback control [55]. A constant arc length control system is schematically shown in Figure 28, demonstrating the ability of the system to adjust to random variations in CTWD without changing the arc length. [5, 56]

Modern electronics allow engineers to design software that supports welders in control of the weld process. Nowadays, extensive memory functions allow storage and retrieval of optimal settings for process parameters.

Figure 28 presents a configuration of a digitally controlled arc welding power source. The instruction is given to the inverter section, which controls the power, directly from the computer without digital-analogue (DA) conversion, and this

enables faster operation. Moreover, since the wire supply rate can be controlled digitally by a computer while it is sensed unfailingly by devices such as rotary encoders, the wire supply becomes reliable and stable. [57, 58]

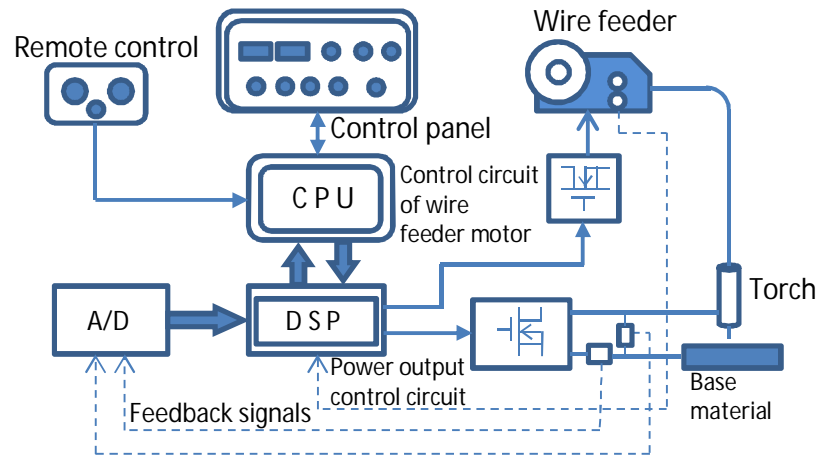


Figure 28. Configuration of digitally-controlled arc welding machine [59]

Various new systems have been introduced into the market. Based on details of the approaches adopted, names are individually given by the manufacturer and advertised for their advantages. There have been successful achievements of adaptive GMAW processes to specific joints, metal and position in the actual in-service execution. This section reviews different concepts of adaptive GMAW and highlights their applications and benefits.

4.1 Modified short arc GMAW methods

The automotive and motorcycle industries have been promoting the use of thinner sheet metals to reduce the weight of vehicle bodies, as well as methods to decrease welding spatter, to reduce industrial waste and the costs associated with post-weld spatter removal. Currently, the pulsed gas metal arc welding (P-GMAW) process is used to reduce spatter. With non-pulsed gas metal arc welding (GMAW), low heat input to the base metal is desired to mitigate melt-through in welding sheet metals. However, use of the non-pulsed GMAW process causes much more spatter. In non-pulsed GMAW using low currents, spatter is mostly

generated from the moment of re-arc, right after the short circuit. In order to suppress such spatter generation, a specific method has been suggested that senses the molten metal squeezed at the tip of the wire during the short circuit and rapidly decreases the current just before re-arc to transfer the molten metal to the weld pool using only surface tension. [60-62]

The modified short circuit consist of a special waveform control short circuit which differs from the traditional one. The precise shape of the current and voltage are different for WiseRoot, STT, and Cold Process, for example, but there are common principles. In general, the software controls the electrode current during all phases of the droplet transfer. After the droplet on the end of the wire wets out in the weld pool, the current curve shape is increased to a level sufficient to start pinching the droplet. The current is then gradually increased further until the short circuit is about to occur. Once the short circuit happens, the current is rapidly decreased so that transfer occurs with lower current to the weld pool. Moreover, curves are also designed to allow smooth transfer, to stabilise the pool and allow easy re-ignition. The current is monitored and, if necessary, is dropped even further to avoid an arc force that could agitate the pool. [63]

The right balance between wire feed speed and burn-off rate is crucial for successful short arc welding. To achieve this, the arc voltage and wire speed need to be carefully matched. Among other factors affecting the short circuit time, the choke setting also affects heat input. More choke results in a longer arc period, lower short circuit and higher heat input. Inversely, less choke gives a shorter period, higher short circuit frequency and lower heat input. Figure 29 shows an ESAB concept that is achieved by the QsetTM function. The settings of the choke inductance are synchronised with the short circuit timing, which results in a cold or hot arc and has an effect on the arc length. [35]

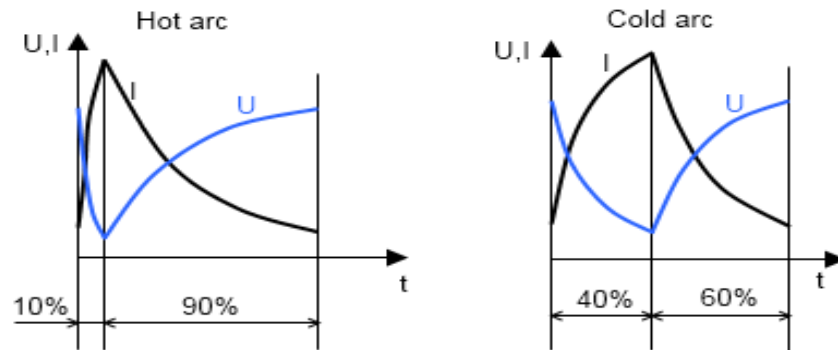


Figure 29. Setting of arc frequency by inductance, capability of control of short-circuit and arcing time [35]

4.2 Modified pulsed GMAW methods

In the past there was little scope for process modification of the pulsed GMAW method. Notable exceptions were dual power source concepts for dip transfer and the early introduction of pulsed transfer GMAW using sinusoidal current pulses [64]. Pulsed GMAW (P-GMAW) provided additional control of the GMAW process by using a current waveform consisting of a low background level to maintain the arc and a superimposed pulse current to detach the material. The objective was to produce spray type projected transfer at mean currents below the spray transition threshold. The process gave good positional spray performance and was particularly beneficial in the welding of aluminium alloys and stainless steel [65, 66]. The main limitation of the process was the power source design constraint, which meant that pulse frequency was usually a multiple of mains frequency and the pulse profile and duration were dependent on the fixed power source design. The introduction of solid state power control meant that power source statics and dynamics characteristics, and output waveforms could be varied. Based on the early work of J. Ma [29] it became possible to produce the drop spray transfer mode discussed above in a controllable and repeatable manner over a wide current range. Nowadays, structural steel has been added amount material weldable by P-GMAW.

Increase in the welding current in the P-GMAW process reduces the columnar growth of dendrites in the matrix. The morphology of the bainite was found to change with variation in welding parameters. The pulse current resulted in a coarse microstructure with respect to the growth of dendrites, especially at higher pulse frequency and pulse duration, due to reduced cooling rates. However, pulse current welding carried out at higher arc voltage was found to be beneficial for the production of a finer weld microstructure [67, 68]. In recent decades, as a result of power source technology improvement different approaches have been implemented successfully and have significantly improved the pulsed GMAW process. Main variants are reviewed in the sub-section below.

4.2.1 Synergic control

Synergic control mode can also be regarded as wire-feed speed control of the mean current [69]. The power supply and wire-feeder are directly linked in such a way that the mean current is determined by the wire-feed rate to ensure a stable arc. The circuit arrangement for this system is shown in Figure 30. [70]

The pulse waveform produced by this type of control, shown in Figure 30, has constant peak duration and excess current. Variable pulse parameters are peak current, base current and base current duration. This control can only be operated in fixed ranges of the mean current as a large mean current might produce multiple droplet detachments per pulse. [69, 70]

In a typical synergic control system, the pulse duration and amplitude for single-drop detachment are pre-set. The system may incorporate a tachometer that measures wire feed speed and feeds the speed signal to a control circuit that generates the appropriate pulse frequency. [71]

The major advantage of this control technique is that the mean current can be varied continuously over a wide range by means of a single control (e.g. 50–300 A with a 1.2 mm diameter carbon steel wire) and stable projected drop spray type transfer is maintained throughout the control range.

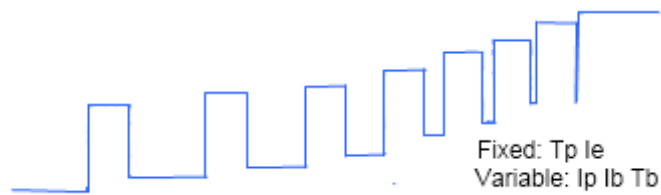


Figure 30. Pulse waveform of synergic control [72]

4.2.2 Self-regulating control

Self-regulating control mode can also be regarded as voltage control of the mean current or error voltage system [69]. The welding voltage varies according to the arc length. This system always tries to restore arc length to the set reference voltage by automatically modifying the burn off rate. The circuit arrangement for this system is shown in Figure 31.

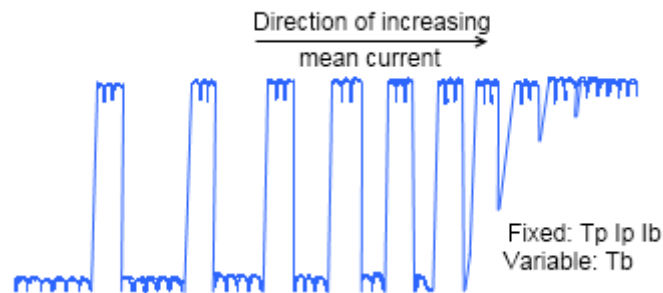


Figure 31. Pulse waveform of self-regulating control [72]

4.2.3 Dual-pulse

Dual pulsed GMAW (DP-GMAW) technology is refers to a low frequency current pulse which is superimposed on a high-frequency current pulse (Fig. 32). Compared with P-GMAW, DP-GMAW has wider welding current range, can be applied for all position and bridges larger air gap, and reduces heat input and porosity [73-75]. The role of the high-frequency current pulse is to control the droplet transfer behaviour and obtain welding penetration. The main function of the low frequency current pulse (thermal pulse) is to have a series of regular pulses to stir the weld pool [76]. The two difference pulses have benefits for refining grains and reducing crack sensibility of weld joint. [77, 78]

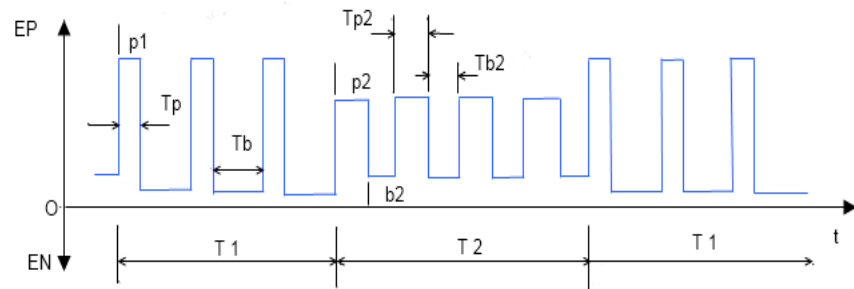


Figure 32. Dual-pulsed current waveform [77]

4.2.4 AC pulse

AC MIG (Alternative Current MIG) also called VP-GMAW (Variable Polarity GMAW) welding is not very common and is used mostly in Japan. AC MIG welding was not commercially available in Europe before the end of the 1990s. This type of equipment is used for short arc and pulsed arc welding of details for vehicles in a lower current range up to 200 A. [2]

Negative polarity on the electrode means lower heat input and higher variable deposition rate. Arc re-ignition at the time of polarity switching is a problem for VP-GMAW welding. For this reason a re-ignition device is customarily fitted to the AC power sources of commercial frequencies in order to prevent arc blow and welding faults, thus making possible high-current multi-electrode GMAW of thick sheets. [79]

Fast zero-crossing is necessary to secure re-ignition of the arc. A balance control allows the user to adjust the ratio of negative to positive polarity. In practice, this gives the user a tool to change the ratio of heat and amount of filler material. At 50% negative polarity, only 40% of the current is needed to melt the wire compared to welding with normal positive polarity. The advantage is that thinner material can be welded and it is possible to allow more variations of the gap width. Heat input and deformations decrease. [2]

Figure 33 presents the current waveform of AC pulse GMAW, which can be expressed in the EN ratio as shown in Equation 2. The symbols, I_p , I_b , I_{EN} , represent respectively the peak current, the background current of DCEP, the base current of DCEP, and the pulse current of DCEN. T_p , T_b and T_{EN} indicate the peak current time of DCEP, base current time of DCEP and time of DCEN, respectively. [80]

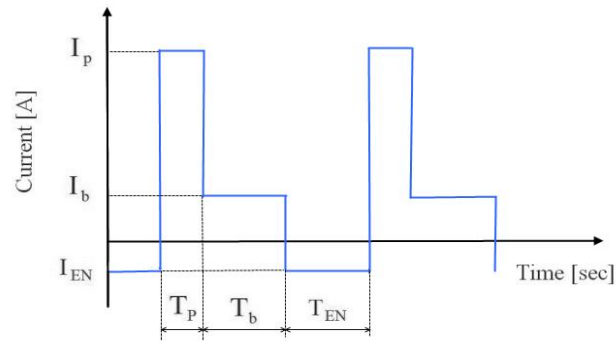


Figure 33. Current waveform for AC pulse GMA welding [80]

$$ENratio = \frac{I_{EN} \times T_{EN}}{(I_p \times T_p + I_b \times T_b) + I_{EN} \times T_{EN}} \quad (2)[80]$$

Where

I_{EN} : The average current of the section EN, (A)

I_p : The average current of the peak section EP, (A)

I_b : The average current of background section EP (A)

T_{EN} : The time of the section EN, (s)

T_p : The time of the peak section EP, (s)

T_b : The time of the background section EP, (s)

The variable pulsed welding process introduces less heat input to the base metal than DC pulsed GMAW and the molten amount of wire is greater at the same welding mean current. Therefore, AC-GMAW is regarded as an effective consumable electrode arc welding process able to address important factors such as melt-through, gap tolerance and deformation, which are common difficulties encountered during welding of thin sheet metal. For example, AC-GMAW is now

being used in the fabrication of welded structures such as aluminium alloy auto bodies, motorcycle frames, stainless steel exhaust system components, and railway rolling stock roofs. [81, 82]

4.3 Mechanically assisted metal transfer GMAW

The Control Short Circuit (CSC) process in which the orientation and the rate of wire feeding are changed as the time progresses was developed by Huisman in 1999 [83]. This triggered acceptance of the idea of controlling the current waveform and wire supply at the same time, and expanded the range of welding phenomena available for control and their tolerances. This approach has been further refined by combined current waveform and wire oscillation. [84]

Mechanical control of the states is performed by advancing and retracting the wire at the arc. An advance followed by retraction defines one process cycle. The process cycle, as used herein, includes one cycle of the states of the process, and starts with an arc state, followed by a short circuit state, or starts with an arc state, followed by a short circuit state, then by a pulse state, etc. The advancing and retracting are accomplished using a pair of motors placed on either side of the wire, opposite one another, and near to (or mounted on) the torch. The motors are, depending on the precise system, stepper motors, servo motors, planetary drive motors, zero backlash motors, gearless motors, or replaced with a linear actuator. [83]

A study was conducted by Y. Wu et al. [85] aiming to investigate mechanically assisted drop transfer in the GMAW process. The experiment used an oscillating wire feeder developed by the welding research group of the Harbin Institute of Technology [86] to generate an additional force to cause detachment of the droplet. Thus, the projected transfer mode can be achieved much more easily. The oscillation can be activated by a stepping motor that is controlled by a single-chip computer.

The results showed that the additional mechanical force resulting from wire electrode oscillation can make the droplet size smaller and produces a higher droplet transfer rate, thus greatly improving the droplet transfer process. In addition, for welding at a higher wire-feeding rate, 100 mm/s, a significant improvement in the weld quality is achieved for welding currents ranging between 210 and 220 A. For a wire-feeding rate of 60 mm/s, an acceptable weld quality is obtained for welding currents ranging from 160 to 180 A. The wire oscillation frequency plays a key role in improving the droplet transfer process. The higher the oscillation frequency, the greater is the improving effect. In the research by Y. Wu et al [85], 85 Hz oscillation yielded the best effect at which a projected spray transfer mode was established and a very stable uniform detachment of small droplets was achieved. [85]

4.4 Combination of waveform and reversal electrode motion control

The combination of a special waveform and reversal of the electrode motion is a modified short circuiting transfer mode. The approach assists the molten metal transfer from the electrode to the weld pool by using a mechanical force generated when retracting the wire. Furthermore, the current and voltage waveform are designed to control the arc burning and short circuiting period. The process is enhancement of mechanically assisted droplet transfer. There has been little interest in this concept, and only few manufacturers have adopted the method, for example, CMT process from Fronius, MicroMIG process from SKS. Cold Metal Transfer (CMT) is a well-known practical application of this combination.

Cold Metal Transfer is a modified Gas Metal Arc Welding (GMAW) process that links waveform control and mechanically assisted droplet transfer. The moment the power source detects a short circuit, the welding current drops, and the filler wire starts to retract. Exactly one droplet is detached into the molten weld puddle. The filler wire then moves forwards again and the cycle is repeated. The filler wire is constantly retracted at very short intervals. The precisely defined retraction of the wire facilitates controlled droplet detachment to give a clean, virtually

spatter-free material transfer. Figure 34 illustrates the droplet detachment sequence. [87-89]

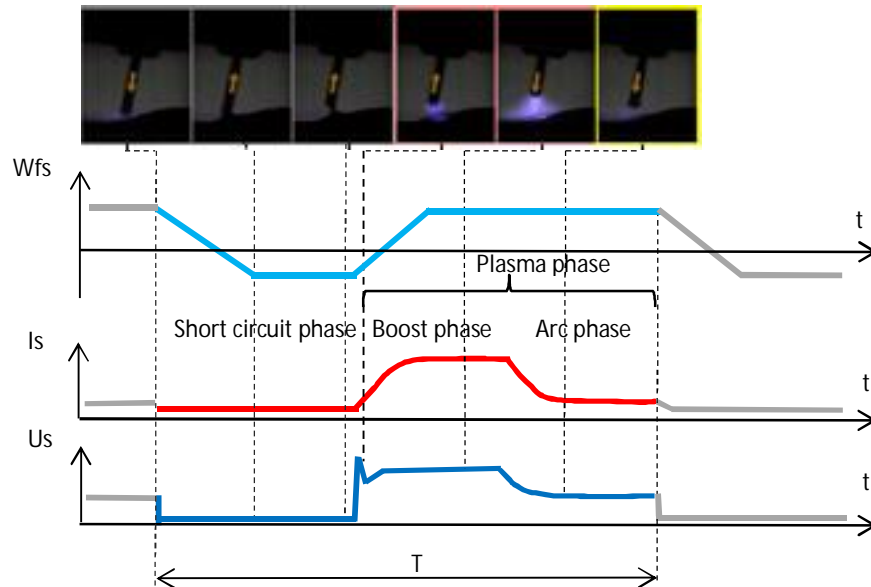


Figure 34. Waveform current (I_s) and voltage (U_s) with electrode alternative feeding motion (W_{fs}) [90]

The process has shown usability to welding corrosion resistance alloys (CRA) materials, such as martensitic and duplex stainless steel, and welding tests and development projects have been conducted on carbon steel pipe materials. In addition, welding tests on pressure vessels with stringent requirements for fatigue life and low temperature toughness welded with CMT root passes have been carried out with proven quality and mechanical performance. Double-welding of a steel catenary riser (SCR) - prolongation of a sub-sea pipeline attached to a floating production structure in catenary shape - is an additional application where CMT may be applied. [90]

Welding of cross-country pipelines with HSLA steel grades X80 and above could be a further application, as mechanized CMT and P-GMAW tie-in welding provides the low hydrogen solution that meets the need for elevated mechanical properties. Low heat inputs, minimized bevel volume, accommodation of

4.6 Determination of heat input with complex waveform

Modern welding waveforms are often not symmetric. They operate on inductive loads, contain high frequency harmonics, and are not repetitive. Traditional methods of calculating heat input involve measuring of either the average or root mean square (RMS) voltage and the average or (RMS) current. While traditional methods produce relatively consistent results with high-energy processes such as traditional spray arc, the results become less consistent or accurate with short arc and pulse modes due to the continually changing output of the machine.

Debate has taken place concerning the most accurate method to obtain power and heat input measurement for complex waveforms. An abundant literature reaches the same conclusion as a new study by Joseph [93]. The study revealed that the most appropriate method to calculate heat input for complex waveforms is Average Instantaneous Power (AIP), which requires the use of high-speed data acquisition of a minimum of 8-10 kHz to capture the brief change in welding waveforms. Figure 36 depicts different methods of heat input calculated. It can be clearly seen that the Average Instantaneous Power parallels the true heat input. RMS measurements of voltage and current provide up to 10% higher than true heat input. Power calculated from average voltage and current yield heat inputs up to 15% lower than actual power. In addition, pulse parameter waveforms changed heat input by 17% for a given wire feed speed, although the corresponding changes in bead shape, penetration, and dilution were small. [94-99]

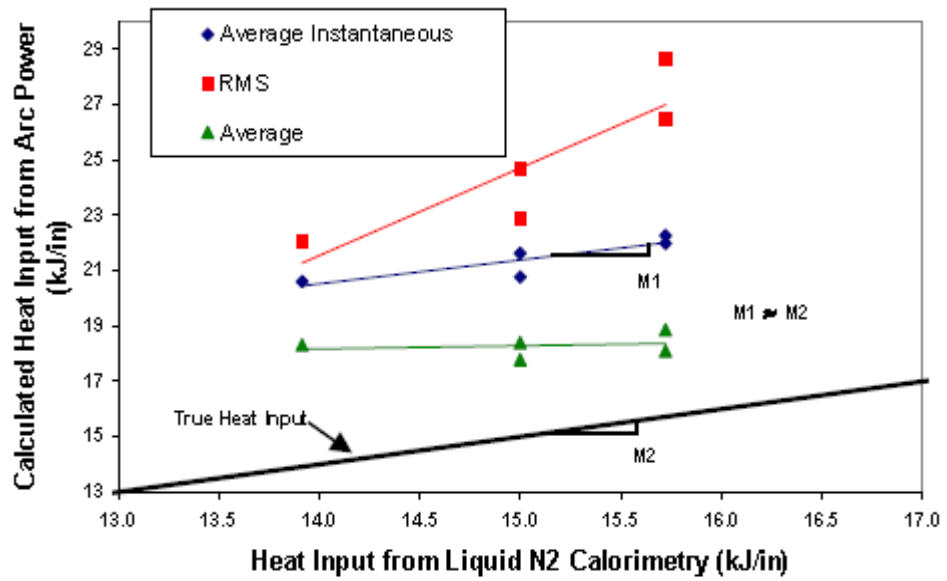


Figure 36. Graph comparing calculated heat input to actual heat input for P-GMAW [100]

The current trend is to fully integrate complex waveforms in standard codes, because the welding power source needs to capture data and calculate heat input, i.e. the trend is to avoid specific data acquisition devices. A new approach as suggested by ASME Section IX is for power sources that compute complex waveforms to directly output an energy reading made using instantaneous measurement and calculation methods. The heat input is calculated by dividing the energy reading by the length of the weld, as shown in Equations (3) and (4). [101]

$$Q(\text{Joules/mm}) = \frac{\text{Energy (J)}}{\text{Weld bead length (mm)}} \quad (3)$$

or

$$Q(\text{Joules/mm}) = \frac{\text{Power (J/s)} \times \text{Arc times (s)}}{\text{Weld bead length (mm)}} \quad (4)$$

5 COMPARISON BETWEEN CONVENTIONAL AND ADAPTIVE GMAW

Table 8 compares different approaches of the adaptive GMAW process. The concepts differ depending on the parameters being controlled. The main concerns are; the electrode extension control, the current polarity control, the waveform current and voltage control, the electrode reversal control, the combination of waveform and electrode reversal control, and the combination of different transfer modes.

Electrode extension significantly improves the melting rate; however, it requires a high current and it is only applied in automated welding. The variable polarities overcome difficulties in welding aluminium. With a direct negative electrode, the melting rate is higher but specific requirements for the zero fast crossing and low dilution are drawbacks.

The pulse allows better control of droplet transfer, which reduces spatter; unfortunately, the arc should be long to prevent any unexpected short arc during metal transfer. When a short circuit is needed, the software controls the percentage of short circuit occurrence to reduce spatter. Waveform control of the short circuiting transfer mode reduces spatter and heat input and increases welding speed. With a reversal electrode, the heat is reduced by a low current at the electrode pinch. The process needs a special torch, and a special waveform, if added, results in even lower heat and an increase in welding speed.

Table 8. Comparison between conventional and adaptive GMAW process [102]

Category		Advantage	Limitation	Examples
Conventional		Low cost equipment	Unstable arc, higher spatter	
Adaptive	Extended electrode – High current spray	High deposition rate, 15 Kg/hr	High current, Automatic only, steel or resistive wire high range current capacity of power source	T.I.M.E, RapidMelt, MIGFAST
	Extended electrode – low current dip	Low heat input at low current for thin material	High current, Automatic only, steel or resistive wire, high range current capacity of power source	MIGFAST Rapidarc Forcedarc DeepArc
	AC Pulsed	Low heat input, Melting rate increase with EN ratio, welding of aluminium	Fast reactive equipment to overcome polarity crossing	Cold process, AC-MIG process
	DC Electrode Negative	High deposition rate, low heat input to plate	Argon based gas, low dilution	Used with metal cored wires
	Short arc spray	Low fume, deep penetration	Needs appropriate dynamic characteristics	ForceArc, HD-pulse WiseFusion
	Pulsed drop spray	One drop per pulse, low spatter ease of control	Long arc, difficult root control	
	Pulsed spray	Smooth transfer	Less robust control	

	Current controlled dip	Low spatter, lower heat input, good root run performance	Limited to thin section.	STT, RMD, WiseRoot, Cold Arc, Cold Process, Optarc
	Wire controlled Dip	Dip with larger wire diameters, simple power source	More complex feed system	CSC
	Current + wire controlled dip	Low heat input, high speed on thin material, Fe and Al alloys	Normally automatic	CMT
	Dual Pulse	Improved control, TIG like bead appearance	Require careful selection of balance between high and low frequency	

6 ADAPTIVE GMAW PROCESS: WISEROOT™, WISEFUSION™ AND WISEPENETRATION™

The Wise concept from Kemppi Oy started with the introduction in September 2005 of the FastRoot process. FastRoot was designed for root pass and thin sheet metal, mainly for structural and stainless steel. The process digitally controls the power source's current and voltage. Its ability to weld thin sensitive sections and its gap bridge-ability has been successfully tested [103]. The concept is a software application that can be installed in specific Kemppi welding machines. New adaptive processes that have subsequently emerged, such as WiseRoot, WiseThin, WiseFusion and WisePenetration, are detailed in the paragraphs below. [104]

6.1 WiseRoot™

The patented WiseRoot process controls the power source's current and voltage parameters digitally. The principle by which the WiseRoot process operates is illustrated in Figure 37. Comparison with a conventional dip transfer mode clearly shows the difference that characterises the innovation. The curve is a modified short circuit and presents two main periods: the short circuit and the arc period. The process monitors the short circuit and ensures correct timing of the filler droplet's transmission from the filler wire into the weld pool. This is a modified short-arc welding process and as a MIG/MAG welding process it is in category 131, 135, 136, or 137 as defined in the EN ISO 4063 standard. [104-106]

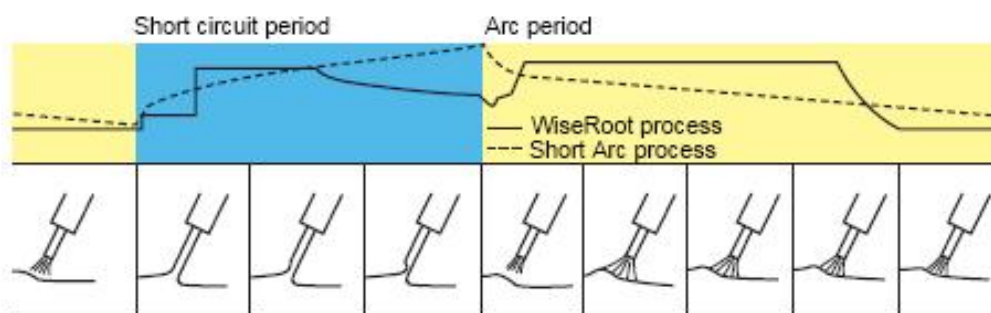


Figure 37. Current waveform of WiseRoot compared with a conventional current waveform [106]

In the first upslope stage, there is a short peak in the welding current, during which the filler material wire contacts the weld pool; the rapid increase of the current to the desired level generates a so-called pinch force, which allows the droplet to detach from the tip of the filler wire. The detachment is ensured by slowly decreasing the current. Once the droplet has been transmitted to the weld pool, a second stage of increasing current begins and initiates the arc stage. The control system of the device monitors the droplet detachment moment throughout the arc. Correctly timed rise and fall of the current guarantees a spatter-free transfer from the short circuit to the open arc. [105, 106]

The second upslope stage is characterised by a sudden increase that is sustained at the desired level. The second upslope stage shapes the weld pool and ensures sufficient penetration in the root pass. After the two upslope stages, one following upon the other, the current is reduced to the desired base level. Use of a specified base current level ensures that the next filler droplet will be transmitted during the next short circuit.

In normal short arc welding, as illustrated in Figure 37, droplet detachment occurs at a high current value, which depends on the voltage control. After that, the current slowly decreases, prior to the arc period ending, and the next short circuit begins. In the WiseRoot process, droplet detachment happens at a low current value, which results in soft transmission to the weld pool. After that, in the arc period, the process gives a precisely measured strong boost to the arc and then rapidly cuts the current to the predetermined level before the next short circuit. A rapid response and correct timing in the power source control combine with the correct shape of the current waveform to allow uninterrupted, spatter-free droplet detachment and transmission into the weld pool. This keeps the arc stable and the welding process easy to control.

Below is a list of the key benefits of the modified root pass welding process:
[105, 106]

- Easy to learn and use.
- Fewer spatters than with a normal short arc.

- Wider root gap makes it possible to use a smaller groove angle and decrease groove volume.
- No need for use of a backing ring.
- A highly efficient process: 10 % faster than normal MAG welding, and three times faster than TIG welding.
- Suitable for different position welding

6.2 WiseThin™

GMAW process has developed such that it is now possible to weld with low heat input, especially in the short-arc area. For sheet metal welding, low heat input is a desirable feature and various laser-welding applications have been used for this purpose. However, lasers have their limitations. As regards sheet metal laser welding applications, the biggest problems arise from the narrow gap tolerances. The tolerance window is wider with GMAW processes because they are not so sensitive to air gap variations. WiseThin is a modified short-arc welding process and as a GMAW process is in categories 131, 135, 136, or 137 as defined in the EN ISO 4063 standard. [105, 106]

The principle of the WiseThin process is similar to that of the tailored WiseRoot process for root pass welding. The difference is that WiseThin is optimised for sheet metal welding. Kemppi's WiseThin is a tailored GMAW short-arc process that enables 5–25 % less heat input than with a normal short arc, depending on the welding case. In welding of high-strength steels, this is of great benefit, because its microstructure is sensitive to heat and impossible to restore by post weld treatments. [105, 106]

6.3 WisePenetration™

In the manual GMAW process, the stick-out length always varies to some extent, depending on the welder's skills, and this has an effect on the weld penetration. Sometimes the welder must increase the stick-out length because of limited

visibility or accessibility, out-of-position welding, difficult joints or weld design problems.

In mechanised and automated welding, dimensional and geometrical deviations of the joints can cause variation of stick-out length. These deviations can originate from various phases of the joint preparation or fit up work. The welding heat also causes distortion, which increases deviations during welding. Various joint tracking systems can be used to alleviate this problem, but they are expensive and do not operate reliably in all welding conditions.

WisePenetration offers constant welding current with stick-out length within limits defined in the welding procedure specification (WPS). When welding with stick-out lengths within the permitted limits, WisePenetration operates like a conventional GMAW process and allows the welding current to fluctuate with the stick-out length. However, if the stick-out length increases above the permitted level, WisePenetration takes control and ensures that the current remains constant.

Changes in stick-out length have no effect on wire feed speed or arc voltage. Instead, welding current fluctuates according to the changes in stick-out length.

As an example, Figure 38 shows how welding current changes with stick-out length when welding S235 steel with 1.2 mm wire and using Ar + 18% CO₂ shielding gas and the following welding parameters: wire feed speed 8.8 m/min, voltage 29 V, travel speed 58.0 cm/min. [105, 106]

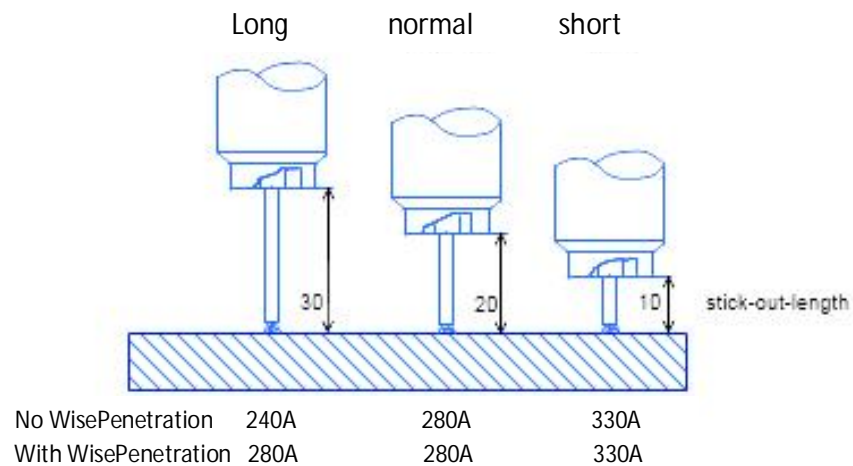


Figure 38. Welding current changes with the stick-out length [107]

6.4 WiseFusion™ function

The WiseFusion function keeps arc length more constant and prevents the arc from becoming longer as the stick-out length changes. In out-of-position welding (other than flat or horizontal vertical), during traditional GMAW, the most common problem is how to control the welding arc and the molten weld pool. This issue is accentuated in pulse arc and spray arc welding. For example, it is very difficult to find the correct pulse welding parameters when welding aluminium in the horizontal overhead position. To meet the needs of all position welding, the arc length is kept constant and prevents the arc from becoming longer as stick-out length changes.

The principle of the WiseFusion function is based on controlled regulation of the pulse or spray arc current and voltage waveform, as seen in Figure 39. Welding in the medium current globule transfer region to high-current spray transfer region is carried out as spray transfer welding, it is possible to reduce spatter but there is an increase in heat input to the base metal. As the problems of humping and undercut occur when high speed is performed, in many cases welding is applied with lower welding voltage.

To increase travel speed, in normal pulse welding waveform, the arc length must be kept short, the number of short circuits increases and short circuit is at the

pulse peak current. Consequently, short arc length results in stubbing, humping and spatter. The WiseFusion control short circuit occurrence in the waveforms at low current, which minimizes spatter and keep the arc focused for optimum energy. The percentage of short circuit occurrence can be adjusted by selection to the power source to improve weld quality and efficiency. In pulsed arc WiseFusion welding, the %-value indicates the number of short circuits in a pulse sequence. For example, if %-value is 50, half of the droplets detach in open arc and half of them in short circuit. The power source keeps track of the number of short circuits so that it remains on the level defined by the WiseFusion %-value. [105, 106]

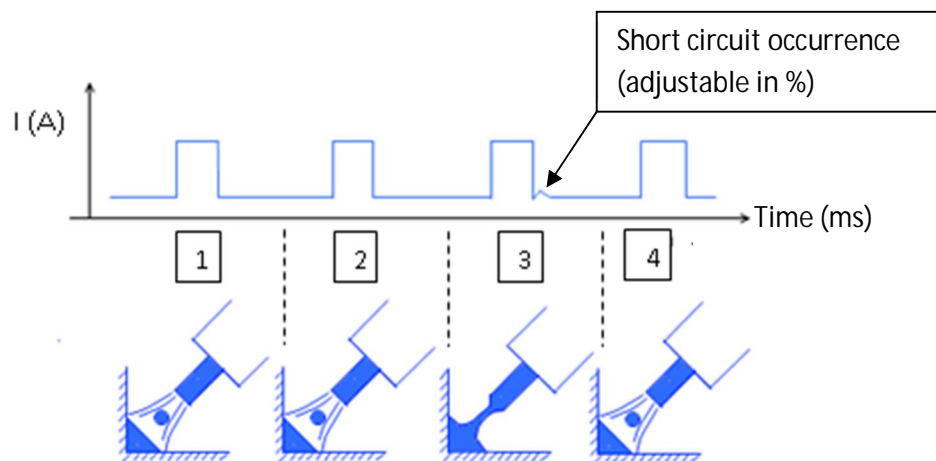


Figure 39. Pulse sequence where the filler droplet short-circuits before detaching [107]

7 EXPERIMENTS

The experiments in this thesis aim to identify advantages from using the adaptive pulsed GMAW process. Optimal parameters are selected with respect to the small number of specimens, material cross-section and time available. The section is divided into four sub-sections: The first sub-section defines the usability targeted in this study. The second sub-section then presents consumables such as the base material composition and properties, as well as the filler wire and shielding gas. The third sub-section describes welding equipment characteristics to understand the hypothesis of the welding experiment. The last part describes the welding procedure and includes weld design, weld processes and different tests.

7.1 Usability of the process

One of the primary objectives of this study is to evaluate the usability of adaptive pulsed GMAW processes. Usability is defined as the ability to produce reliable, high quality, cost effective welds, over a wide range of gap widths and welding parameters, even when the welded joint contains gouges or other local defects.

A higher melting rate involves not only a larger quantity of filler material melted, but also a higher arc heat input, which may have an unfavourable effect on the mechanical properties of the weld. In welding, it is, therefore, necessary to be cautious and take into account the chemical composition and the mechanical properties of the material. [108]

The usability must also be based on the ability of the final weldment to pass non-destructive as well as destructive, testing with a low reject rate. As with conventional GMAW methods, high-current arc welding is characterized by a very deep weld pool depression (gouging region), where the molten metal under the arc turns into a thin film that flows toward a bulk of liquid (trailing region) at the rear of the weld pool. This large depression is the direct cause of several weld pool defects such as humping, undercutting, split bead, parallel humping, and tunnel porosity. [54]

7.2 Materials

The material and filler material must match and present a high degree of weldability. The driving forces behind the choice of structural steel for this study is based on their increasing use, often connected to a wish to achieve the best structural performance at the lowest possible weight and cost. One should consider, for example, that by using thermo-mechanically controlled process structural steel, it is possible to reduce the material thickness and deadweight of a structure, which in turn gives higher payloads.

7.2.1 Base metals

S355 MC structural steel plate is a low-alloy European standard structural steel, EN 100149 – 2, with a yield strength of 355 MPa, MC refers to thermo-mechanically rolled (M) and cold formable (C). Careful attention should always be placed on the specific variation of S355 required if considering substitute material. S355 MC is very widely used and typical applications include:

- Structural steel works: bridge components, and components for offshore structures
- Power plants
- Mining and earth-moving equipment
- Load-handling equipment
- Wind tower components

Table 9 and 10 present respectively the chemical and tensile properties of S355MC .

Table 9. Chemical properties of S355 MC [109]

Symbol	Chemical composition, (wt%)					
	C	Si	Mn	P	S	Al
S355 MC	≤0.12	≤0.03	≤1.50	≤0.020	≤0.015	≥0.015

Table 10. Tensile properties transverse of S355 MC [109]

Symbol	Tensile properties		
	R _e (MPa)	R _m (MPa)	Strain at fracture (%)
S355 MC	355	430-530	18

Hydrogen cracking is one of the main problems that has to be considered when welding steel structures. Hydrogen cracking is also called cold cracking or delayed cracking and occurs at temperatures below 200°C. Crack formation is often delayed and it can appear a few days after welding. A common requirement is that inspection should not be performed before, at the earliest, 16 or 24 hours after welding.

For cracking to occur, three simultaneous conditions are necessary: [2]

- The presence of hydrogen.
- A sensitive microstructure (usually martensite) or a high carbon equivalent.
- High tensile stresses.

For hydrogen cracking to occur, the microstructure has to be hard and brittle. The martensitic microstructure is particularly sensitive to hydrogen cracking. The carbon equivalent is a measure of the weldability of the material. A high carbon equivalent indicates an increased risk of hydrogen cracking. There are several different carbon equivalents. The most common is (IIW) Equation (5): [2]

$$CE(IIW) = C + \frac{Mn}{6} + \frac{(Cu + Ni)}{15} + \frac{(Cr + Mo + V)}{5} \quad (5)$$

As a rule of thumb, materials or weld metals with a $CE(IIW) \leq 0.40$ are not sensitive to hydrogen cracking. The material selected for the experiment in this Thesis meet the condition $CE(IIW) = 0.37$.

High tensile stresses are caused by residual stresses. Residual stresses up to the yield strength of the weld metal are nearly always present in a welded joint. Residual stresses are the driving force for hydrogen cracking. Factors that influence the level of residual stresses are the level of restraint, plate thickness, joint fit-up, weld geometry, weld sequence, and the filler material strength [2].

7.2.2 Filler metal

Classification EN ISO 14341-A G3Si1 and approval SFS EN 440, OK Autrod 12.51 is an ESAB copper-coated, Mn-Si-alloyed G3Si1/ER70S-6 solid wire for the GMAW of non-alloyed steels, as used in general construction, pressure vessel manufacture and shipbuilding. The diameter of the consumable electrode used during the experiment was 1.0 mm. When welding low alloy steels, filler wire generally contains less than 0.2 % carbon and less than 0.5% of other elements such as manganese, nickel, chromium and molybdenum. Unfortunately, low alloy steels and consumable electrode may also have impurities like phosphorus, sulphur, oxygen and nitrogen, which must be kept at a minimum to prevent harmful effects on the weldment (Table 11). [110]

Typical applications of G3Si1 are found in general steel construction and the welding of pipes. It is suited for the production of (multi-layer) fillet and butt welds in all welding positions and can be welded with Ar/CO₂ mixed shielding gas or with pure CO₂.

Table 11. Chemical properties of the consumable electrode [111]

Symbol	Chemical composition, (wt%)								
	C	Si	Mn	P	S	Ni	Mo	Al	Ti+Zr
G3Si1	0.06-0.14	0.70-1.00	1.30-1.60	0.025	0.025	0.15	0.15	0.02	0.15

7.2.3 Shielding gas

Argon is one of the most popular shielding gases, thanks to its suitable properties. As an inert gas, it has no chemical interaction with other materials. CO₂, or a small amount of oxygen, improve the welding properties, especially for short arc welding. A content of up to 20% CO₂ improves the penetration (limits the risk of lack of fusion) while 5-8% will give reduced spatter. Therefore, a mixture of 82% Argon and 18% CO₂ was selected for the experiment. [1, 6, 15]

7.3 Experimental set-up

Figure 40 presents the welding setting of the workstation. The set-up used during the experiment included a gas regulator, welding machine, a support torch mechanized unit, a flexible fume extractor and workpiece support, and fixtures. The power source characteristic and electrode filler wire were read on the machine rating data plate.

The power source was FastMIG 450 from Kemppi Oy, which is digitally controlled multi-process equipment. FastMIG 450 can be shifted from synergic GMAW to synergic pulsed or Wise GMAW processes. The Wise concept software was installed in the equipment used during the experiment. The indication on the rating plate showed the International and European Standard IEC/EN 60974-1-5-10 class and specifies demands on power sources regarding electrical safety. The enclosure class is IP 23 S and the power source rating is determined by its duty cycle, which indicates for what proportion of a period of ten minutes that the power source can be operated at the specified load. 450 A at 60 % duty factor, means that the power source can supply 450 A for 6 minutes in every ten minutes indefinitely without overheating.

According to the wire feeder specification unit, it is designed with respect to EC/EN 60974-5-10 JB/T 9533-1999 with 550 A of 60 % duty. The range of wire feed speed varies from 1 to 25 m/min.

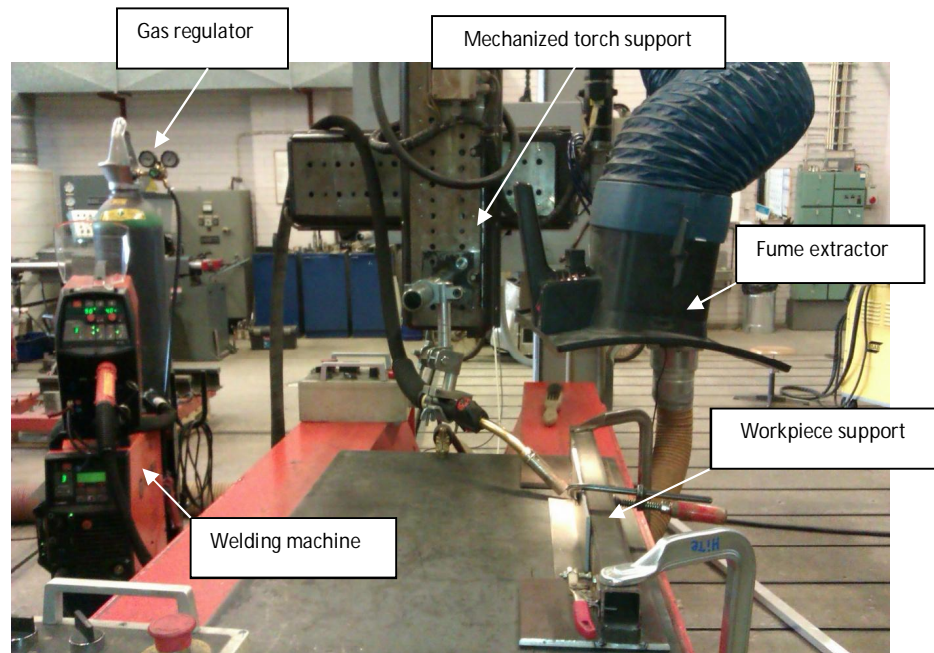


Figure 40. Welding equipment and setting

7.4 Experimental procedure

The evaluation of usability was tested on a T-joint, as shown in Figure 41. The runs were carried out with welding processes such as (1) synergic pulsed GMAW, (2) WiseFusion and (3) synergic GMAW. Welding parameters such as welding speed, wire feed rate, gas flow, and CTWD were kept constant and a calibrated digital oscilloscope was used as data acquisition equipment for amperage and voltage values storage. The specimens were inspected and different tests were performed to identify the benefits of adaptive pulsed GMAW and to provide a better perspective regarding acceptable welds (i.e. good sidewall fusion, no centre line cracking, no undercut, and very little spatter).

7.4.1 Sample preparation

Structural steel plates S355 MC with the dimensions of 5x100x300 were prepared. Ten parts were cut to produce five specimens of the same size. A positional weld was then performed to constitute a T-joint. An increasing gap between the workpieces from 0 to 2.5 mm was calibrated for each specimen. Figure 41 shows

the position of the upright and base member as well as the electrode orientation and travel direction.

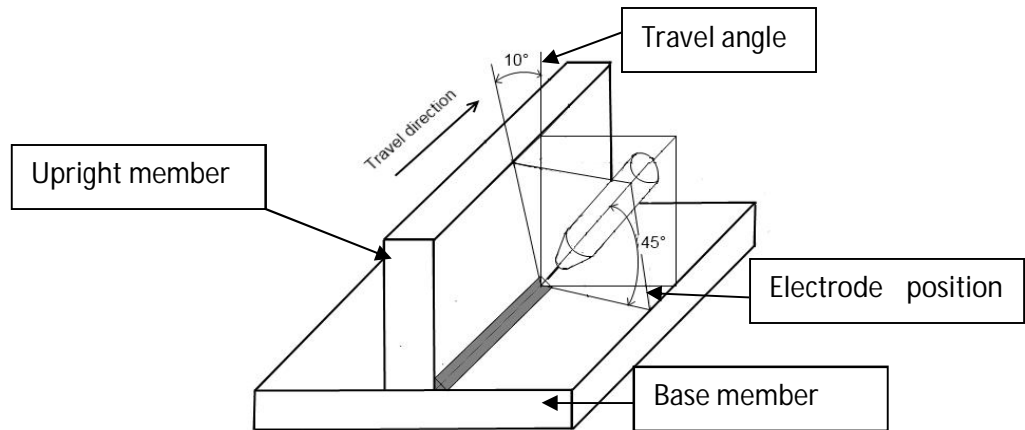


Figure 41. Welding design and electrode orientation in horizontal position

Travel angle refers to the angle of the welding gun in the direction of travel. The electrode position is at a 45° angle between the top and bottom base metal and about 10° – 15° in the direction of travel. The travel angle is for left-hand welds. A right-hand welder would tilt the welding gun 10° – 15° to the right. If the welding gun were closer to the vertical, the weld would penetrate more of the base member and have insufficient fusion to the upright member. [1]

7.4.2 Visual inspection of the specimens

Visual examination (VT) SFS-EN 970 is the non-destructive examination method used most extensively for weldments. The technique is used to detect inaccuracies in size and shape, surface cracks and porosity, undercut, overlap and crater faults. The control is performed at the end of the welding process, as well as during the operation. [6, 112]

7.4.3 Metallographic specimens preparation

The metallographic process analysis was based on the SFS-EN 1321 standard. Metallographic specimen preparation began with a sectioning operation. Specimens were sectioned at specific air gaps corresponding to 0, 1 and 2 mm. The base metal was re-sized using a saw to provide convenient measurement on the grinding machine and to permit focus on the weld zone and its immediate vicinity. No mounting operation was performed since the cut specimens were large enough for handling during preparation and examination. In addition, sharp edges and corners were eliminated to increase safety and to avoid damage to the papers and cloths used in preparation.

In the grinding operation, the section surface was roughened using successively finer grades of silicon carbide papers starting from a grit size of 80 and following with 120, 220, 500 and finally 800. The surface was then polished with a radial contact finishing grinding machine to remove a surface layer of about 6 μm . A bright mirror-like polished surface, free of scratches, was obtained.

Etching was done to reveal the microstructure of the specimens and show the weld bead penetration. Nital etchants, containing 4 % nitric acid (HNO_3) in ethanol, were used to produce variation of contrast for optical examination.

7.4.4 Vickers hardness test

The hardness test was based on the SFS-EN 1043-2 destructive test on welds in metallic materials [113]. A DuraScan hardness tester was used, which is a state-of-the-art hardness testing system covering many applications, with a unique test load range from 10^{-3} kgf (0,098 N) to 10 kgf (98,07 N). Fully automatic test cycles and hardness evaluation ensure the highest repeatability and reproducibility. The optional overview camera makes it easy to select starting points and test series with just a few mouse clicks. Figure 42 shows the heat affected zone, fusion line and fusion zone, and Figure 43 presents the hardness

test line and its orientation for the Vickers hardness test. It can be seen that the line covers the important areas targeted by the test.

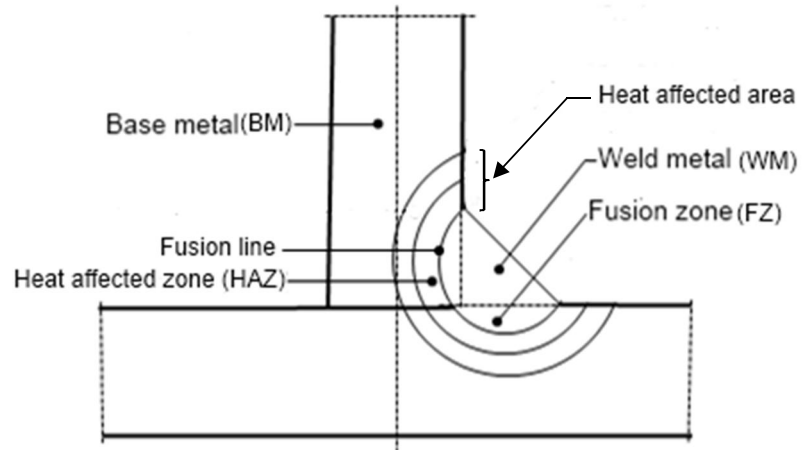


Figure 42. Weld profile description

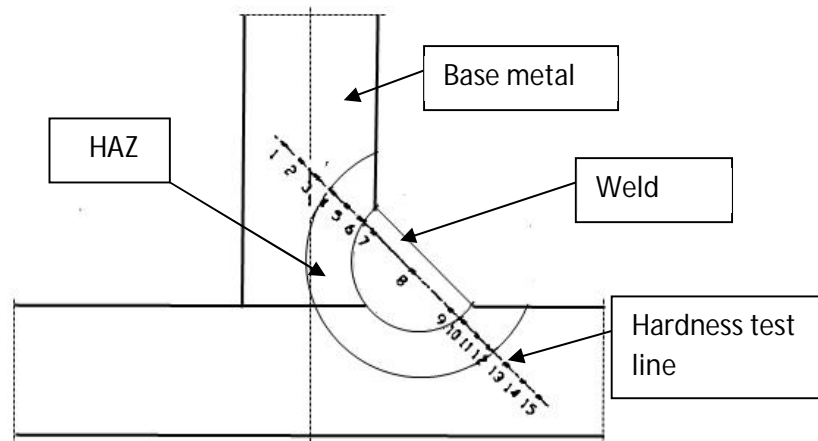


Figure 43. Profile repartition of hardness test

7.4.5 Bead penetration measurement

Bead penetration measurements help to understand the interrelationship between variations of current, voltage and weld bead penetration of the adaptive pulsed GMAW process. Figure 44 shows different measurements investigated during bead penetration evaluation.

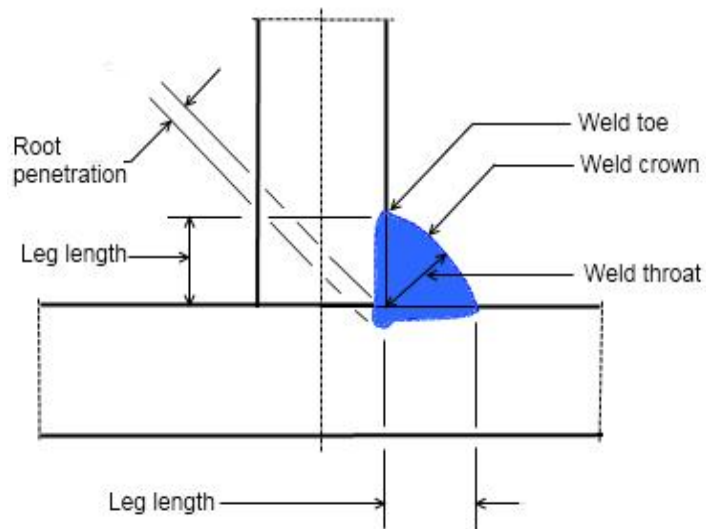


Figure 44. Bead penetration measurement

7.4.6 Dilution analysis

Dilution is the measurement used to describe the amount of penetration in terms of the base metal. It is described in terms of a percentage of base material within the deposit. Figure 45 depicts dilution areas. The cross section of the weld was divided into three sub-surfaces, and AutoCAD 2011 was used to estimate the areas a, b and c, and the dilution was then calculated based on Equation (6). [114]

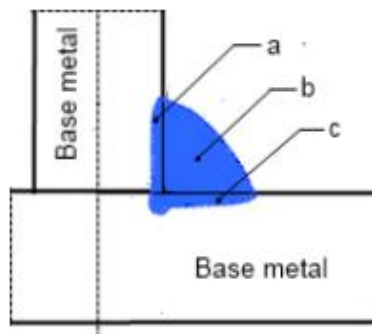


Figure 45. Filler metal dilution [114]

$$\% \text{ dilution} = \frac{a+c}{a+b+c} \times 100 \quad (6) \quad [114]$$

8 RESULTS AND DISCUSSION

The results of the welding process described in this work are discussed in this section. The discussion compares the visual appearance of specimens and data values during welding performance and after welding analysis. Thus, four main issues are considered; the heat input, the visual inspection of the weld, the penetration of the weld, and the microstructure analysis and Vickers hardness test.

8.1 Heat input

The same values were used for wire feeding speed, welding speed, flow gas, CTWD as in Table 12. The highest current and voltage were observed when applying synergic GMAW and the lowest values were noticed with WiseFusion. Consequently, the reduction in current and voltage affected the heat input. In addition, Table 12 shows that the percentage number of short circuits has no effect on the heat input when operating with WiseFusion. Lower spatter and a more stable arc were found with WiseFusion compared to synergic pulsed GMAW, and higher spatter was observed with the synergic GMAW process. The results are similar from claims by the manufacturer. The difference between the synergic GMAW and WiseRoot in the software manual [107] can be justified by the different parameters applied during the experiments. In addition, the welding procedure of the experiments may be the reason for variation in the outcome of the results, as may be the small number of samples.

Table 12. Welding experiment parameters

Test	Processes	I [A]	U [V]	Ws [cm/min]	Wfs [m/min]	Flow gas [L/min]	CTWD [mm]	Q [kJ/mm]
1	Synergic pulsed	170	26.7	34	9	14	18	0.64
2	WiseFusion™ (35% short circuit)	167	25.1	34	9	14	18	0.59
3	WiseFusion™ (50% short circuit)	167	25.1	34	9	14	18	0.59
4	WiseFusion™ (20% short circuit)	167	25.1	34	9	14	18	0.59
5	Synergic GMAW	200	24.3	34	9	14	18	0.69

8.2 Visual inspection of the weld

Comparisons of the weld joints by visual inspection did not immediately reveal apparent differences, as can be seen from Figures 46 to 50 below, particularly when attempting to differentiate synergic pulsed GMAW and WiseFusion welded joints. However, closer inspection permitted some conclusions to be drawn and these are highlighted in the next paragraph.

Visual inspection performed during welding indicated that the arc process was much more stable with WiseFusion than when using conventional welding, and resulted in fewer spatters. Visual inspection after the weld (Figure 46) showed a good bead appearance from 0 mm up to 1.5 mm gap, then the quality started decreasing, with less convexity. The appearance was worst from 2.3 mm, indicating the unsuitability of synergic pulsed GMAW for use above the 2.3 mm gap limit.

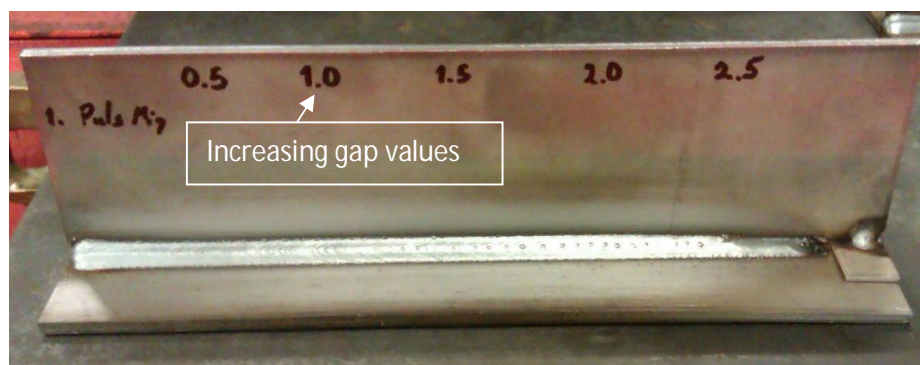


Figure 46. Increasing gap values bead appearance of the Synergic Pulsed GMAW process welded specimen.

The experiment performed with synergic GMAW was unstable; there was spatter and the process was noisy. Visual inspection revealed spatter, which will require cleaning and extra work in production, and consequently additional cost. The bead appearance in Figure 47 is acceptable from 0 mm to 1.5 mm gap, after which it started reducing dramatically in both size and in quality. The effects of heat on the surface of the base metal around the weld indicated that a coated layer, had there been one, would have been negatively affected.

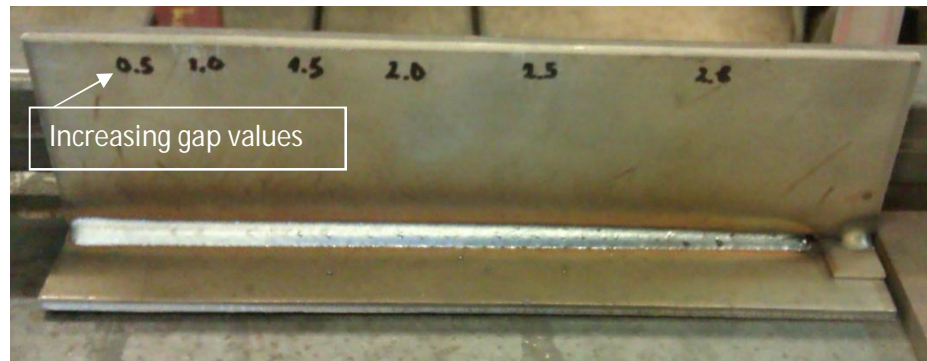


Figure 47. Increasing gap values bead appearance of the Synergic GMAW process welded specimen.

WiseFusion™ demonstrated a far more stable arc compared to synergic GMAW and a slightly better arc than the synergic pulsed GMAW process. There was very low spatter and little noise. It was however not easy to really notice the difference when changing the percentage. Figure 48 shows the specimen obtained from the default curve at 35% short circuit, then a random setting at 20% and a 50% short circuit. Examination of the 35% and 50% (Figures 48 and 49) welded specimens, shows good bead appearance up to 1.5 mm gap then the size decreases steadily. For 20% (Figure 50) the quality is better and reaches 2 mm air gap. Further analysis, for example cross section microstructure study, indicated that the shrinkage of the weld in the side was caused by molten metal that had flowed in the air gap. The heat effect on the base metal layer could clearly be observed, with accentuation on the lower percentage welded specimen, but its impact was not evaluated in this study.

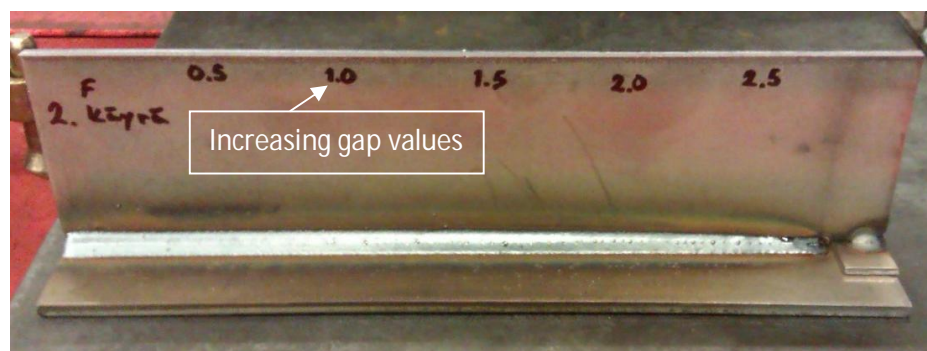


Figure 48. Increasing gap values sample using WiseFusion™ , 35% short circuit.

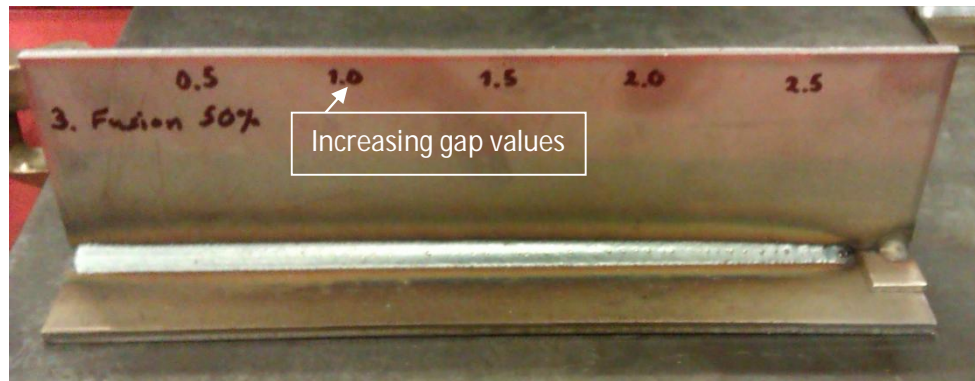


Figure 49. Increasing gap values sample using WiseFusion™, 50% short circuit.



Figure 50. Increasing gap values sample using WiseFusion™, 20% short circuit.

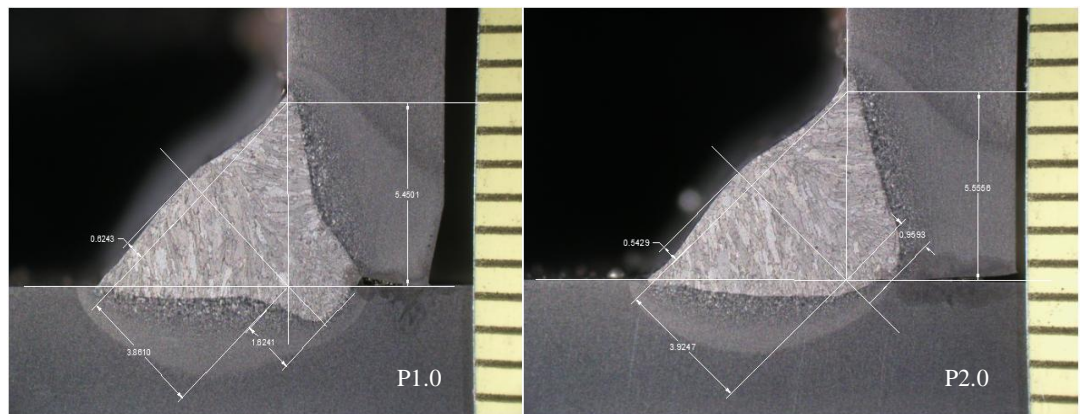
8.3 Macro-sections analysis

Macro-sections analysis was used to evaluate the wall and root penetration, as well as the throat (Figures 51, 52 and 53). Three different categories of air gap were considered (0; 1 and 2 mm) and cut from five weld specimens. The images were attached in AutoCAD 2011 version, and scaled measurements of convexity, throat leg length and root penetration were then carried out. Table 13 shows different specimens cut from the welded samples.

Table 13. Specimen designation

Processes		Air gap		
		0 mm	1 mm	2 mm
Synergic Pulsed GMAW		P1.0	P1.1	P1.2
WiseFusion™	35 % short-circuit	P2.0	P2.1	P2.2
	50% short-circuit	/	P3.1	P3.2
	20% short-circuit	/	P4.1	P4.2
Synergic GMAW		/	P5.1	P5.2

The Figures 51 (a) and (b) present respectively samples from the specimens welded using synergic pulsed GMAW (P1.0) and the WiseFusion™ default curve at 35% of short circuit (P2.0) at 0 gap of the T-joint. It can be seen that the heat affected zone of P1.0 is higher than that of P2.0, which confirms the increase in heat input resulting when using the synergic pulsed GMAW process. In addition, there is a significant difference of root penetration length and profiles; however, both samples present quite similar legs length.



(a)

(b)

Figure 51. Cross section dilution analysis at 0 air gap (a) Synergic Pulsed GMAW (b) Default curve 35% short circuit.

Table 14 clearly shows slight differences in the weld measurements. It can be observed that the leg length of P2.0 is 0.1 mm longer than P1.0, and 0.06 longer at its throat. However, the convexity of P2.0 is 0.08 lower than P1.0, and root penetration 0.66 smaller.

Table 14. Weld dimension at 0 mm gap

Specimen	Leg length (mm)	Throat (mm)	Convexity (mm)	Root penetration(mm)
P1.0	5.4501	3.8610	0.6243	1.6241
P2.0	5.5556	3.9247	0.5429	0.9593

Figure 52 (a) shows a synergic pulsed sample and Figure 52 (b) depicts the WiseFusion default curve at 35% short circuit from a welded specimen at 1 mm gap of the T-joint. The heat affected zone in P1.1 is larger than in P2.1, which confirms the increase in heat input resulting from using the synergic pulsed GMAW process. Table 15 presents measurements of the weld from five samples at 1 mm air gap. The difference in root penetration length between P1.1 and P2.1 is rather small, about 0.01 mm. However, both samples present quite similar legs length. It can be observed that the convexity using the default curve at 35% is symmetric, which is advantageous in stress repartition.

Analysis of the effect of the short circuiting percentage on the penetration measurements in Table 15 reveals that the wall penetration increases with the increase in the number of short circuits. The penetration is significantly higher at 35% and 50% (Fig. 52 b and c) short circuiting, respectively P2.1 and P3.1. It can be also observed that the legs lengths of P2.1 and P3.1 are longer than P4.1 (Fig. 52 d) with 20% short circuiting, about 0.2 mm. Moreover, it is evident that the lower the percentage of short arc, the closer the weld shape is to the synergic pulsed GMAW process. The synergic GMAW process, sample P5.1, presents the

lowest penetration and a greater porosity defect, indicated by the red circle and arrow in Figure 52 (e).

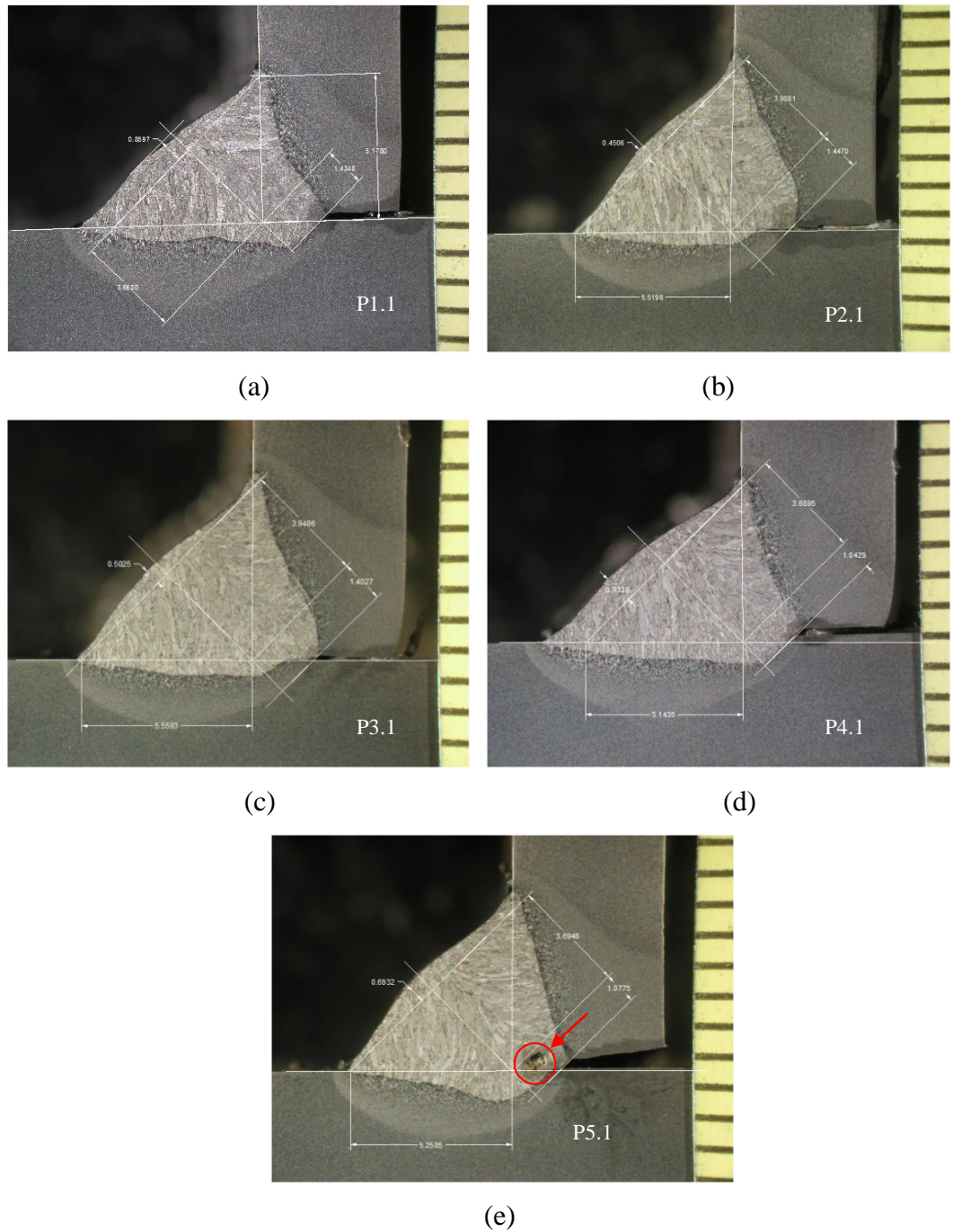


Figure 52. Cross section dilution analysis at 1 mm gap (a) Synergic Pulsed GMAW (b) WiseFusion 35% short circuit, (c) 50%, (d) 20% and (e) Synergic GMAW.

Table 15. Weld dimension at 1 mm gap

Specimen	Leg length (mm)	Throat (mm)	Convexity (mm)	Root penetration(mm)
P1.1	5.1780	3.6620	0.8597	1.4346
P2.1	5.5198	3.9081	0.4506	1.4470
P3.1	5.5593	3.9486	0.5025	1.4027
P4.1	5.1435	3.6595	0.9338	1.0429
P5.1	5.2585	3.6946	0.6932	1.0775

Figure 53 (a) and (b) describe samples welded using synergic pulsed GMAW and the WiseFusion with 35% short circuit with a 2 mm air gap of the T-joint. The heat affected zone in sample P1.2 (Fig.53 a) is larger than in sample P2.2 (Fig.53 b), which indicates an increase in heat input from using the synergic pulsed GMAW process. In addition, measurement of the weld in Table 16 indicates that a slight difference appears in root penetration length between P1.2, P2.2 and P2.3, but P4.2 is medium and P5.2 root length is the smallest. It can be observed that the vertical leg length of sample P2.2 is greater than sample P1.2 and inversely the horizontal leg of sample (a) is longer than in sample P1.2. WiseFusion shows the ability to produce symmetric share of the weld pool downward and upward regardless of the gravity force. Sample P4.2 presents the highest throat (3.7 mm) but also the lowest reinforcement, which can weaken the joint strength.

The WiseFusion gap bridgeability was evaluated and depended considerably on the percentage of short circuit. It can be noted that the bridge at 35% and 50% short circuit, sample P2.2 (Fig. 53 b) and P3.2 (Fig. 53 c), respectively is higher than the 20% short circuit sample P4.2 (Fig. 53 d). Therefore, in WiseFusion, the bridgeability decreases with the reduction in short circuit percentage.

The synergic GMAW process sample P5.2 (Fig. 53 e) exhibits an absence of root penetration and bridge ability. Moreover, the HAZ and porosity defect (red arrow) are greater, as shown in Figure 53 (e).

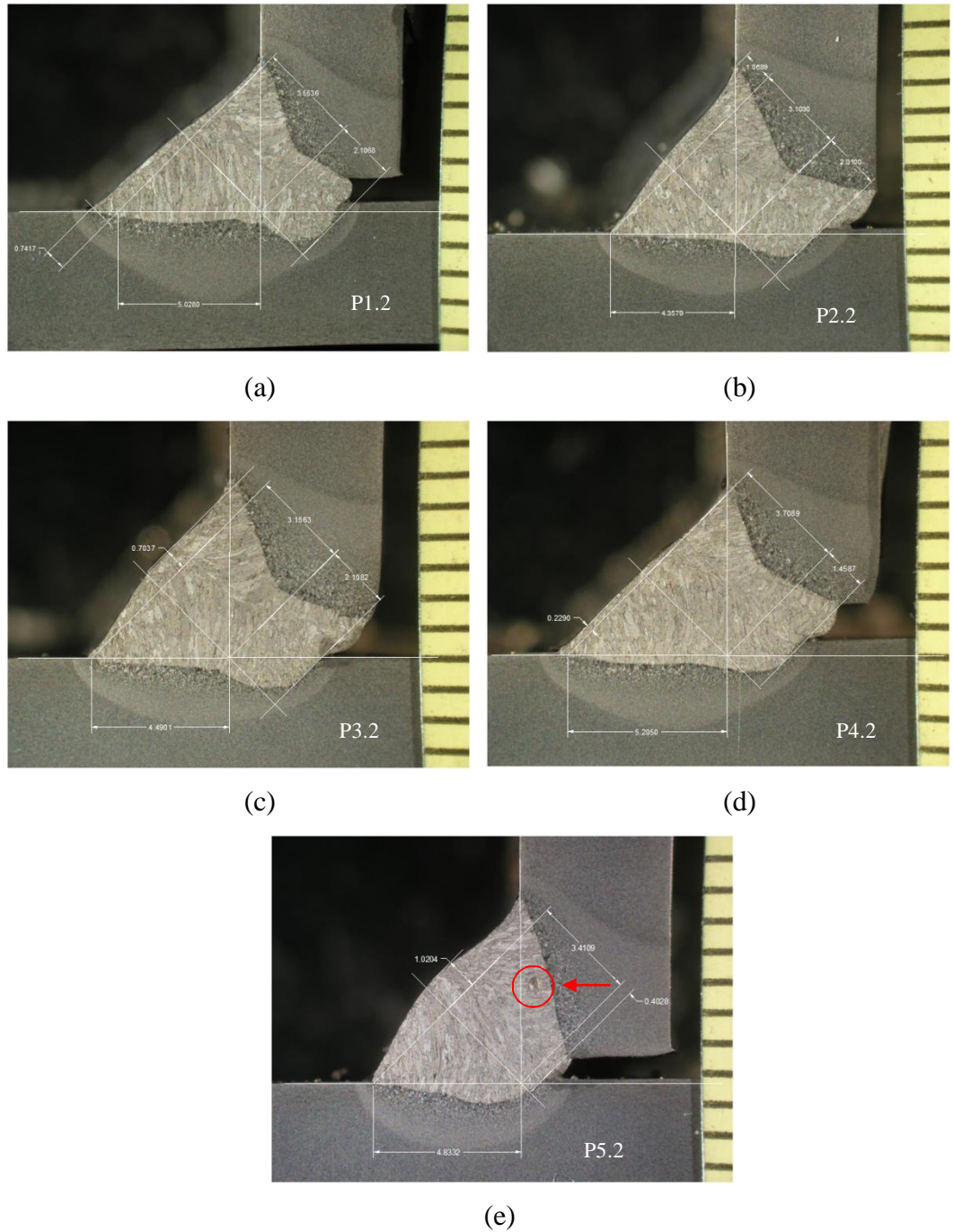


Figure 53. Cross section dilution analysis at 2 mm gap (a) Synergic Pulsed GMAW (b) WiseFusion 35% short circuit, (c) 50%, (d) 20% and (e) Synergic GMAW.

Table 16. Weld dimension at 2 mm gap

Specimen	Leg length (mm)	Throat (mm)	Convexity (mm)	Root penetration(mm)
P1.2	5.0280	3.5536	0.7417	2.1068
P2.2	4.3579	3.1030	1.0689	2.0100
P3.2	4.4901	3.1563	0.7037	2.1082
P4.2	5.2050	3.7089	0.2290	1.4587
P5.2	4.8332	3.4109	1.0204	0.4028

8.4 Dilution analysis

Dilution analysis was used to evaluate the percentage of weld metal in the base metal. The paragraph below discusses values for different air gaps. Three different categories of air gap were considered and cut from five weld specimens, thus the same macro-section images were used.

Table 17 shows specimens P1.0 and P2.0 at 0 mm gap. It can be seen that the dilution of the vertical wall of P1.0 is slightly higher than that of P2.0, at 1.8 mm², and there is a similar difference in the horizontal walls; however, the difference in the weld metal is small. The dilution percentage of P1.0 is higher than that of P2.0, a result of the heat input difference.

Table 17. Dilution comparison of P1.0 and P2.0

Area (mm²)	P1.0	P2.0
a	6.0289	5.807
b	17.9377	17.7903
c	3.8989	2.2669
Dilution %	35.6276	31.2165

The dilution at an air gap of 1 mm, presented in Table 18, is at a maximum for WiseFusion, particularly at 35% short circuit for specimen P2.1. The WiseFusion software manual states that this percentage is required for steel. The results clearly show different dilution compared with the 0 air gap. The wall dilution of the synergic controlled sample P1.1 at 3.39 mm² is lower than that of the WiseFusion sample P2.1. It should be noted that the smaller the number of short-circuits the closer the wall dilution of WiseFusion™ becomes to synergic pulsed and synergic GMAW.

Table 18. Dilution comparison at 1 mm air gap

Area (mm²)	P1.1	P2.1	P3.1	P4.1	P5.1
a	5.2963	9.0672	7.4813	4.9985	5.756
b	18.2772	17.9051	17.9363	17.5121	16.942
c	4.4947	2.0329	2.5838	4.3726	3.2768
Dilution %	34.8829	38.2693	35.9450	34.8586	34.7752

Table 19 shows a reduction of dilution as the air gap increases. There is a considerable decrease in dilution for both synergic pulsed and synergic GMAW. However, the dilution increases for WiseFusion at 50% short circuit. The

difference in the trends needs further investigation to explain the factors leading to this specific behaviour.

Table 19. Dilution comparison at 2 mm air gap

Area(mm ²)	P1.2	P2.2	P3.2	P4.2	P5.2
a	4.2725	6.3166	6.6059	4.5694	4.7618
b	17.7467	17.7779	17.7948	18.074	17.2414
c	3.0314	3.2875	3.4832	4.1374	2.3592
Dilution %	29.1566	35.0745	36.1825	32.5114	29.2295

8.5 Microstructure analysis

The heat input directly influences the microstructures formed in the weld metal [115, 116]. The typical microstructure formed in weld metal (WM) of low carbon steels consists of grain boundary ferrite (GBF), Widmanstätten ferrite (WF) (side plates), acicular ferrite (AF) and others microphases (a small amount of martensite, retained austenite or degenerate pearlite depending on the cooling rate and composition). High heat input and a low cooling rate result in coarse grain structure and consequently impart low hardness, less tensile strength and yield strength, and a less ductile weldment. [117-119]

Grain boundary ferrite (GBF) or pro-eutectoid ferrite forms along the austenite grain boundary when the weld metal is cooled in the stage of austenite-ferrite transformation. Elongated or granulated, this grain boundary ferrite grows into the austenite grain on one side of the boundary. This reaction is known as ferrite veining due to its branching aspects throughout the weld metal. [120]

Polygonal ferrite (PF) occurs in the form of coarse ferrite islands inside the prior austenite grains. Its presence reduces the toughness of the weld metal. Its amount

increases with the increase in heat input during welding and decreases with the increase in carbon and chromium content of the weld metal [121]. As PF has a poor ability to resist cracks, crack initiation occurs easily at PF and it is propagated along the PF structure. An AF structure with high dislocation enhances the tensile strength of weld metal in the joints. [119, 122]

Acicular ferrite (AF) is a microstructure of ferrite that is characterized by needle shaped crystallites or grains when viewed in two dimensions. The grains are actually three dimensional in shape and have a thin, lenticular shape. Acicular ferrite is formed in the interior of the original austenitic grains by direct nucleation from the inclusions, resulting in randomly oriented short ferrite needles with a 'basket weave' appearance. This interlocking nature, together with its fine grain size, provides maximum resistance to crack propagation by cleavage. Acicular ferrite is also characterized by high angle boundaries between the ferrite grains. This further reduces the chance of cleavage because these boundaries impede crack propagation. [119, 122]

The microstructure of the weld, for different processes and heat-input, is shown in Figures 54, 55 and 56 below with magnification scale bare 100 μm . The figures show that ferrite veining (elongated fine grain boundary ferrite), acicular ferrite and polygonal ferrite are present in the weld. It can be observed that the amount of grain boundary ferrite and polygonal ferrite decreases and the amount of acicular ferrite increases with the growth of heat-input. This can be attributed to the coarsening of the ferrite at higher heat input.

Figure 54 shows the base metal microstructure, the strength and toughness derive from very fine ferrite and second-phase microstructure (finely dispersed pearlite or bainite) that occurs during acceleration cooling of the manufacturing of thermo-mechanically controlled process. The carbon content can then be reduced and the carbon equivalent, consequently, the steel significantly improve their resistance to hydrogen-induced cold crack. However, HAZ softening, especially at high heat inputs, is a concern, because the favourable microstructure of TMCP steel is reversed during the slow cooling in the HAZ at high heat input levels. [123]

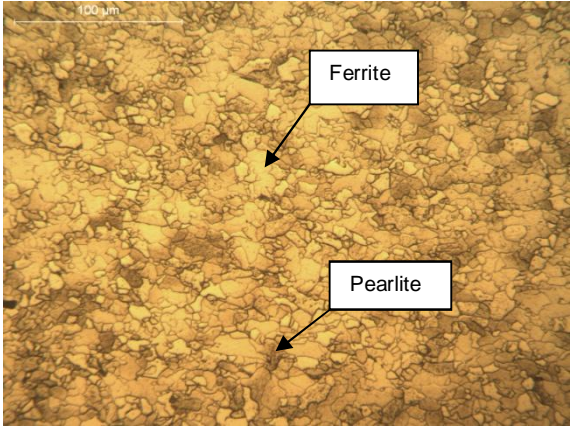
Microstructure	Observation
	<p>Base metal Ferrite (lighter area) and pearlite (darker area) resulting from the structural steel S355 MC process of manufacturing based on thermo-mechanically controlled process (TMCP)</p>

Figure 54. Microstructure of specimen P1.1 Base metal S 355 MC.

The phase transformation is observed from the base microstructure to dendritic grain structure and it is visible in the heat affected zone (HAZ) structure in Figure 55 (a), specimen P1.1, welded using the synergic pulsed GMAW process. The microstructure of the weld consists of the primary dendritic phase (lighter) and the secondary interdendritic phase (darker area) that forms during the terminal stage of solidification. A mixture of a significant amount of equi-axed dendrite grain structures and a considerable number of long columnar structures was observed in the weld zone (Figure 55 b). The weld microstructure consists of mainly acicular ferrite (AF) and Widmanstätten ferrite (WF).

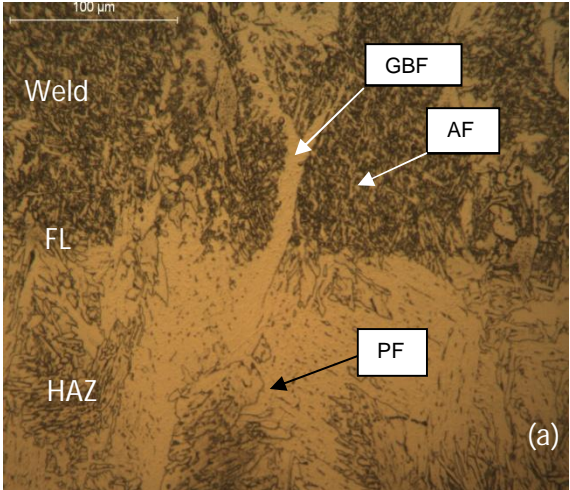
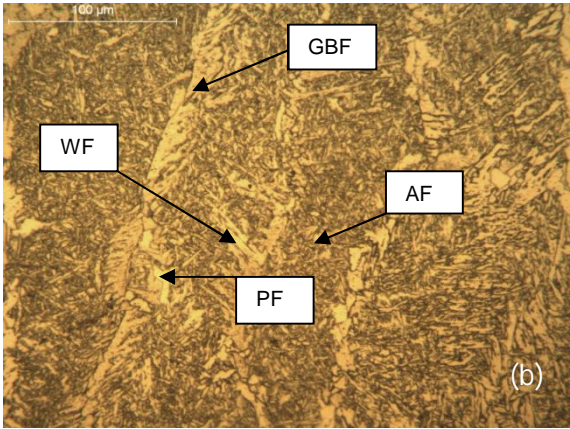
Microstructure	Observation
 <p>(a)</p>	<p>Weld-HAZ</p> <p>Below the fusion line (FL) the heat affected zone is composed of cellular and columnar dendritic grain structure. In contrast, the weld metal on top is mainly acicular ferrite (grain boundary ferrite) outlining the prior austenite boundary.</p>
 <p>(b)</p>	<p>Weld</p> <p>The weld microstructure of P1.1 reveals the presence of GBF, AF, WF and an important number of columnar dendritic with grain cellular structure.</p>

Figure 55. Microstructure of specimen P1.1 (a) HAZ-Base and (b) Weld.

The microstructure in Figure 56 (a) of specimen P2.1 shows a higher amount of fine equi-axed grains compared to the synergy pulsed GMAW specimen P1.1, and relatively more equi-axed dendritic structures with finer grain size are observed in the weld zone of Figure 56 (b). Compared to P1.1, P2.1 has much concentrate of weld microstructure consisting predominantly acicular ferrite (AF) and Widmanstätten ferrite (WF). In addition, slight long columnar structures were noted in the weld zone.

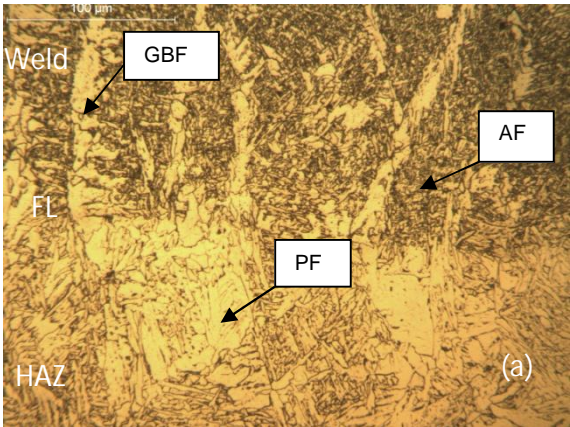
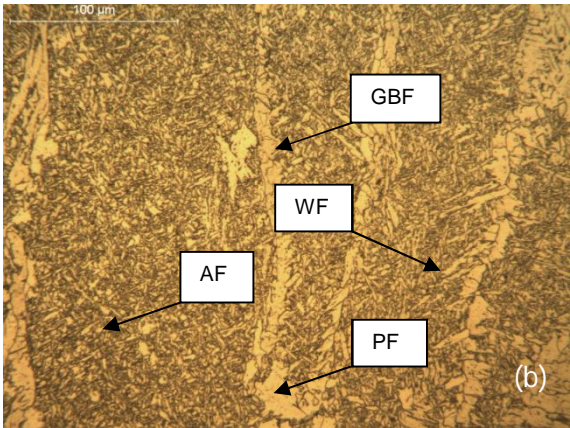
Microstructure	Observation
	<p>Weld-HAZ</p> <p>Below the fusion line (FL) the heat affected zone is composed of cellular and columnar dendritic grain structure. In contrast, the weld metal on top is mainly acicular ferrite (grain boundary ferrite) outlining the prior austenite boundary.</p>
	<p>Weld</p> <p>For P2.1 with 35% short circuit the amount of AF is higher than in specimen P1.1. In addition, the GBF and PF are larger compared to P1.1.</p>

Figure 56. Microstructure of specimen P2.1 (a) HAZ-Base and (b) Weld.

Figure 57 (a) shows the presence of finer equi-axed grains. WiseFusion welded specimens P2.1 and P4.1 have more long columnar dendritic compared to P3.1. The primary columnar structure predominantly occurs in the weld in Figure 57 (b). The weld microstructure comprises principally acicular ferrite (AF) and significant formation of Widmanstätten ferrite (WF). Higher long columnar structures were noted in the weld zone.

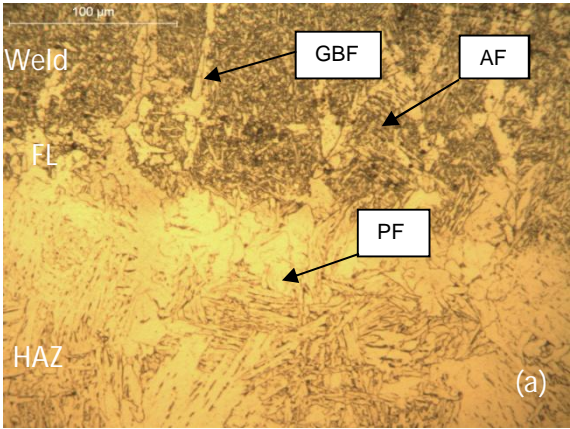
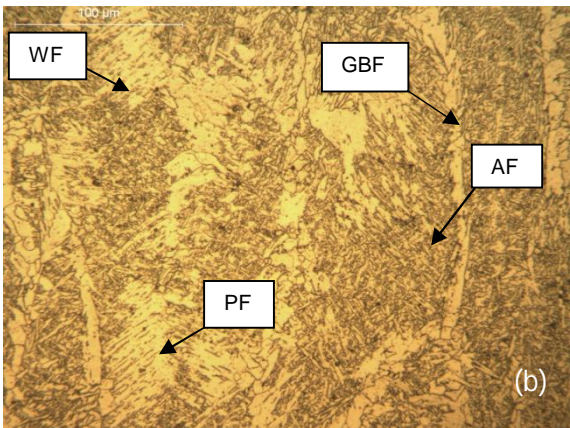
Microstructure	Observation
 <p>(a)</p>	<p>Weld-HAZ</p> <p>Below the fusion line (FL) the heat affected zone is composed of cellular and columnar dendritic grain structure. In contrast, the weld metal on top is mainly acicular ferrite (grain boundary ferrite) outlining the prior austenite boundary.</p>
 <p>(b)</p>	<p>Weld</p> <p>For P3.1 with 50% short circuit the amount of AF is reduced compared to P1.1 and is lower than in P2.1. In addition, the GBF decreased and PF is larger compared to P1.1 and P2.1</p>

Figure 57. Microstructure of specimen P3.1 (a) HAZ-Base and (b) Weld.

Figure 58 (a) shows a similar amount of fine equi-axed grains compared to specimen P1.1 and relatively more equi-axed dendritic structures with finer grain size are observed in the weld zone (Figure 58 b). A slightly lower in P4.1 compare specimen P1.1 of amount of equi-axed dendrite grain structures and considerable long columnar structures are observed in the weld zone (Figure 58 b). The Weld microstructure consists of mostly acicular ferrite (AF).

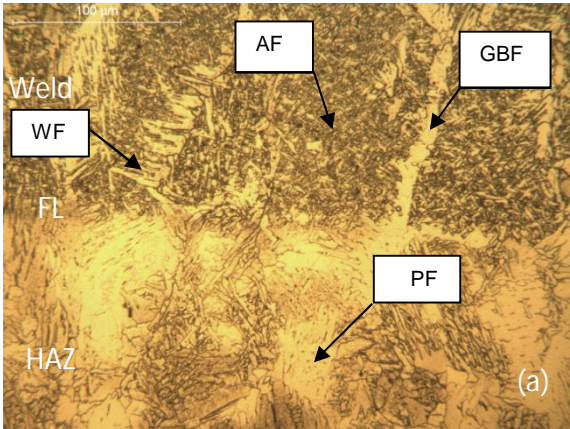
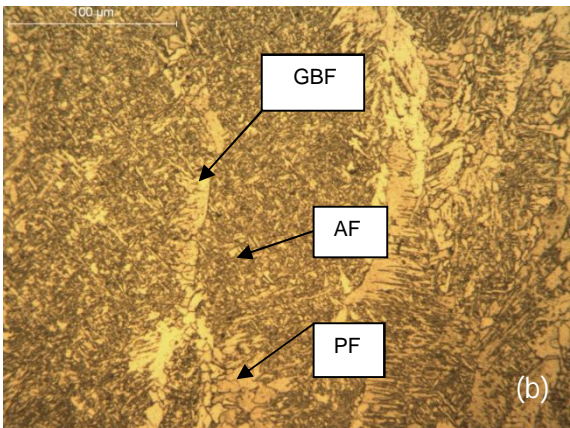
Microstructure	Observation
 <p>(a)</p>	<p>Weld-HAZ</p> <p>Below the fusion line (FL) the heat affected zone is composed of cellular and columnar dendritic grain structure. In contrast, the weld metal on top is mainly acicular ferrite (grain boundary ferrite) outlining the prior austenite boundary.</p>
 <p>(b)</p>	<p>Weld</p> <p>At P4.1 with 20% short circuit the amount of AF increases and is higher than P2.1 and slightly more compared to P1.1. Consequently, the GBF decreases, however, there is moderate presence of PF in P1.1 compared to P4.1.</p>

Figure 58. Microstructure of specimen P4.1 (a) HAZ-Base and (b) Weld.

Specimen P5.1 was welded using the synergic GMAW process. A bigger concentration of the weld microstructure contains of acicular ferrite (AF) than in P1.1, P2.1, P3.1 and P4.1. It can be observed that the microstructure contains predominantly coarser and elongated primary austenite phases with fine interdendritic structures, Figure 59 (b).

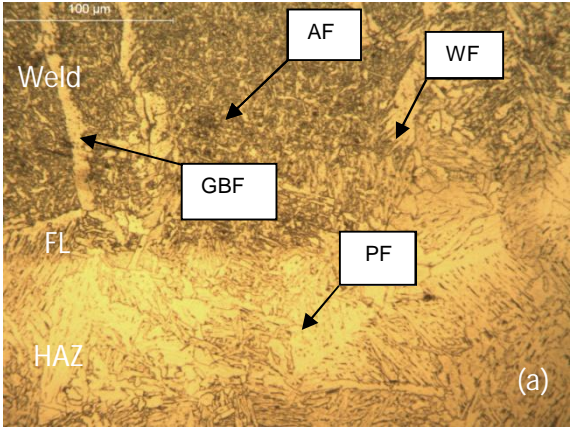
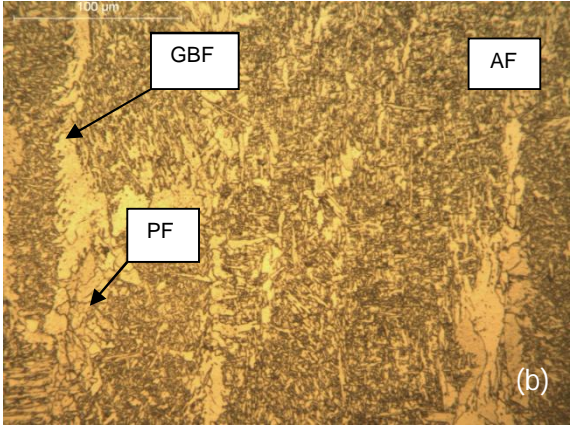
Microstructure	Observation
 <p>(a)</p>	<p>Weld-HAZ</p> <p>Below the fusion line (FL) the heat affected zone is composed of cellular and columnar dendritic grain structure. In contrast, the weld metal on top is mainly acicular ferrite (grain boundary ferrite) outlining the prior austenite boundary.</p>
 <p>(b)</p>	<p>Weld</p> <p>For P5.1 with Synergic GMAW the amount of AF increases and is the highest of all the specimens. GBF and PF decrease.</p>

Figure 59. Microstructure of specimen P5.1 (a) HAZ-Base and (b) Weld.

8.6 Vickers-Hardness Test

The macro-hardness test was performed from the base metal to the centreline by considering the symmetric of the weld. The analysis compared the same range of air gap for the base metal, HAZ and weld hardness with HV 5. The results are given in tabular form with recorded values and data in the Appendices I-VII and are plotted in Figures 60, 61 and 62.

Macro-hardness data from P1.0 (synergy pulsed GMAW) and P2.0 (WiseFusion, 35% short-circuit), given in Figure 60, indicate that softening of the base metal due to heat input is located between 1 and about 2 mm for specimen P2.0. Meanwhile for P1.0, the hardness is lower, at the 0 mm point, which clearly indicates a larger heat affected zone when using synergic pulsed GMAW compared to the default WiseFusion. The hardness of both specimens grows gradually as fusion is approached. However, a net difference is observed at the fusion zone (FZ), with 190 HV 5 for P1.0 and 175 HV 5 for P2.0. From 1.5 to 5.5 mm from the centre line corresponding to the weld (WM), P2.0 hardness is slightly greater than that of the P1.0 specimen.

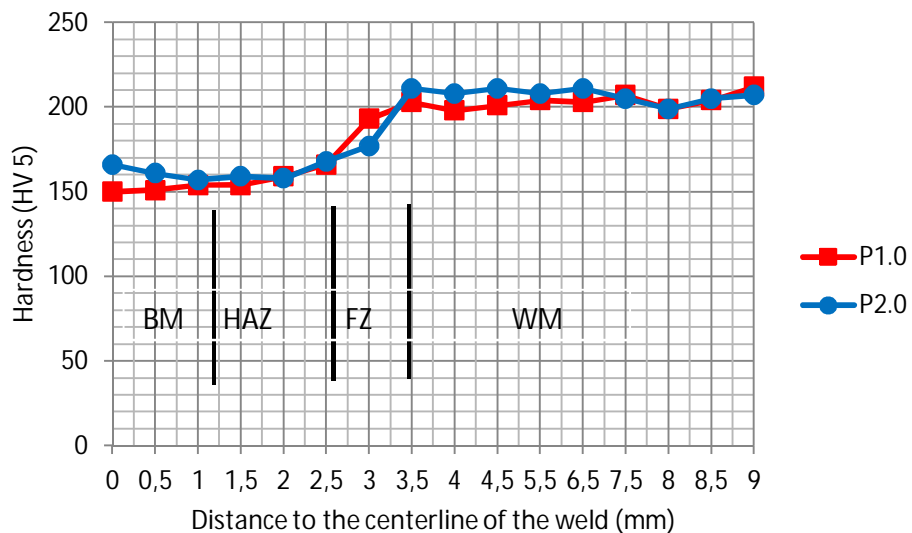


Figure 60. Hardness test results comparison between specimen P1.0 and P2.0.

The macro-hardness test at 1 mm air gap is given in Figure 61, which shows highest hardness for specimen P5.1 at point 3.5 to 6.5 mm. Although, the WiseFusion specimens (P2.1, P3.1 and P4.1) hardness (HV5) is very close, from 0.5 to 3.5 mm points, it is observed that the hardness of P1.1 increases sharply while that of P2.1 and P5.1 grows moderately at the fusion zone (FZ). In contrast, the hardness growth of P3.1 and P4.1 is steady in the same range. The fluctuation observed correlates with noticed with heat input, which is high in both P1.1 and P5.1, respectively, synergic pulsed control and synergic GMAW processes.

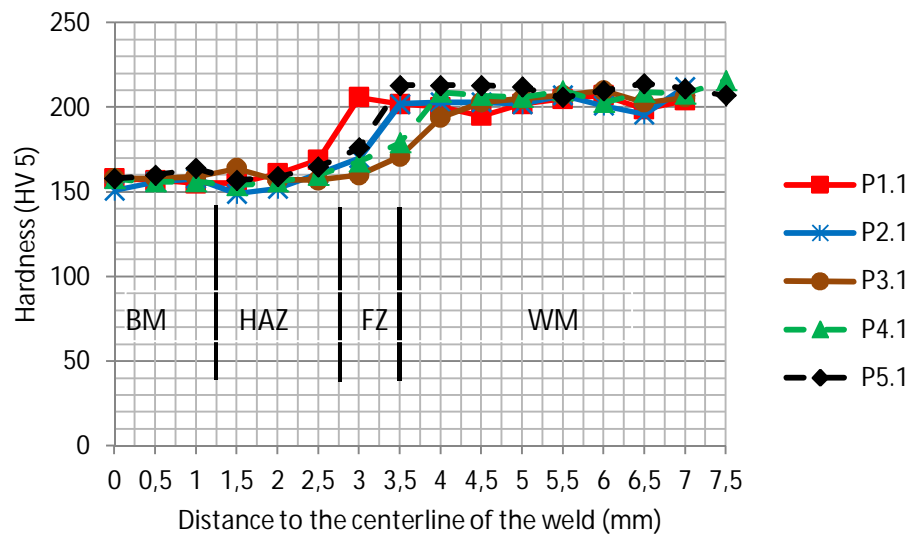


Figure 61. Hardness test results comparison P1.1, P2.1, P3.1, P4.1 and P5.1.

The macro-hardness test was also performed on specimens with a 2 mm air gap, and the results are plotted in Figure 62. Specimen P1.2 (synergic pulsed control) presents a softened area at heat affected zone (HAZ), as does P3.2 (WiseFusion, 50 % short circuit). However, for P5.2 (synergic GMAW) the softened area is between 1.5 and 2.5 mm points located respectively at HAZ and Fusion zone (FZ). The hardness increases sharply for P3.2 and P4.2 (WiseFusion, 20% short circuit). P4.2 has the longest hardness zone, beginning at 3 mm. That of P3.2 begins at 3.75 mm.

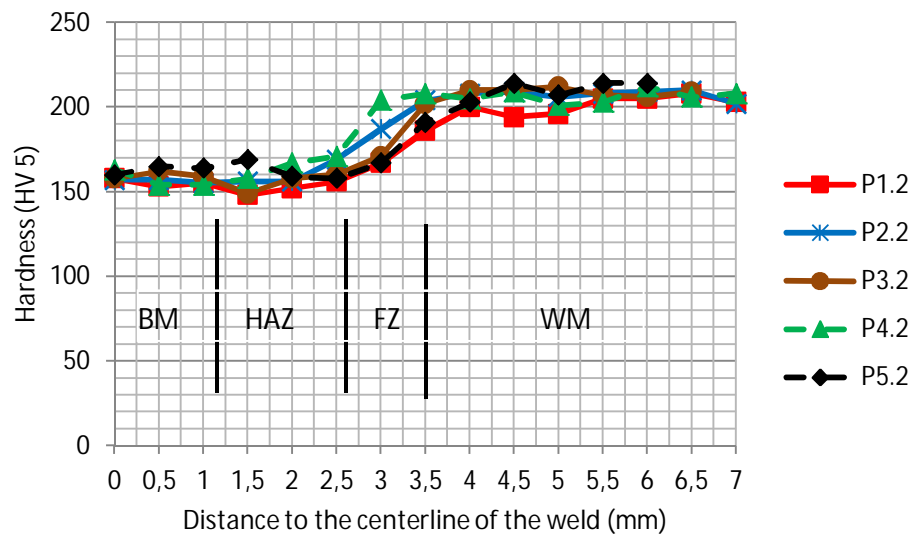


Figure 62. Hardness test results comparison P1.2, P2.2, P3.2, P4.2 and P5.2.

9 CONCLUSIONS

During this study, whose objective was to evaluate the applications and benefits of adaptive GMAW processes, three different processes; Synergic Pulsed GMAW, WiseFusionTM and Synergic GMAW were used to weld a fillet weld (PB position). It was decided to search for the best result and optimal conditions and parameters. Based on visual, mechanical and chemical analysis, the following conclusions can be drawn.

The high current density welding process is suitable for automation because it requires high speed at its upper range to avoid humping. However, manual applications can be performed at the lower speed range, due to the adaptive control and stability of the arc. The low heat input compared to traditional GMAW observed when using adaptive pulsed GMAW can be beneficial with a structure subject to multiple welds, as it reduces significantly the total heat, and thus limits distortion.

The thermal conductivity of the shielding gas affects the temperature of the arc and the weld pool. Moreover, the electrical conductivity of the shielding gas increases as the temperature increases. Therefore, shielding gas choice and mixture influence the droplet transfer mode. Furthermore, the shielding gas mixture also affects the weld penetration; for example, the PB weldment position conducted with various portions of Argon and CO₂ revealed higher penetration with a maximum of 18% CO₂.

The welding speed increases proportionally to the depth of penetration but it decreases as the speed is increased beyond certain limits. This means that for any welding condition, there is an optimum value of welding speed beyond which if the speed is increased the depth of penetration drops. Based on the effect of welding speed, arc current and welding voltage, higher welding bead penetration is obtained with a larger electrode diameter and the gas flow rate has negligible impact.

Conventional single wire heavy duty GMAW is based on wire extension, a high current and relatively low voltage for high-energy short circuit processes and a high voltage for high-energy spray processes. The productivity achieved with high-energy short circuiting arc processes varies between 8-18 kg/h, and that of high-energy spray arcs is 20 kg/h. The drawbacks of conventional high energy processes are the instability of the arc, humping and excessive heat. These problems can be successfully solved by utilization of a digitally controlled power source machine.

Compared to synergic pulsed GMAW, the profile of the weld generated with WiseFusion is bigger, with deeper side wall and a shorter root penetration. This reduces the risk of burn-through when welding plate of thin sections smaller or equal to 5 mm by increasing the welding speed and energy input.

Weld design with difficult access, such as narrow angles, has been challenging for weld torch orientation and has resulted in arc stability problems and poor weld quality. Adaptive pulsed GMAW provides an alternative to electrode extension and better control of the arc. A concrete example is the ForceArc process.

Adaptive pulsed GMAW processes are based on complex waveform current and voltage. It is difficult to evaluate the mean current and voltage, which can result in error when estimating the heat input. A new approach has been suggested by ASME section IX which gives more accurate results, although the power source must be able to display the total energy after welding.

Increase in the welding current in the synergic pulsed GMAW process reduces the columnar growth of dendrites in the matrix. The morphology of the bainite was found to change with variation in welding parameters. The pulse current resulted in a coarse microstructure with respect to the growth of dendrites, especially at higher pulse frequency and pulse duration, due to reduced cooling rates. However, pulse current welding carried out at higher arc voltage was found to be beneficial for the production of a finer weld microstructure. Compared to synergic pulsed GMAW, the weld zone in short circuit GMAW contained a more dendritic

microstructure with significant epitaxial growth of dendrites. The aspect ratio of the dendrites reduced to unity at the weld centre. There was no significant variation of the weld microstructure in both processes at a constant heat input, but the morphology of the dendrites changed with variation of the pulse parameters.

Weld penetration has a major impact on joint strength and service life. The weld dilution dictates the degree of base metal fusion, which must be adequate to maintain weld quality. The hardness variation at the interface of the weld zone (WZ) and heat affected zone (HAZ) correlate highly with the joint strength. The joint weakening tendency can be significantly reduced in ferrous welds, as well as non-ferrous welds. The WiseFusion process exhibited better wall dilution and penetration. This ability increased when the percentage of short circuits grew. Furthermore, the legs lengths of WiseFusion were much longer than synergic GMAW and slightly superior to synergic pulsed control.

The shape of the weld is defined by the penetration, as well as the dilution of the weld seam. Seam welds were observed for the three processes to investigate whether they differ significantly in shape. Synergic pulsed GMAW, for instance, was manifested by a straighter profile and a longer root, while synergic GMAW exhibited a straight wall fusion line but short root penetration. The straight fusion line and shorter legs length lead to smaller dilution compared to WiseFusion. WiseFusion presented a longer legs length and a more rounded seam weld fusion line with relatively symmetric repartition at the side wall of the weld. The shape of WiseFusion welds exhibited the factors necessary to guarantee strength rigidity and a long life cycle.

10 FURTHER RESEARCH

This study was limited to a moderate energy of about 180 to 250 A of peak current and involved only a limited number of samples. However, the study can be a basis for further work on high currents, in the range of 300 to 450 A. It is clear that work on a greater number of specimens is required. Other parameters which could be considered in future studies might include CTWD, welding speed, electrode feed speed and gas flow.

Another study could take an interest in developing principle that could help to set advanced power sources, which offers, to recall it, a variety of options but with precise requirement according to the materials and type of joint to be produced. The importance of this area could be seen in this study when it was found that applying different percentages of short circuit current affected the results achieved.

11 SUMMARY

This study reviewed some adaptive GMAW welding processes suggested originally by pioneers of the TIME, RapidMelt and RapidArc processes. These processes are able to increase production using a single electrode and relatively high energies. A major disadvantage of the methods as originally designed is the requirement for a particular gas mixture. This special mixture made the processes expensive, even if the processing speed compensated somewhat for this handicap. It was necessary, furthermore, to have specialised equipment. New modern digitalised welding machines provide an improved and more efficient use of the process, thanks to their memory capacity that allows the storing, saving and retrieving of data for rapid switches to achieve optimal results. In addition, thanks to the monitoring capability of modern welding machines, new curves of current and voltage have enabled satisfactory results to be achieved which are virtually spatter-free and with reduced heat input. This latter development is significant as excess heat affects the microstructure and weakens welding.

An experiment comparing Synergic Pulsed GMAW, WiseFusionTM welding and Synergic GMAW demonstrated that the heat introduced during the adaptive processes is indeed reduced. The heat reduction was confirmed by evaluation of the hardness and microstructure of the welds. WiseFusion showed the ability to weld pieces even with open gaps and irregularity; this is an advantage for the preparation of joints that do not need high accuracy. The weld dilution is another advantage of these processes as it guarantees a long life cycle of the weldments. It should, however, be noted that the study did not include higher current (300-450 A), which would have required many more specimens and a variation of other parameters. Such experiments would have allowed estimation of the limits of adaptive GMAW processes using high energy and it is strongly recommended that this area be explored.

The research and experiments carried out as part of this study clearly show the benefits that adaptive pulsed GMAW process has on the welding of structural steel (S355MC) in terms of microstructures quality and wider weld shape.

Heavy-duty adaptive GMAW using single wire was successfully applied to a wider range of thickness. The risk of joint softening which arises when using traditional high energy GMAW processes is mitigated because adaptive welding process allows the user to select optimal parameters, for example, the optimum heat in the weld to produce acicular ferrite appropriate for crack propagation resistance. Adaptive pulsed GMAW processes such as WiseFusion, ForceArc, DeepArc and RapidArc, also opens the possibility for manual use; thus far high energy arc GMAW has been limited to mechanized production. The adaptive pulsed GMAW process has considerable potential and is clearly an interesting field of study.

REFERENCES

- [1] K. Ferjutz and J. R. Devis, ASM Handbook, Volume 6, Welding Brazing and Soldering, Metals Park, Ohio: ASM International, 1993.
- [2] K. Weman and L. Gunnar, MIG Welding Guide, Cambridge: Woodhead Publishing and Maney Publishing, 2006.
- [3] J. Norrish, "Arc welding power sources – design evolution and welding characteristics," *IW Doc, XII-1215-91*, 1991.
- [4] S. Adolfsson, P. Bahrami et al, "On line quality monitoring in short circuit GMA welding," *Welding Journal, Research Supplement*, pp. 59s–73s, Feb 1999.
- [5] K. Himmelbauer, "Digital Welding," Fronius International, Property reports and presentations, 2003.
- [6] K. Weman, Welding Process Handbook, Cambridge, England: Woodhead Publishing Limited, 2003.
- [7] J. F. Lancaster, The Physics of Welding, Oxford: Pergamon Press, 1984.
- [8] J. Norrish, "A review of metal transfer classification in arc," in *IW Doc*, Bucharest, 2003.
- [9] J. Nadzam, "Gas metal arc welding: process overview," Lincoln Electric Company, Technology Center, Internal report, 2003.
- [10] C. Howard B, Modern Welding Technology, 3 rd ed., New Jersey: Regents/Prentice Hall, Englewood Cliffs , 1994.
- [11] Robert W. Messler Jr., Principles of Welding, Processes, Physics, Chemistry, and Metallurgy, Singapore: WILEY-VCH Verlag GmbH & Co. KGaA, Weinheim, 2004.

- [12] J. Taylor, *An Engineer's Guide to Fabrication Steel Structures; Fabrication Methods*, Sydney: Australian Institute of Steel Construction, 2001.
- [13] R. Killing, H. Sönnichsen and G. Glowicki, "Beitrag zur Klassifizierung des Werkstoffüberganges beim Metallschutzgasschweißen," *Schweissen und Schneiden*, vol. 36, no. 12, pp. 575-578, 1984.
- [14] E. Smårs and K. Acinger, "Material transport and temperature distribution in arc melting," *IIW-Document 212-168-68, International Institut of Welding Study Group SG212, Physics of Welding*, 1968.
- [15] C. L. Jenney and A. O'Brien, *Welding Handbook, 9th Edition, Volume 1, Welding Science and Technology, 9th; vol. 1 ed.*, C. L. Jenney and A. O'Brien, Eds., Miami, FL 33126, USA: (AWS) American Welding Society, 2001.
- [16] H. Granjon, *Fundamentals of Welding Metallurgy*, Cambridge: Woodhead Publishing, 1991.
- [17] D. G. Deyev and G. F. Deyev, "Surface Phenomena in Fusion Welding Processes," London, CRC Press Taylor & Francis Group, 2006, pp. 135-139.
- [18] S. I. Pinchuk, V. F. Postaushkin and G. D. Kulikov, "Nature of action of surface," *Avtom. Svarka*, pp. 11, 24, 1974.
- [19] M. Beckert et al, "Neues in der schweisstechnik 1985. werkstoffgrundlagen und," *Schweisstechnik (DDR)*, vol. 36, no. 5, p. 214, 1985.
- [20] R. Killing, "Angewandte Schweißmetallurgie-Anleitum für die Praxis, Fachbuchreihe Schweißtechnik Band 113," Düsseldorf, Deutscher verlag für schweißtechnik DVS-verlag GmbH, 1996, pp. 74-77.
- [21] Y. S. Kim and T. W. Eagar, "Analysis of metal transfer in Gas Metal Arc

Welding,” *Welding Journal*, pp. 269-278, June 1993.

- [22] R. Killing, “Schutzgase zum Lichtbogenschweißen -,” *Der Praktiker*, vol. 45, no. 8, pp. 451-454, 1993.
- [23] H. Matzner, “Qualitätssteigerung beim spritzerarmen MAGM-impulslichtbogenschweißen durch Regelung der Prozeßgrößen, Schweißtechnische Forschungsberichte, Band 40,” Düsseldorf, Deutscher Verlag für Schweißtechnik (DVS) GmbH, 1991, pp. 9, 13.
- [24] D. Dzelnitzki, “Increasing the deposition volume or the welding speed?- Advantages of heavy-duty MAG welding,” *Welding and Cutting*, no. 9, pp. E197-E204, 1999.
- [25] ISF, “5-Gas-shielding metal arc welding,” The Welding and Joining Institute (ISF) of RWTH, Aachen University in Germany, 2002.
- [26] F. Jeffus Larry, “Welding: Principles and Applications,” Clifton Park, New York, Delmar Cengage Learning, ISBN 1401810462, 2002, p. 218 – 225.
- [27] L. Baum and V. Fichter, “Der schutzgasschweisser, teil 2, MIG/ MAG schweissen,” *Die schweißtechnische Praxis*, DVS- Verlag, no. 12, 1999.
- [28] Anon, “Classification of metal transfer,” in *IIW Doc. XII-636-76*, 1976.
- [29] J. Ma, “Metal Transfer in MIG Welding,” Cranfield Institute of Technology, Bedfordshire, U.K., PhD Thesis, 1982.
- [30] W. Lucas, D. Iordachescu and V. Ponomarev, “Classification of metal transfer modes in GMAW,” in *IIW Doc. No XII-1859-05*, Prague, 2005.
- [31] D. Iordachescu and L. Quintino, “Steps toward a new classification of metal transfer in gas metal arc welding,” *Journal of Materials Processing Technology*, vol. 202, pp. 391-397, 2008.

- [32] E. Karadeniz, U. Ozsarac and C. Yildiz, “the effect of process parameters on penetration in gas metal arc welding processes,” *Journal of Materials and Design*, vol. 28, pp. 649-656, 2007.
- [33] S. Liu and T. A. Siewert, “Metal transfer in gas metal arc welding: droplet rate,” *Welding Journal*, vol. 68, no. 2, pp. 52-58, 1989.
- [34] W. J. So, M. J. Kang and D. C. Kim, “Weldability of pulse GMAW joints of 780 MPa dual-phase steel,” *International Scientific Journal*, vol. 41, no. 1, pp. 53-60, January 2010.
- [35] H. Wolters and P. Åberg, “QSet™ - a breakthrough in welding technology!,” *The ESAB Welding and Cutting Journal*, vol. 61, no. 1, pp. 36-37, 2006.
- [36] M. Suban and J. Tusek, “Dependence of melting rate in MIG/MAG welding on the type of shielding gas used,” *J. Mater. Process. Technol.*, vol. 119, pp. 185–192, 2001.
- [37] J. N. Pires, A. Loureiro and G. Böllmsjo, *Welding Robots Technology, System Issues and Application*, London: Springer/978-1-85233-953-1, 2006.
- [38] V. Stenke, *Besonderheiten und Eigenschaften von Mehrkomponentengas in der Schweißtechnik*, Düsseldorf: DVS-Berichte 155, DVS-verlag, 1993.
- [39] V. Stenke, “Schutzgasauswahl - vom CO₂ zum T.I.M.E. Gas.,” in *Dodatni i pomoćni materijali za zavarivačke i srodne postupke*, Poreč, 1996.
- [40] K. A. Lyttle, “Shielding gases, Welding, Brazing and Soldering,” in *ASM Handbook, Vol 6*, Metals Park, Ohio, ASM International, 1993, pp. 64-69.
- [41] I. Pires, T. Rosado, A. Costa and L. Quintino, “Influence of GMAW shielding gas in productivity and gaseous emissions,” in *10th International Aachen Welding Conference*, Aachen, Germany, October

2007..

- [42] I. S. Kim, A. Basu and E. Siores, "Mathematical models for control of weld bead penetration in the GMAW process," *Int. J. Adv. Manuf. Technol.*, vol. 12, pp. 393-401, 1996.
- [43] J. S. Allen and D. Wildgery, "Cored Wire developments and objectives of BS 7084," *Weld. Met. Fabr*, vol. 6, pp. 274-282, 1990.
- [44] H. Imaizumi and J. Church, "Welding characteristics of a new welding process, T.I.M.E process," in *IIW Doc No. XII-1199-90*, 1990.
- [45] Publ AGA Co, Facts About: Rapid Arc, Rapid Melt-High Productivity MIG/MAG, 1993.
- [46] S. Trube, "High performance MAG welding with the Linfast," in *IIW Doc No. XII-1499-97*, 1997.
- [47] B. Czwornog, "High energy MAG welding - arc shielding gases," *Biul Inst Spawalnictwa*, vol. 1, pp. 30-34, 1997.
- [48] B. Czwornog, "Properties of weld and joints MAG-weld using high arc energy levels," *Welding Journal*, vol. 15, no. 6, pp. 425-430, 2001.
- [49] M. Schellhase, "Der Schweißlichtbogen-ein technologisches Werkzeug, Fachbuchreihe Schweißtechnik, Band 84,," Düsseldorf, Deutscher Verlag für Schweißtechnik (DVS) GmbH, 1985, pp. 60, 68-70, 144.
- [50] S. Trube, "MAG-Hochleistungsschweißen mit dem LINFAST®-Konzept," Linde AG, Hoellriegelskreuth, 1997.
- [51] N. V. Pepe, "Advances in GMAW and application to corrosion resistant alloy pipes," Cranfield University, UK, PhD Thesis, 2010.
- [52] D. S. West, J. Neuberger, R. Lahnsteiner and A. Overton, "Revolutionary improvements in automated robot welding," in *TWI Conf. Automated*

welding systems in manufacturing, 17-19 November 1991. TWI paper 35, Gateshead, North East UK, 1991.

- [53] E. Halmoy et al, "The T.I.M.E. welding method compared with GMAW," *Doc. XII-1248-91, IIW 1991.*, 1991.
- [54] P. F. Mendez and T. W. Eagar, "Penetration and defect formation in high-current arc welding," *Welding Journal*, pp. 296s-306s, October 2003.
- [55] S. Adolfsson, P. Bahrami et al, "On line quality monitoring in short circuit GMA welding," *Welding Journal, Research Supplement*, pp. 59s-73s, Feb 1999.
- [56] N. Ahmed, *New Development in Advanced Welding*, Cambridge: Woodhead Publishing Limited, 2005.
- [57] Hamamoto et al, "Development of Digitally-Controlled Welding Machines," in *Welding Process Guide Book Vol.5 'Improvement of efficiency in welding processes'*, W. P. S. C. I. Welding Society, Ed., Welding Society, Welding Process Study Committee II-99., 2004.
- [58] Furukawa, "Inert gas arc welding machine in Europe," *Light Metal Welding*, vol. 43, no. 4, 2005.
- [59] Mita, "Present state of our company's inert gas arc welding machine and its prospect," *Light Metal Welding*, vol. 53, no. 8, 2005.
- [60] T. Ogasawara, T. Maruyama, T. Saito, M. Sato and Y. Hida, "A power source of gas shielded arc welding with new current waveforms," *Welding Journal*, vol. 66, no. 3, pp. 57-63, 1987.
- [61] E. K. Stava, "A new, low spatter," *Welding Journal*, vol. 72, no. 1, pp. 25-29, 1993.
- [62] S. F. Goecke, "Energiereduziertes Lichtbogen-Fügeverfahren für Wärmeempfindliche Werkstoffe (Reduced Energy Laser Process for Heat

- Sensitive Materials),” *DVS-Berichte*, vol. 237, pp. 44–48, 2005.
- [63] J. Cuhel, “Modified short circuit and pulsed gas metal arc welding technologies increase pipe welding productivity, improve quality, and ease training,” *welding Journal*, pp. 66-68, June 2008.
- [64] J. C. Needham and A. W. Carter, “Material transfer characteristics with pulsed current,” *Br. Welding J.*, vol. 12, no. 5, pp. 229-41, 1965.
- [65] J. C. Needhan, “Control of transfer in aluminium consumable electrode welding,” *Physics of Welding Arc, The Institute of Welding, London*, pp. 114-124, 1962.
- [66] W. Shimada and Ukai, “Effects of pulsed current control on welding quality improvement,” *IIW Document XII-B-81*, 1981.
- [67] P. K. Ghosh and B. K. Rai, “Characteristics of pulsed current bead on plate deposite in flux cored GMAW process,” *ISIJ Int*, vol. 36, no. 8, pp. 1036-1045, 1996.
- [68] P. K. Ghosh, S. R. Gupta and H. S. Randhawa, “Characteristics of a pulsed-current, vertical-up gas metal arc weld in steel,” *Metall. Mater. Trans. A*, vol. 31A, pp. 2247-2259, 2000.
- [69] S. Elliott, *Met. Construction*, pp. 148–151, 1985.
- [70] M. Amin and P. V. C. Watkins, “Synergic pulse MIG welding,” *Weld. Inst. Res. Rep.*, p. 46, 1977.
- [71] J. Norrish, *Advanced Welding Process; Technologies and Process Control*, Cambridge: Woodhead Publishing Limited, 2006.
- [72] C. J. Allum, “MIG welding —time for a reassessment,” *Met. Construction*, vol. 15, no. 6, pp. 347–353, 1983.
- [73] C. L. Mendes da Silva and A. Scotti, “Performance assesment of the

- (Trans) Vareststraint test for determining solidification cracking suceptibility when using welding processes with filler metal,” *Meas Sci Technology*, vol. 15, pp. 2215–2223, 2004.
- [74] C. L. Mendes da Silva and A. Scotti, “The influence of double pulse on porosity formation in aluminum GMAW,” *J Mater Process Technol*, vol. 171, pp. 366–372, 2006.
- [75] Mita, “IT processing for welding power,” *J Jpn Wels Soc*, vol. 1, 1997.
- [76] M. R. Bosworth and R. T. Deam, “Influence of GMAW droplet size on fume formation rate,” *J Phys D: Appl Phys*, vol. 33, pp. 2605–2610, 2000.
- [77] Matsui, “Study for improvement of weld quality in thin sheet welding execution,” in *Proc Conf 10th Seminar, Welding and joining Engineering Bureau*.
- [78] A. R. Doodman Tipi, “The study on the drop detachment for automatic pipeline GMAW system: free flight mode.,” *Int J Adv Manu Tech*, vol. 50, pp. 137–14715, 2010.
- [79] M. F. Iwami, “Development of a large-current AC-MIG welding method,” *J Jpn Weld Soc*, vol. 10, no. 5, pp. 83-88, 1992.
- [80] J. Tanimoto, M. Minooka and Y. Nishida, “Development of the AC pulse MIG welding process,” in *Proceedings of the IIW Asian Pacific Regional Welding Congress, 36th Annual AWI Conference.*, 1988.
- [81] H. Harada et al, “The state-of-the-art of AC GMAW process in Japan,” *IIW Doc XII-1589-99*, 1999.
- [82] H. Tong et al, “Quality and productivity improvement in aluminium ally thin sheet welding using alternating current pulsed metal inert gas welding system,” *Science and Technology of Welding and joining*, vol. 6, no. 4, pp. 203-208, 2001.

- [83] G. Huismann, "Introduction of new MIG process-advantage and possibility," in *IIW*, 1999.
- [84] D. Cuiuri, J. Norrish, G. Dean, P. Di Pietro and C. David Cook, "Control method and system for metal arc welding". Patent WO/2003/101658, 2003, 2003.
- [85] Y. Wu and R. Kovacevic, "Mechanically assisted droplet transfer process in gas metal arc welding," *J Engineering Manufacture*, vol. Proc Instn Mech Engrs Vol 216, no. Part B, pp. 555-564, 2002.
- [86] S. Y. Yang, "Projected droplet transfer control with additional mechanical forces (AMF) in MIG/MAG welding process," Harbin Institute of Technology, PhD dissertation, 1998.
- [87] Fronius, "CMT Advanced-New development," *Schweissen & Schneiden*, pp. 8-10, 2009.
- [88] Gerd Trommer Gernsheim, "'Fronius: Technologie – und Anwendungsinnovationen mit dem, CMT Advanced, - Prozess,'" *Welding and Cutting Today*, no. 2, p. 12, 15.9 2009.
- [89] Maritime-executive, "Reaching the limit of arc welding," 24 September 2009, <http://www.maritime-executive.com/pressrelease/latest-news-fronius-international-gmbh/>.- [Accessed 15 March 2012].
- [90] R. Fokens, "Cold Metal Transfer - CMT - A revolution in mechanized root pass pipeline welding," in *4th Pipeline Technology Conference*, Hannover Messe, Hannover, Germany, 2009.
- [91] V. Ponomarev, A. Scotti, A. Silvinskiy and O. Al-Erhayem, "Atlas of MIG/MAG welding metal transfer modes," in *Proc conf IIW, Doc.XII-1771 to 1775-03*, Bucharest, 2003.
- [92] T. Anderson, "Aluminium Q&A," *Welding Journal*, pp. 20-23, 8 2009.

- [93] A. P. Joseph, "Assessing the effect of GMAW-Pulse parameters on arc power and welding heat input," Master's Thesis, Ohio state university, 2001.
- [94] M. R. Bosworth, "Effective Heat input in pulsed current gas metal arc welding with solid wire electrodes," *Welding Journal*, vol. 70, no. 5, pp. 111s-117s, May 1991.
- [95] J. C. Needham, "What do you mean by current?," *Welding Institute Research Bulletin*, vol. 26, no. 8, pp. 273-277, August 1985.
- [96] J. C. Needham, "What do you mean by voltage?," *Welding Institute Research Bulletin*, vol. 26, no. 9, pp. 331-316, September 1985.
- [97] G. B. Melton, "Measurement of the arc welding parameters and validation of equipment," in *Eurojoin 2*, Florence, 1994.
- [98] U. Dilthey and R. Killing, "Heat input for pulse GMAW," *Welding Design Fabrication*, vol. 63, no. 9, pp. 51-53, Septembre 1990.
- [99] A. I. Sergeev, A. V. Mitulinskaya and K. L. Serpilin, "Selection methods of measuring the energy parameters of welding with control of active power," *Paton Welding Journal*, vol. 2, no. 9, pp. 650-653, 1990.
- [100] A. Joseph, D. D. Harwig, D. F. Farson and R. Richardson, "Assessing the effects of GMAW-P parameters on arc power and weld heat input," in *84th AWS Annual Conference*, Detroit, MI, USA, 2003.
- [101] T. Melfi, "New code requirements for calculating heat input," *welding Journal*, pp. 61-63, June 2010.
- [102] J. Norrish, "Process modification in Gas Metal Arc Welding for enhanced performance," in *WTIA/IIW Congress*, Cairns, Queensland, Australia, 25-28 September 2011, 2011.

- [103] J. Uusitalo, "FastMig™ synergic and pipe welding," *Kemppi Pro News*, p. 8, 3 2005.
- [104] P. Kah, "Welding of sheet metal using modified short arc," Lappeenranta University of Technology, Master's Thesis, 2007.
- [105] J. Uusitalo, "Modified short arc process-new way of welding root passes.' Economic and Ecological Aspects," in *Proceeding of the IIW International Conference: Welding & Materials-Technica*, Croatia: Dubrovnik & Cavtat, 2007.
- [106] T. Peltola, J. Kumpulainen and M. Veikkolainen, "Novel tailored welding arcs help welders meet quality and productivity demands," *Innovation and Business Development at Kemppi Oy, Finland*, pp. 15-18.
- [107] Kemppi Oy, "files/Kemppi Wise,Match Software Manual," <http://www.rapidwelding.com/files/Kemppi%20Wise,Match%20Software%20Manual.pdf>. [Accessed 20 March 2012].
- [108] A. M. Torbati, R. M. Miranda, L. Quintino, S. Williams and D. Yapp, "Optimization procedures for GMAW of bimetal pipes," *Journal of Materials Processing Technology*, vol. 211, no. 6, p. 1112–1116, 2011.
- [109] SFS Suomen Standardisoimisliitto "SFS-EN 10149-2:1996.(EN 10149-2:1995), Kuumavalssatut lujat kylmämuovattavat teräslevytuotteet," Osa 2: Termomekaanisesti valssattujen terästen toimitusehdot., Suomen Standardisoimisliitto SFS ry. 14 s., 1995.
- [110] R. Stout, "Weldability of steels," *Welding Research Council*, pp. 3–4, 263, 1987.
- [111] SFS Suomen Standardisoimisliitto, "SFS-EN 440, Hitsausaineet. Hitsauslangat ja hitsiaineet seostamattomien terästen ja hienoraeterästen metallikaasukaarihitsaukseen. Luokittelu," Suomen Standardisoimisliitto SFS, 1995.

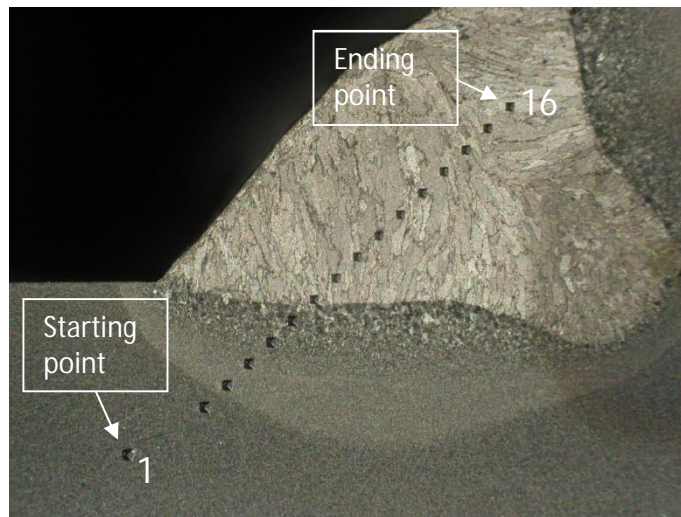
- [112] SFS Suomen standardisoimisliitto, Hitsien tarkastus. Osa 1. Rikkomaton aineenkoetus, Syyskuu 2001.
- [113] SFS Suomen standardisoimisliitto, Hitsien tarkastus. Osa 2. Rikkova aineenkoetus, Huhtikuu 1999.
- [114] C. L. Estes and P. W. Turner, "Filler metal dilution and composition in dissimilar-metal welding," *Welding Journal*, vol. 43, p. 541s, 1964.
- [115] L. E. Svensson, *Control of Microstructures and Properties in Steel Arc Welds*, London: CRC Press, 1994.
- [116] K. Easterling, *Introduction to the Physical Metallurgy of Welding*, 2nd ed., Oxford: Butterworth-Heinemann, 1992.
- [117] M. Aksoy, M. Ero and N. Orhan, "Effect of coarse initial grain size on microstructure and mechanical properties of weld metal and HAZ of a low carbon steel," *Material Science and Engineering*, vol. 1, no. 269, pp. 1-9, 1999.
- [118] S. S. Babu, "Current opinion in solid state and materials science," *Curr. Opin. Solid State Mater. Sci.*, vol. 8, p. 267, 2004.
- [119] S. S. Babu, "The mechanism of acicular ferrite in weld deposits," *Curr Opin Solid State Mater Sci*, vol. 8, no. 3-4, pp. 267-278, 2004.
- [120] R. E. Dolby, "Advances in welding metallurgy of steel," *Metals Technology*, no. 10, pp. 349 - 362, 1983.
- [121] D. J. Abson, A. Duncan and R. J. Pargeter, "Guide to the light microscope examination of ferritic steel weld metals," *IIW DOC. IX-1533-88, IXJ-123-87, revision 2*, June 1988.
- [122] M. Q. Johnson, G. M. Evans and G. R. Edwards, "The effect of thermal cycles on high strength steel SMA weld metal microstructures and properties," in *Proc 4th int. conf on "Trends in welding research"*,

Gatlinburg, USA, June 1995.

- [123] H. J. Kim and J. G. Youn, "Characteristics of TMCP steel and its softening," *Welding Metallurgy of Structural Steel*, J.Y. Koo, Ed., AIME, 1987.

APPENDICES

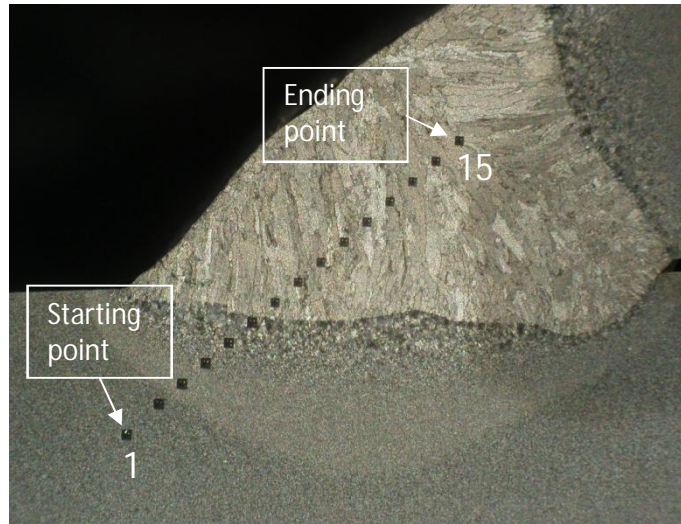
Appendix I: Macro-hardness data and macro section of macro-hardness indents specimen P1.0



Specimen P1.0 macro-hardness indents

Point of measurement	Method	Lens	X-distance from the starting point	Y-distance from the starting point	Hardness	Diagonal
1	HV 5	10x	0	0	150	248,958
2	HV 5	10x	0,5	0	151	247,796
3	HV 5	10x	1	0	154	245,371
4	HV 5	10x	1,5	0	154	245,371
5	HV 5	10x	2	0	159	241,482
6	HV 5	10x	2,5	0	166	236,335
7	HV 5	10x	3	0	193	219,182
8	HV 5	10x	3,5	0	203	213,715
9	HV 5	10x	4	0	198	216,397
10	HV 5	10x	4,5	0	201	214,776
11	HV 5	10x	5	0	204	213,19
12	HV 5	10x	5,5	0	203	213,715
13	HV 5	10x	6	0	207	211,64
14	HV 5	10x	6,5	0	199	215,852
15	HV 5	10x	7	0	204	213,19
16	HV 5	10x	7,5	0	212	209,129

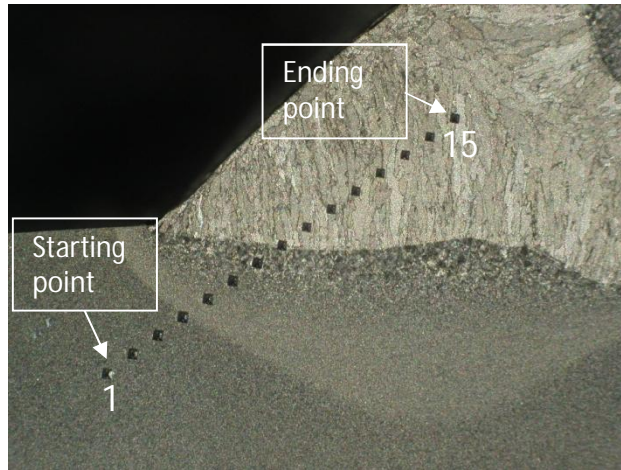
Appendix II: Macro-hardness data and macro-section of macro-hardness indents specimen P1.1



Specimen P1.1 macro-hardness indents

Point of measurement	Method	Lens	X-distance from the starting point	Y-distance from the starting point	Hardness	Diagonal
1	HV 5	10x	0	0	158	242,188
2	HV 5	10x	0,5	0	157	243,015
3	HV 5	10x	1	0	155	244,578
4	HV 5	10x	1,5	0	155	244,578
5	HV 5	10x	2	0	161	239,977
6	HV 5	10x	2,5	0	169	234,228
7	HV 5	10x	3	0	206	212,153
8	HV 5	10x	3,5	0	202	214,243
9	HV 5	10x	4	0	200	215,312
10	HV 5	10x	4,5	0	195	218,055
11	HV 5	10x	5	0	202	214,243
12	HV 5	10x	5,5	0	205	212,67
13	HV 5	10x	6	0	207	211,64
14	HV 5	10x	6,5	0	199	215,852
15	HV 5	10x	7	0	204	213,19

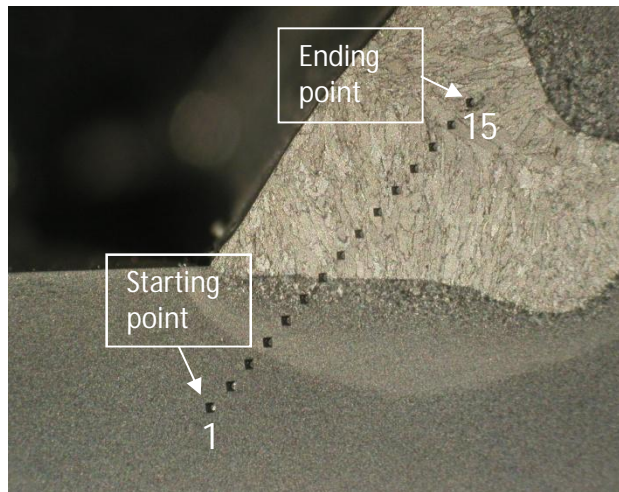
Appendix III: Macro-hardness data and macro-section of macro-hardness indents specimen P1.2



Specimen P1.2 macro-hardness indents

Point of measurement	Method	Lens	X-distance from the starting point	Y-distance from the starting point	Hardness	Diagonal
1	HV 5	10x	0	0	158	242,245
2	HV 5	10x	0,5	0	153	246,171
3	HV 5	10x	1	0	155	244,578
4	HV 5	10x	1,5	0	148	250,295
5	HV 5	10x	2	0	152	246,98
6	HV 5	10x	2,5	0	156	243,793
7	HV 5	10x	3	0	167	235,627
8	HV 5	10x	3,5	0	186	223,268
9	HV 5	10x	4	0	200	215,312
10	HV 5	10x	4,5	0	194	218,616
11	HV 5	10x	5	0	196	217,498
12	HV 5	10x	5,5	0	205	212,67
13	HV 5	10x	6	0	205	212,67
14	HV 5	10x	6,5	0	208	211,131
15	HV 5	10x	7	0	203	213,715

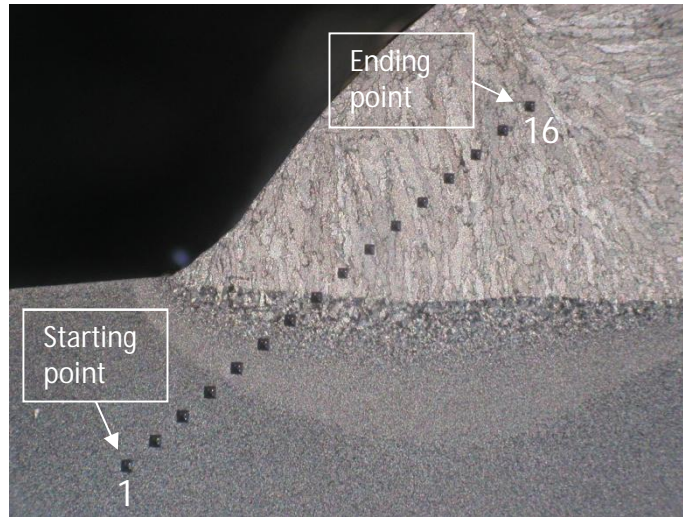
Appendix IV: Macro-hardness data and macro-section of macro-hardness indents specimen P2.2



Specimen P2.2 macro-hardness indents

Point of measurement	Method	Lens	X-distance from the starting point	Y-distance from the starting point	Hardness	Diagonal
1	HV 5	10x	0	0	157	243,015
2	HV 5	10x	0,5	0	157	243,015
3	HV 5	10x	1	0	155	244,578
4	HV 5	10x	1,5	0	156	243,793
5	HV 5	10x	2	0	156	243,793
6	HV 5	10x	2,5	0	169	234,228
7	HV 5	10x	3	0	187	222,67
8	HV 5	10x	3,5	0	204	213,19
9	HV 5	10x	4	0	208	211,131
10	HV 5	10x	4,5	0	209	210,625
11	HV 5	10x	5	0	206	212,153
12	HV 5	10x	5,5	0	208	211,131
13	HV 5	10x	6	0	209	210,625
14	HV 5	10x	6,5	0	210	210,123
15	HV 5	10x	7	0	202	214,243

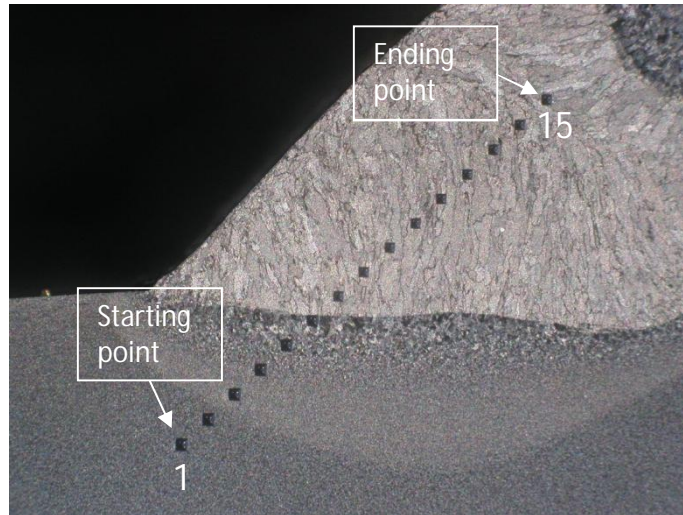
Appendix V: Macro-hardness data and marco-section of macro-hardness indents specimen P4.1



Specimen P4.1 macro-hardness indents

Point of measurement	Method	Lens	X-distance from the starting point	Y-distance from the starting point	Hardness	Diagonal
1	HV 5	10x	0	0	158	242,245
2	HV 5	10x	0,5	0	156	243,793
3	HV 5	10x	1	0	156	243,793
4	HV 5	10x	1,5	0	154	245,371
5	HV 5	10x	2	0	156	243,793
6	HV 5	10x	2,5	0	160	240,726
7	HV 5	10x	3	0	168	234,924
8	HV 5	10x	3,5	0	179	227,592
9	HV 5	10x	4	0	209	210,625
10	HV 5	10x	4,5	0	207	211,64
11	HV 5	10x	5	0	206	212,153
12	HV 5	10x	5,5	0	210	210,123
13	HV 5	10x	6	0	203	213,715
14	HV 5	10x	6,5	0	209	210,625
15	HV 5	10x	7	0	208	211,131
16	HV 5	10x	7,5	0	216	207,184

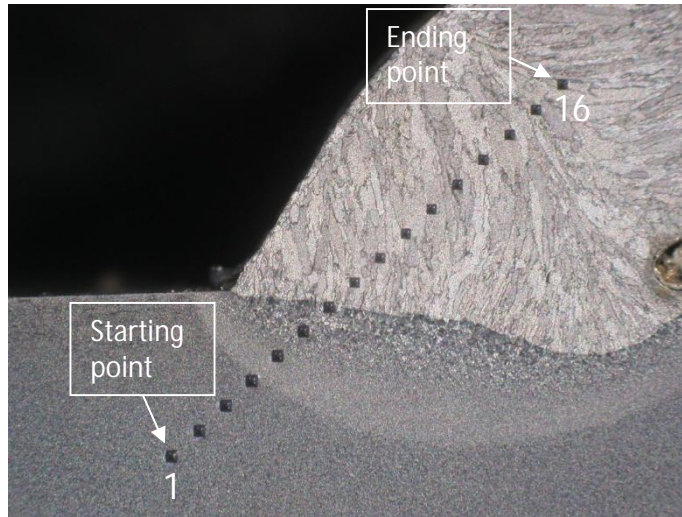
Appendix VI: Macro-hardness data and macro-section of macro-hardness indents specimen P4.2



Specimen P4.2 macro-hardness indents

Point of measurement	Method	Lens	X-distance from the starting point	Y-distance from the starting point	Hardness	Diagonal
1	HV 5	10x	0	0	163	238,5
2	HV 5	10x	0,5	0	154	245,371
3	HV 5	10x	1	0	154	245,371
4	HV 5	10x	1,5	0	158	242,245
5	HV 5	10x	2	0	167	235,627
6	HV 5	10x	2,5	0	171	232,855
7	HV 5	10x	3	0	204	213,19
8	HV 5	10x	3,5	0	208	211,131
9	HV 5	10x	4	0	205	212,67
10	HV 5	10x	4,5	0	209	210,625
11	HV 5	10x	5	0	201	214,776
12	HV 5	10x	5,5	0	203	213,715
13	HV 5	10x	6	0	212	209,129
14	HV 5	10x	6,5	0	206	212,153
15	HV 5	10x	7	0	208	211,131

Appendix VII: Macro-hardness data and macro-section of macro-hardness indents specimen P5.0



Specimen P5.0 macro-hardness indents

Point of measurement	Method	Lens	X-distance from the starting point	Y-distance from the starting point	Hardness	Diagonal
1	HV 5	10x	0	0	158	242,245
2	HV 5	10x	0,5	0	160	240,726
3	HV 5	10x	1	0	164	237,772
4	HV 5	10x	1,5	0	157	243,015
5	HV 5	10x	2	0	159	241,482
6	HV 5	10x	2,5	0	165	237,051
7	HV 5	10x	3	0	176	229,523
8	HV 5	10x	3,5	0	213	208,638
9	HV 5	10x	4	0	213	208,638
10	HV 5	10x	4,5	0	213	208,638
11	HV 5	10x	5	0	212	209,129
12	HV 5	10x	5,5	0	206	212,153
13	HV 5	10x	6	0	210	210,123
14	HV 5	10x	6,5	0	214	208,15
15	HV 5	10x	7	0	211	209,624
16	HV 5	10x	7,5	0	207	211,64